

**CHARACTERIZATION OF SMOKE PLUME EMISSIONS AND DYNAMICS
FROM PRESCRIBED AND WILDLAND FIRES USING
HIGH-RESOLUTION FIELD OBSERVATIONS AND
A COUPLED FIRE-ATMOSPHERE MODEL**

By

KARA M YEDINAK

A dissertation submitted in partial fulfillment of
the requirements for the degree of

DOCTOR OF PHILOSOPHY

WASHINGTON STATE UNIVERSITY
College of Engineering and Architecture

DECEMBER 2013

© Copyright by KARA M YEDINAK, 2013
All Rights Reserved

To the Faculty of Washington State University:

The members of the Committee appointed to examine the dissertation of KARA M YEDINAK find it satisfactory and recommend that it be accepted.

Brian Lamb, Ph.D., Chair

Heping Liu, Ph.D.

Serena Chung, Ph.D.

Philip Higuera, Ph.D.

ACKNOWLEDGEMENTS

I would like to thank the International Association of Wildland Fire for awarding me a graduate scholarship in 2008, which partially funded my travel to conference during my time as a graduate student.

Many thanks to the National Center for Atmospheric Research and Dr. Janice Coen for hosting me during my graduate student ASP visit for three months in the spring of 2011. I would also like to thank Dr. Coen for all of her help and insight that resulted in the enrichment of this dissertation. I was inspired and supported by many scientists and graduate students during my stay at NCAR, including Pedro Jimenez, Ned Patton, May Wong, Anna Fitch, Yaitza Luna, Corwin Wright, Natalie Laube, Jean-François Cossette, and Joanna Maja Slawinska. Thank you for your camaraderie, technical support, and inspiration.

I was supported in my decision to return to graduate school by several fire behavior colleagues whom I consider to be friends, including Colin Hardy, Mark Finney, Jack Cohen, Bret Butler, Jason Forthofer, Rod Linn, Penny Morgan, Alistair Smith and Chad Hoffman. Your support of my journey has been a driving force when all other hope seems lost.

I would never have made it to WSU and LAR if it hadn't been for Dr. George Mount, who has been an inspiration, a wonderful mentor, and an upholder of scientific standards.

There are numerous colleagues in LAR that have made my graduate student struggles bearable, and dare I say, fun. I would like to thank Dr. Steve Edburg, Natalie Wagenbrenner, and my fellow office mates in Dana 334, past and present, in particular

for all of their support and laughter. Dr. Steve Edburg has played a critical part in this dissertation work and has been an invaluable source of knowledge and support.

Dr. David Wollkind from the WSU mathematics department was a tremendous inspiration to me when all other creative lights were dimming. Your unbridled passion for beautiful science and appreciation for creativity will never be forgotten.

The support, from the men and women who worked beside me in GWIS and GAIA, has been invaluable. Your friendship and good advice are irreplaceable and will never be forgotten.

I would like to thank my committee; Dr. Brian Lamb, Dr. Serena Chung, Dr. Heping Liu, and Dr. Philip Higuera; for all the hours of advice, edits, and creative thinking they put forth in signing on to my committee.

Special thanks go to Dr Brian Lamb for having the faith in me to succeed and for supporting me through all the personal and professional challenges that came my way. Special thanks also goes to Dr. Tara Strand for her words of encouragement and tremendous technical support on the emissions factors portion of this dissertation.

The support of my family has been incredible during this experience. It was so wonderful to have their support and occasionally be reminded that I should laugh at myself more often. Mom and Dad, I could not imagine having done this without you both there to talk to, hypothesize with, and remind me that I can do this. Thanks for having such unflappable faith in your quirky daughter! Kevin and Karsten, you two remind me to keep it real and silly as often as possible. Thank you for believing I could do this and for making sure I never forgot I was your smaller sister. James, I have no words. I can't believe we decided to embark on graduate school together, and despite the

crazy ride, I don't regret it at all. You have been a strong sounding board and my constant defender. Thank you for all your love and support.

CHARACTERIZATION OF SMOKE PLUME EMISSIONS AND DYNAMICS
FROM PRESCRIBED AND WILDLAND FIRES USING
HIGH-RESOLUTION FIELD OBSERVATIONS AND
A COUPLED FIRE-ATMOSPHERE MODEL

ABSTRACT

by Kara M Yedinak, Ph.D.
Washington State University
December 2013

Chair: Brian Lamb

Smoke plumes associated with wildland fires are difficult to characterize due to the non-linear behavior of the variables involved. Plume chemistry is largely modeled using emission factors to represent the relative trace gas and aerosol species emitted. Plume dynamics are modeled based on assumptions of plume vertical distribution and atmospheric dispersion. In the studies presented here, near and in-source measurements of emissions from prescribed burns are used to characterize the variability of emission factors from low-intensity fires. Emissions factors were found to be in the same range as those from other, similar studies in the literature and it appears that the emission factors may be sensitive to small differences in surface conditions such as fuel moisture, surface wind speed, and the ratio of live to dead fuels. We also used two coupled fire atmosphere models, which utilize the Weather Research and Forecasting (WRF) model called WRF-

Fire and WRF-Sfire, to investigate the role that atmospheric stability plays in influencing plume rise as well as developing a technique for assessing plume rise and the vertical distribution of pollutants in regional air quality models. Plume heights, as well as rate of growth of the fire, were found to be sensitive to atmospheric stability while fire rate of spread was not. The plume center-of-mass technique was demonstrated to work well but has slightly low estimates compared to observations.

TABLE OF CONTENTS

ACKNOWLEDGEMENTS	III
CHARACTERIZATION OF SMOKE PLUME EMISSIONS AND DYNAMICS	VI
ABSTRACT	VI
TABLE OF CONTENTS	VIII
LIST OF FIGURES	XI
LIST OF TABLES	XIV
DEDICATION	XV
ATTRIBUTION	XVI
CHAPTER 1: INTRODUCTION AND LITERATURE REVIEW	1
1.1. OVERVIEW	1
1.2. GOAL AND OBJECTIVES	2
1.3. BACKGROUND	3
1.3.1. Modeling wildland fire production of particulates and traces gases	3
1.3.2. The influence of atmospheric stability on wildland fire plume dynamics	5
1.3.3. Regional scale representation of wildland fire plume dynamics	8
1.4. SUMMARY	9
1.5. REFERENCES	10
CHAPTER 2: POLLUTANT EMISSIONS FROM LOW INTENSITY PINE FOREST PRESCRIBED BURNS	17
2.1. ABSTRACT	17

2.2. INTRODUCTION	18
2.3. METHODS.....	20
2.3.1. Tower Instrumentation.....	21
2.3.2. Unit 18 and 19	22
2.3.3. Unit 27	24
2.4. ANALYSIS AND RESULTS.....	25
2.4.1. Meteorological Conditions	25
2.4.2. Chemical Measurements.....	28
2.5. DISCUSSION.....	44
2.5.1. Comparison with Other Studies	47
2.6. CONCLUSIONS.....	49
2.7. REFERENCES	50
CHAPTER 3: AN ANALYSIS OF SENSITIVITY TO AMBIENT ATMOSPHERIC STABILTIY ON FIRE BEHAVIOR AND SMOKE PLUME RISE USING WRF- FIRE.....	57
3.1. ABSTRACT.....	57
3.2. INTRODUCTION	57
3.3. METHODS.....	59
3.3.1. WRF-Fire model setup.....	59
3.3.2. Two cases: idealized stability regimes.....	62
3.3.3. Analysis Methods	64
3.4. RESULTS	66
3.4.1. Fire-line ROS.....	66
3.4.2. Plume Rise	68
3.5. DISCUSSION.....	70

3.6. <i>SUMMARY AND CONCLUSIONS</i>	71
3.7. <i>REFERENCES</i>	74
CHAPTER 4: DEVELOPMENT OF A PLUME RISE ANALYSIS TECHNIQUE FOR LARGE WILDLAND FIRES USING WRF-SFIRE	81
4.1. <i>ABSTRACT</i>	81
4.2. <i>INTRODUCTION</i>	81
4.3. <i>METHODS</i>	82
4.3.1. <i>Case Studies</i>	85
4.4. <i>RESULTS</i>	86
4.5. <i>DISCUSSION</i>	90
4.6. <i>SUMMARY AND CONCLUSIONS</i>	94
4.7. <i>REFERENCES</i>	95
CHAPTER 5: SUMMARY AND CONCLUSIONS.....	102
5.1. <i>SUMMARY</i>	102
5.2. <i>CONCLUSIONS</i>	102
5.2.1. <i>Chapter 2</i>	102
5.2.2. <i>Chapter 3</i>	103
5.2.3. <i>Chapter 4</i>	104
5.3. <i>FUTURE WORK</i>	105

LIST OF FIGURES

Chapter 2

- Figure 1 Counterclockwise from the top left corner, the blue square denotes the region of North Carolina, near Fort Bragg (lower left) where multiple prescribed burn (white outline) took place. Wire grass and longleaf pine litter (lower right) were the dominant surface fuels in the two burn units sampled in this study (bright green - middle right panel) of this study. The canopy fuels (not burned) are shown in the upper right corner and consisted predominantly of longleaf pine.....21
- Figure 2 Burn units 18 and 19 (outlined in orange) are pictured here with the full suite of campaign instruments shown. The WSU tower is labeled “Super Tower” and denoted by a yellow marker in the upper right of the image.23
- Figure 3. Unit 27 (outlined in yellow) is shown with the WSU tower (labeled “Super Tower”) in the southern quadrant.25
- Figure 4 Vertical temperature (left) and wind speed (right) profiles for burns 1 (top) and 2 (bottom) shows an overall increase in magnitude.....26
- Figure 5 Wind speed and direction at the top of the canopy (25.7m AGL) for burn 1 (top) and burn 2 (bottom) were roughly constant for the duration of the prescription. The green and red bars denote the start and stop of the prescribed burn, while the grey dashed bar indicates the first smoke plume impact on the tower. The blue shaded area marks the range in wind direction that resulted in impact of the smoke plume on the tower.27
- Figure 6 The 5-minute averaged time series of MCE and excess concentrations of CO, CO₂, NO_x, NO, CH₄, NH₃, PM_{2.5}, PAH, and BC (where applicable) are shown for burn 1. The time series starts when the smoke plume first encounters the tower and the red vertical line denotes the end of the prescribed burn.....30
- Figure 7 The excess concentrations for burn 2 were higher due to the in-source location of the sampling tower. The vertical red line denotes the end of the burn...31
- Figure 8 From top to bottom, excess concentrations of CO, CH₄, NH₃, and NO_x are plotted against CO₂ and CO for burns 1 (blue) and 2 (red). Trend lines and regression equations are shown for only flaming combustion.....33
- Figure 9 The time series of MCE and EFs for burn 1 are shown. The time series starts at the beginning of the burn and the red vertical line denotes the end of the prescribed burn. The gray dashed line in the MCE (top) plot denotes the threshold between flaming and smoldering combustion.36

Figure 10 The time series of burn 2 is shown with the red vertical line denoting the end of the prescribed burn. The highest EFs of all gasses and particulates occur after the end of prescription except for CO₂.37

Figure 11 The relationship between emission factors (EF) and modified combustion efficiency (MCE) for CO (top) and CO₂ (bottom) are shown for both burn 2 (red) and burn 1(blue). The regressions lines and corresponding equations are only representative of flaming combustion.....40

Figure 12 A comparison of EF to MCE for NO (top), NO_x (middle), and CH₄ (bottom) shows very poor correlation of NO and NO_x during burn 2 (red), and a slightly stronger correlation to MCE during burn 1 (blue). The correlations of CH₄ have the opposite trend.41

Figure 13 The EF of NH₃ compared to MCE during burn 1 (blue) and burn 2 (red). Overall, these correlations were very low.....42

Figure 14 The EFs of PAH (top) and PM_{2.5} (bottom) are shown for burn 1 (blue) and burn 2 (red) along with regression lines and correlations to flaming combustion....43

Figure 15 Emission factors of CO, CO₂, CH₄, NO_x, NH₃, and PM_{2.5} from this study are compared with results from similar pine understory measurements.....48

Chapter 3

Figure 1 A schematic of the idealized model domain is shown above. The back panel of the schematic shows an example of the water vapor released in the model during the combustion process.....60

Figure 3 The potential temperature(a), wind speed(b), and water vapor(c) profiles just after turbulence spin up and before ignition are shown here.63

Figure 4 Time series of surface momentum and heat fluxes as well as the standard deviation of U-direction winds show stable behavior after 37 minutes from the start of the simulation.....63

Figure 5 The solid and dashed lines denote the average forward ROS for the neutral (blue) case and unstable (red) case respectively. The shaded areas denote the standard deviation for the unstable (red dots) and neutral (blue lines) cases.66

Figure 6 The dashed red line denotes the average fire area for the unstable case and the solid blue line denote the average fire area for the neutral case. The patterned areas show the standard deviation for the unstable (red) and neutral (blue) cases.67

Figure 7 A Rate of Growth (ROG) time series is shown for the unstable (red) and neutral (blue) cases with the shaded red and blue areas denoting the standard deviation of the two cases respectively.....68

Figure 8 The solid lines represent the average plume centerline for the unstable (red) and neutral (blue) stability cases. The shaded areas represent the standard deviations for the unstable (red dots) and neutral (blue lines) cases. The gray dashed lines denote the top and bottom of the thermal inversion at 1.3km and 0.5 km AGL respectively. The bottom gray dashed line is also defined as the top of the CBL.....69

Chapter 4

Figure 1 Model domain locations for the domains 1-4 (D1-D4) were centered over southern California. The Witch Fire (WF) and Guejito Fire (GF) locations are shown on the D4 inset at left.....83

Figure 2 Column vertical profiles of PM are shown for 1.1 (black dash), 5.0 (red), 8.0 (blue), 12.0 (green), and 16.5 (grey dots) km downwind from the fire.84

Figure 3 The rows of this panel, from left to right, represent the 6-hr averaged plume height (1), the 6-hr standard deviation of the plume height (2), and a single instance 3 hours into the 6-hr time frame (3). The rows depict three time frames, the first night (A), daytime (B), and the second night (C) during the simulation. The fire area, at the end of each time period, is shown as a black outline in each plot. The domain is 62.5 x 52.5 km.87

Figure 4 The panel depicts 6-hr averaged vertical profiles (black dashed line) of temperature (1) and wind speed (2) for first nighttime period (A), the daytime (B), and the following nighttime (C) during the simulation. The shaded areas represent the standard deviation of the 6-hr average for temperature (blue) and wind speed (orange).....89

Figure 5 Example of vertical column PM concentration profiles that shows a double peak.92

Figure 6 Panel A is a 6-hr averaged plume rise using a 20 $\mu\text{g m}^{-3}$ filter on the PM data. Panel B is the same 6-hr time period with a 10 $\mu\text{g m}^{-3}$ filter on the PM data.....93

LIST OF TABLES

Chapter 3

Table 1. Background concentrations of the measured trace gasses and particulates for burn 1 and burn 2.29

Table 2 The average and standard deviation of MCE and emissions factors (g kg^{-1}) are separated by flaming and smoldering combustion for both burn 1 (top) and burn 2 (bottom). The sample size (#) of each calculation is included.38

Table 3 Whole-event averages and standard deviations for MCE and trace-gas emission factors [g/kg dry fuel] are listed for both burns.47

Chapter 4

Table 1 The eight unique median plume height measures, taken using MISR retrievals during the same time period as our simulations, give estimates of the average plume height occurring in the vicinity of the Witch and Guejito fires.90

DEDICATION

To my family

ATTRIBUTION

The research presented in this dissertation is a collection of one field study and two modeling studies: emissions measurements from a southeastern longleaf pine understory prescribed burn (Chapter 2), sensitivity analysis of a coupled fire-atmosphere model to changes in stability (Chapter 3), and development of a center-of-mass plume analysis tool for use with coupled fire-atmosphere models. Kara Yedinak is the primary author for each of these manuscripts. However, the results presented in this dissertation represent efforts and contributions from many collaborators.

Data from chapter 2 would not have been possible without the guidance of Dr. Tara Strand (SCION) who graciously and quickly brought me up to speed on this study. Her help in forming the goals and layout of this work were instrumental in pulling this study together. Dr. Brian Lamb (Washington State University) also gave a tremendous amount of time and input in educating on the nuances of field data and interpretation of the results presented here. There was also a large body of graduate students and technicians from Washington State University whose hard work and expertise went into collecting the data presented here. The funding of this project was provided by a Joint Fire Science Program (JFSP) grant 09-1-04-2.

Development of chapter 3 would not have been possible without the help of Dr. Janice Coen (NCAR). Dr. Coen made it possible for me to visit NCAR on a three month fellowship where I received help and insight from her as well as many of the students and scientists there. Dr. Adam Kochanski (University of Utah) provided critical advice on modeling techniques specific to WRF-Fire. Dr. Brian Lamb (Washington State University) was instrumental and his continued efforts and reframing of the research

objectives as well as contributing his expertise in evaluating modeled results. Dr. Steve Edburg (Washington State University) was incredibly helpful in educating us on the nuances of Large Eddy Simulation as well as critical thinking regarding data interpretation and manuscript editing.

Chapter 4 was developed out of conversations with Dr. Steve Edburg and Dr. Brian Lamb (Washington State University) to support an ongoing project funded by a NASA grant (11-FIRES11-0003). This work would not have been possible without access to WRF-Fire simulations run by Dr. Adam Kochanski (University of Utah).

It becomes difficult to determine where one person's ideas end and another's begin, however, this entire body of work would not have been possible without the guidance, mentoring, and open sharing of ideas from Dr. Brian Lamb (Washington State University).

CHAPTER 1: INTRODUCTION AND LITERATURE REVIEW

1.1. OVERVIEW

Smoke production from wildland fires impacts local and regional air quality through increases in air pollutants and reduction in visibility (Urbanski 2013). There is ongoing work to characterize the chemical makeup (Yokelson et al., 2013; Akagi et al., 2011; Urbanski 2013; Burling et al., 2011) and physical transport variables (Goodrick et al., 2013; Jain et al., 2007; Trentmann et al., 2002) needed to better characterize smoke plumes in air quality models.

Recent characterization of the pollutant emissions from fires has largely focused on measurement and compilation of species-specific emission factors (Yokelson et al. 1999; Yokelson et al. 2007; Akagi et al. 2012), including how fuel type affects specific emission factors from flaming combustion. Characterization of these emission factors from smoldering combustion is less well understood. Likewise, there is little work published on how emissions change during the course of a burn and with changes in the modified combustion efficiency (a measure of the combustion characteristics of the fire).

Smoke plume dynamics are largely non-linear due to the non-linear characteristics of the atmosphere (Potter 2012a). This non-linearity influences both the fire behavior and plume rise, making smoke plumes difficult to model. Potter's (2012a) definition of fire behavior is used here: “the manner in which fire reacts to the influences of fuel, weather, and topography.” For the purposes of this work, a plume is defined as the wildland fire produced emissions injected into the atmosphere and plume dynamics are

defined as the plume rise, and plume dispersion measures. Common practice has been to use basic environmental variables such as the fire area and heat flux, as well as knowledge of the general dispersion of the atmosphere to develop estimates of total plume rise (Goodrick et al., 2013). Because fire behavior and atmospheric dynamics have largely been treated as separate entities, little is known about the influence their natural coupling has on both plume rise and fire behavior.

Plume rise and fire behavior are largely evaluated through the use of satellite tools such as MISR or through model-to-receptor comparisons. Due to the nature of these evaluation techniques, the vertical distribution of plumes is still largely unknown, often resulting in arbitrary partitioning of the emissions into different model layers (Pharo et al., 1976) or use of Gaussian distributions (VSMOKE: (Lavdas 1996) and SASEM: (Arizona Department of Environmental Quality 2003)). Likewise, the resolution from satellite observations of fire growth is extremely coarse in space and time, and at times non-existent. More detailed descriptions of fire growth can be obtained on a daily basis through wildland firefighter ground crews. This information is not often well correlated in time and space and thus detailed information regarding high-resolution fire behavior is, at best, difficult to obtain. There is much still to be learned about the interactions between wildland fires and the atmosphere.

1.2. GOAL AND OBJECTIVES

A better understanding of the plume dynamics from wildland fires will require further study of the coupled fire-atmosphere system. Knowing how these two seemingly separate systems interact will improve our understanding of the energy exchange between the two systems. Likewise, wildland fire plume chemistry is not wholly detached from

its source and a better understanding of the links between combustion efficiency, fuels, and meteorology is needed to better characterize emissions. The overall goal of this total work is to better characterize smoke plume dynamics and emissions through a combination of field measurements and modeling.

The goal of this work is focused in on three separate areas: (1) Investigation of the variability of emission factors from prescribed burns in the southeastern United States (US); (2) use of a coupled fire-atmosphere large eddy simulation (LES) model to investigate the sensitivity of plume rise and fire behavior to atmospheric stability; and (3) development of an analysis technique for evaluating plume rise simulated with a coupled fire-atmosphere model for improvement of wildland fire treatment within regional air quality models.

This dissertation is divided into five chapters. Chapter 1 gives an overview of current understanding in wildland fire emissions and plume dynamics. Chapter 2 investigates the variability of emission factors in a longleaf pine forest based on measurements collected on a tall tower located next to and within prescribed burn units. Chapter 3 describes a sensitivity analysis of the WRF-Fire coupled fire-atmosphere model applied in LES mode for an ideal grass fire, and Chapter 4 applies a plume rise analysis tool to a large historical fire in California simulated with the WRF-Sfire model. Chapter 5 pulls together the conclusions of this dissertation and offers up directions for future work.

1.3. BACKGROUND

1.3.1. Modeling wildland fire production of particulates and traces gases

The development of emission factors (EF), as a way to report wildland fire emissions, has been a boon for air quality modeling. The concept behind an EF is that the amount of pollutant released in the combustion process is normalized to the amount of fuel consumed during combustion. A carbon mass balance approach (Yokelson et al., 1999) is used along with the assumption that half of the mass in the dry fuel is made up of carbon (Burling et al., 2010). Thus, by accounting for the major pollutant carbon sinks (mainly CO, CO₂, CH₄, and particulate matter), one can estimate the total carbon contained in the original fuel to within 5% (Yokelson et al., 2007). An example EF calculation is as follows:

$$EF_x = F_c (g_c g_{Fuel}^{-1}) \times 1000 (gkg^{-1}) \times \frac{\Delta X}{\Delta C_{CO_2} + \Delta C_{CO} + \Delta C_{CH_4}} \quad (1)$$

Where F_C is the mass fraction of carbon in the dry biomass (assumed to be 0.5), ΔX is the measured excess concentration of a species of interest, and the denominator of Equation 1 is the sum of the measured excess carbon concentrations in the main products of combustion. The chemical composition of the smoke plume is also related to the combustion dynamics of the fire of origin. In the early 1990s, Ward and Hardy (1991) developed a measure of the combustion dynamics of the fire, termed combustion efficiency (η) which related actual heat released to the potential heat released by a fire. This was approximated through the known carbon containing emissions for fires (Equation 2).

$$\eta = \frac{C_{CO_2}}{C_{CO_2} + C_{CO} + C_{HC} + C_{PM}} \quad (2)$$

The accounting of the carbon species CO, CO₂, particulate matter (PM), and all hydrocarbons (HC) was needed to calculate the total carbon consumed in the combustion process. Thus, Ward and Radke (1993) proposed a simpler approximation, called modified combustion efficiency (MCE), that only required knowledge of the emissions of CO and CO₂:

$$MCE = \hat{\eta} = \frac{\Delta CO_2}{\Delta CO_2 + \Delta CO} \quad (3)$$

Ward and Radke (1993) were able to show that this new metric agreed fairly well with the more intensive combustion efficiency calculation. Since that time, MCE and EFs have become used in tandem, allowing for the separation of emissions based on the calculated MCE threshold of 0.90 (Akagi et al., 2011) to separate flaming and smoldering combustion emissions. Despite having these tools available to better estimate emissions, little is still known about emissions specific to smoldering combustion (Burling et al., 2011; Akagi et al., 2013; Bertschi et al., 2003). Similarly, it has not yet been well quantified how moisture of the combusting vegetation influences EFs or MCE.

1.3.2. The influence of atmospheric stability on wildland fire plume dynamics

Anecdotal knowledge of the atmosphere's role in influencing wildland fire behavior, and how this relates back to wildland fire emission and plume rise, has been passed on since fire behavior first became an object of scientific study at the beginning of the 20th century. However, it was not until 1941 that scientific study of the larger role that the atmosphere plays in dynamically influencing fire behavior took shape. Likewise, the energetic exchange between the upper atmosphere and fire behavior was limited until

World War II, when instrumentation necessary to make these measurements became available (Potter 2012a). Hayes (1941) is thought to be the first fire-weather scientist to consider how vertical profiles of temperature influence fire. Eight years later, Crosby (1949) hypothesized a relationship between atmospheric stability and fire behavior. Hayes (1941) and Crosby (1949) only used surface observation to study fires; a rigorous approach using fluid dynamics was not made until the mid 1950's when Reifsnyder (1954) showed how atmospheric stability related to the extent of economic damages due to fires. He found that although there was not a strong correlation between stability measures and fire behavior, the most devastating fires occurred during unstable atmospheric conditions. During the 1960s and 70s, several data sets of vertical wind speed and temperature profiles were collected during fires and used to relate stability to fire behavior (Potter 2012a). In the late 80s, Dr. Donald Haines developed the still used Haines Index (Haines 1988) which relates measures of upper atmosphere moisture and stability that is commonly associated with fire behavior. However, this index did not fully answer the stability question and is thought to be narrow in its application given that the index was created using results from only two locations within the United States. Nelson (1993; 2003) and (Potter 2002) were among the first to attempt development of theory relating fire behavior to atmospheric stability. Following these studies, Jenkins (2004) used parcel theory to relate fire convection to atmospheric stability and vertical moisture profiles. Jenkins (2004) found that the depth of the convective boundary layer (CBL) and the presence or absence of a thermal inversion were key factors in determining plume height and maximum updraft velocity. Potter (2012a) hypothesized that the plume vertical velocities are largely influenced by atmospheric stability and that this vertical

flow in turn influences the horizontal dispersion of plumes. Potter (2012b) further stated that plume height is largely sensitive to the location of upper atmosphere stable layers. Potter (2012b) followed by saying that current understanding of stability's role in plume height determination is both important and not well understood.

The logical next step in quantifying the influence of atmospheric stability, given the large gap in observations regarding the role of stability on plume rise and fire behavior, was to couple together a fire behavior and an atmosphere model. In this way, the heat released from the fire would influence the atmospheric dynamics, which would, in turn, influence the fire behavior. However, up until the late 1990's this was not an option. The majority of wildland-fire-behavior modeling techniques assumed that either the atmosphere does not dynamically influence the fire or it is always neutral (e.g., no enhancement or suppression of vertical motion by surface heating or cooling). By coupling a fire behavior and atmosphere model, the relationships influencing these two phenomena can move from static empirical relationships to dynamic interactions. Clark et al. (1996) were among the first groups to attempt this using a three-dimensional mesoscale model and an empirical fire behavior model. Later work by Clark et al. (2004) and Coen (2005) further paved the way for coupling the Weather Research and Forecasting mesoscale model (WRF) with an empirical fire behavior model developed by Rothermel (1972). The most recent detailed description of this new coupled model hereafter referred to as WRF-Fire, can be found in Coen et al., (2013).

Fire behavior has long been treated as largely isolated from the dynamic changes present in the CBL outside of grossly averaged surface wind speeds and direction. However, the recent development of coupled fire-atmosphere models in which surface

heating due to the fires presence, diurnal evolution of the CBL, and thus changes to the vertical structure of local temperature, winds, and the resultant fire growth has allowed for testing of these traditional assumptions. Likewise, pyrogenic plume dynamics calculations were modeled as largely static events, relying solely on the previous day's estimated fire size, and energy output, but having little input available as to how the time-variable energy release of the fire interacted with the diurnal trends of the upper atmosphere. As mentioned above, plume rise is a result of complex interactions among variables including atmospheric stability, wind shear, fire heat release rate, and ambient temperature to name a few. Because of this complexity, steady state assumptions are not reasonable at the regional scale (Hardy et al. 2001) nor the local scale.

1.3.3. Regional scale representation of wildland fire plume dynamics

Smoke transport models can often be broken into three pieces: an emission source, a plume vertical profile estimate, and a plume dispersion calculation (Goodrick et al., 2013). Operational chemical transport models often incorporate wildland fire smoke emissions and do so in a number of ways, using everything from simple box models (Pharo et al., 1976), to complex puff (Scire et al., 2000) and Eulerian grid models. The pollutant vertical profile is often estimated in these models as an injection height calculated with a simple stack plume-rise algorithm or through a more complex consideration of the local stability and heat release throughout the fire. This challenge is made more complicated with the added consideration of complex terrain and the subsequent accuracy of meteorological models (Jain et al., 2007). Evaluation of these models is difficult and often requires the use of multiple pollutant receptor locations and the use of satellite imagery to infer the accuracy of these results.

1.4. SUMMARY

A general understanding of the EF from wildland fires as well as corresponding MCE has been given. Lack of a complete understanding of EFs from varying fuel moistures and from smoldering combustion has been outlined. The first study presented in this dissertation was developed to fill the gaps in our understanding of EFs as they relate to fuel moisture and smoldering combustion. A review of our current knowledge on how atmospheric stability influences fire behavior and plume dynamics was outlined. The second study in this dissertation will look into the relative sensitivity of plume rise to atmospheric stability using a coupled fire-atmosphere model. The relative influence that stability has on surface fire behavior will also be explored. The need for inclusion of wildland fire plumes in air quality models has resulted in assumptions in both the fire and atmospheric dynamics that invite large uncertainties into the modeling framework. In the fourth chapter of this dissertation, development of an analysis method for evaluating the performance of these assumptions will be outlined.

1.5. REFERENCES

- Akagi, S. K., J. S. Craven, J. W. Taylor, G. R. McMeeking, R. J. Yokelson, I. R. Burling, S. P. Urbanski, et al. 2012. “Evolution of Trace Gases and Particles Emitted by a Chaparral Fire in California.” *Atmospheric Chemistry and Physics* 12 (3): 1397–1421. doi:10.5194/acp-12-1397-2012.
- Akagi, S. K., R. J. Yokelson, I. R. Burling, S. Meinardi, I. Simpson, D. R. Blake, G. R. McMeeking, et al. 2013. “Measurements of Reactive Trace Gases and Variable O-3 Formation Rates in Some South Carolina Biomass Burning Plumes.” *Atmospheric Chemistry and Physics* 13 (3): 1141–1165. doi:10.5194/acp-13-1141-2013.
- Akagi, S. K., R. J. Yokelson, C. Wiedinmyer, M. J. Alvarado, J. S. Reid, T. Karl, J. D. Crounse, and P. O. Wennberg. 2011. “Emission Factors for Open and Domestic Biomass Burning for Use in Atmospheric Models.” *Atmospheric Chemistry and Physics* 11 (9): 4039–4072. doi:10.5194/acp-11-4039-2011.
- Andreae, Meinrat O., and P. Merlet. 2001. “Emission of Trace Gases and Aerosols from Biomass Burning.” *Global Biogeochemical Cycles* 15 (4): 955–966.
- Arizona Department of Environmental Quality. 2003. “Simple Approach Smoke Estimation Model (SASEM), Version 4.0”. Arizona Department of Environmental Quality.
<http://www.azdeq.gov/environ/air/smoke/download/sasemi.pdf>.
- Bertschi, I., R. J. Yokelson, D. E. Ward, R. E. Babbitt, R. A. Susott, J. G. Goode, and W. M. Hao. 2003. “Trace Gas and Particle Emissions from Fires in Large Diameter and Belowground Biomass Fuels.” *Journal of Geophysical Research-Atmospheres* 108 (D13) (February 15). doi:10.1029/2002JD002100.
- Breyfogle, S., and S. Ferguson. 1996. “User Assessment of Smoke-Dispersion Models for Wildland Biomass Burning”. General Technical Report PNW-GTR-379. Pacific Northwest Research Station: USDA, Forest Service.
- Bunting, S. C., B. M. Kilgore, and C. L. Bushey. 1987. *Guidelines for Prescribed Burning Sagebrush-grass Rangelands in the Northern Great Basin*.
<http://www.treearch.fs.fed.us/pubs/25027>.
- Burling, I. R., R. J. Yokelson, S. K. Akagi, S. P. Urbanski, C. E. Wold, D. W. T. Griffith, T. J. Johnson, J. Reardon, and D. R. Weise. 2011. “Airborne and Ground-based Measurements of the Trace Gases and Particles Emitted by Prescribed Fires in the United States.” *Atmospheric Chemistry and Physics* 11 (23): 12197–12216. doi:10.5194/acp-11-12197-2011.

- Burling, I. R., R. J. Yokelson, D. W. T. Griffith, T. J. Johnson, P. Veres, J. M. Roberts, C. Warneke, et al. 2010. "Laboratory Measurements of Trace Gas Emissions from Biomass Burning of Fuel Types from the Southeastern and Southwestern United States." *Atmospheric Chemistry and Physics* 10 (22): 11115–11130. doi:10.5194/acp-10-11115-2010.
- Chen, L.-W. A., P. Verburg, A. Shackelford, D. Zhu, R. Susfalk, J. C. Chow, and J. G. Watson. 2010. "Moisture Effects on Carbon and Nitrogen Emission from Burning of Wildland Biomass." *Atmos. Chem. Phys.* 10 (14) (July 20): 6617–6625. doi:10.5194/acp-10-6617-2010.
- Christian, T. J., B. Kleiss, R. J. Yokelson, R. Holzinger, P. J. Crutzen, W. M. Hao, B. H. Saharjo, and D. E. Ward. 2003. "Comprehensive Laboratory Measurements of Biomass-burning Emissions: 1. Emissions from Indonesian, African, and Other Fuels." *Journal of Geophysical Research-Atmospheres* 108 (D23) (December 4). doi:10.1029/2003JD003704.
- Clark, T. L., J. L. Coen, and D. Latham. 2004. "Description of a Coupled Atmosphere-fire Model." *International Journal of Wildland Fire* 13 (1): 49–63. doi:10.1071/WF03043.
- Clark, T. L., M. A. Jenkins, J. L. Coen, and D. R. Packham. 1996. "A Coupled Atmosphere-fire Model: Role of the Convective Froude Number and Dynamic Fingering at the Fireline." *International Journal of Wildland Fire* 6 (4) (December): 177–190. doi:10.1071/WF9960177.
- Coen, J. L. 2005. "Simulation of the Big Elk Fire Using Coupled Atmosphere-fire Modeling." *International Journal of Wildland Fire* 14 (1): 49–59. doi:10.1071/WF04047.
- Coen, J. L., M. Cameron, J. Michalakes, E. G. Patton, P. J. Riggan, and K. M. Yedinak. 2013. "WRF-Fire: Coupled Weather-Wildland Fire Modeling with the Weather Research and Forecasting Model." *Journal of Applied Meteorology and Climatology* 52 (1) (January): 16–38. doi:10.1175/JAMC-D-12-023.1.
- Crosby, JS. 1949. "Vertical Wind Currents and Fire Behavior." *Fire Control Notes* 10 (2): 12–14.
- Cunningham, Philip, and Michael J. Reeder. 2009. "Severe Convective Storms Initiated by Intense Wildfires: Numerical Simulations of Pyro-convection and Pyro-tornadogenesis." *Geophysical Research Letters* 36 (June 26). doi:10.1029/2009GL039262.
- Dennis, A., M. Fraser, S. Anderson, and D. Allen. 2002. "Air Pollutant Emissions Associated with Forest, Grassland, and Agricultural Burning in Texas." *Atmospheric Environment* 36 (23) (August): 3779–3792. doi:10.1016/S1352-2310(02)00219-4.

- Dignon, J., and J. E. Penner. 1991. In *Global Biomass Burning: Atmospheric, Climatic, and Biospheric Implications*, by Joel S. Levine. MIT Press.
- Eidsmoe, G. 2007. "Investigation Report: Guejito Fire". Investigation CA-MVU-010484. Guejito Creek drainage: California Department of Forestry and Fire Protection. http://www.fire.ca.gov/fire_protection/downloads/redsheets/CA-MVU-010484_Complete.pdf.
- Ferek, R. J., J. S. Reid, P. V. Hobbs, C. R. Blake, and C. Liou. 1998. "Emission Factors of Hydrocarbons, Halocarbons, Trace Gases and Particles from Biomass Burning in Brazil." *Journal of Geophysical Research: Atmospheres* 103 (D24): 32107–32118. doi:10.1029/98JD00692.
- Freitas, S. R., K. M. Longo, R. Chatfield, D. Latham, M. A. F. Silva Dias, M. O. Andreae, E. Prins, J. C. Santos, R. Gielow, and J. A. Carvalho Jr. 2007. "Including the Sub-grid Scale Plume Rise of Vegetation Fires in Low Resolution Atmospheric Transport Models." *Atmos. Chem. Phys.* 7 (13) (July 2): 3385–3398. doi:10.5194/acp-7-3385-2007.
- Gilbert, M. 2008. "Investigation Report: Witch Fire". Investigation 07-CDF-570. Highway 78 west of Santa Ysabel, San Diego County: California Department of Forestry and Fire Protection. http://www.fire.ca.gov/fire_protection/downloads/redsheets/CA-MVU-010432_Complete.pdf.
- Goodrick, S. L., G. L. Achtemeier, N. K. Larkin, Y. Liu, and T. M. Strand. 2013. "Modelling Smoke Transport from Wildland Fires: a Review." *International Journal of Wildland Fire* 22 (1): 83–94.
- Goodrick, Scott L., Gary L. Achtemeier, Narasimhan K. Larkin, Yongqiang Liu, and Tara M. Strand. 2013. "Modelling Smoke Transport from Wildland Fires: a Review." *International Journal of Wildland Fire* 22 (1): 83–94.
- Haines, D. A. 1988. "A Lower Atmospheric Severity Index for Wildland Fires." *National Weather Digest* 13 (2): 23–27.
- Hardy, C., R. Ottmar, J. Peterson, J. Core, and P. Seamon, ed. 2001. "Smoke Management Guide for Prescribed and Wildland Fire". National Wildfire Coordination Group. <http://www.nwcg.gov/pms/pubs/SMG/SMG-72.pdf>.
- Hayes, G. L. 1941. "Influences of Altitude and Aspect on Daily Variations in Factors of Fire Danger." *US Department of Agriculture, Circular 591* (Washington DC).
- Jain, R., J. Vaughan, K. Heitkamp, C. Ramos, C. Claiborn, M. Schreuder, M. Schaaf, and B. Lamb. 2007. "Development of the ClearSky Smoke Dispersion Forecast System for Agricultural Field Burning in the Pacific Northwest." *Atmospheric Environment* 41 (32) (October): 6745–6761. doi:10.1016/j.atmosenv.2007.04.058.

- Jenkins, M. A. 2004. "Investigating the Haines Index Using Parcel Model Theory." *International Journal of Wildland Fire* 13 (3): 297–309. doi:10.1071/WF03055.
- Jolly, W. M. 2007. "Sensitivity of a Surface Fire Spread Model and Associated Fire Behaviour Fuel Models to Changes in Live Fuel Moisture." *International Journal of Wildland Fire* 16 (4): 503–509.
- Keeley, J. E., G. H. Aplet, N. L. Christensen, S. G. Conard, E. A. Johnson, P. N. Omi, D. L. Peterson, and T. W. Swetnam. 2009. "Ecological Foundations for Fire Management in North American Forest and Shrubland Ecosystems". United States Department of Agriculture, Forest Service, Pacific Northwest Research Station, Portland, OR. <http://www.treesearch.fs.fed.us/pubs/32483>.
- Kilgore, B. M., and G. A. Curtis. 1987. *Guide to Understory Burning in Ponderosa Pine-larch-fir Forests in the Intermountain West*. <http://www.treesearch.fs.fed.us/pubs/32954>.
- Kochanski, A., M. A. Jenkins, J. Mandel, J. Beezley, and S. Krueger. 2013. "Real Time Simulation of 2007 Santa Ana Fires." *Forest Ecology and Management* 294 (April 15): 136–149. doi:10.1016/j.foreco.2012.12.014.
- Kochanski, A., M. A. Jenkins, R. Sun, S. Krueger, S. Abedi, and J. Charney. 2013. "The Importance of Low-level Environmental Vertical Wind Shear to Wildfire Propagation: Proof of Concept." *Journal of Geophysical Research: Atmospheres*: n/a–n/a. doi:10.1002/jgrd.50436.
- Lavdas, L. G. 1996. "Program VSMOKE: Users Manual". General Technical Report GTR-SRS-006. Southeastern Research Station: USDA, Forest Service.
- Lobert, J. M., D. H. Scharffe, W. Hao, T. A. Kuhlbusch, R. Seuwen, P. Warneck, and P. J. Crutzen. 1991. "Experimental Evaluation of Biomass Burning Emissions: Nitrogen and Carbon Containing Compounds." In *Global Biomass Burning*, edited by J. S. Levine, 289–304. MIT Press.
- McMeeking, Gavin R., Sonia M. Kreidenweis, Stephen Baker, Christian M. Carrico, Judith C. Chow, Jeffrey L. Collett, Wei Min Hao, et al. 2009. "Emissions of Trace Gases and Aerosols During the Open Combustion of Biomass in the Laboratory." *Journal of Geophysical Research-Atmospheres* 114 (October 14). doi:10.1029/2009JD011836.
- Naeher, Luke P, Gary L Achtemeier, Jeff S Glitzenstein, Donna R Streng, and David Macintosh. 2006. "Real-time and Time-integrated PM_{2.5} and CO from Prescribed Burns in Chipped and Non-chipped Plots: Firefighter and Community Exposure and Health Implications." *Journal of Exposure Science & Environmental Epidemiology* 16 (4) (July): 351–361. doi:10.1038/sj.jes.7500497.
- NCAR. 2012. *Weather Research and Forecasting Model* (version 3.4). http://www.mmm.ucar.edu/wrf/users/download/get_source.html.

- Nelson, R. M. 2003. "Power of the Fire - a Thermodynamic Analysis." *International Journal of Wildland Fire* 12 (1): 51–65. doi:10.1071/WF02032.
- Nelson, Rm. 1993. "Byram Derivation of the Energy Criterion for Forest and Wildland Fires." *International Journal of Wildland Fire* 3 (3) (September): 131–138. doi:10.1071/WF9930131.
- "NICC Wildland Fire Annual Report." 2012. NIFC. <http://www.predictiveservices.nifc.gov/intelligence/intelligence.htm>.
- Pharo, J. A., L. G. Lavadas, and P. M. Bailey. 1976. "Smoke Transport and Dispersion". General Technical Report SE-10. Southern Forestry Smoke Management Guidebook. Southeastern Research Station: USDA, Forest Service.
- Potter, B. E. 2002. "A Dynamics Based View of Atmosphere-fire Interactions." *International Journal of Wildland Fire* 11 (3-4): 247–255. doi:10.1071/WF02008.
- . 2012a. "Atmospheric Interactions with Wildland Fire Behaviour – I. Basic Surface Interactions, Vertical Profiles and Synoptic Structures." *International Journal of Wildland Fire* 21 (7): 779–801.
- . 2012b. "Atmospheric Interactions with Wildland Fire Behaviour – II. Plume and Vortex Dynamics." *International Journal of Wildland Fire* 21 (7): 802–817.
- Reifsnyder, W. E. 1954. "Atmospheric Stability and Forest Fire Behavior". PhD dissertation, New Haven, CT: Yale University.
- Rothermel, R. C. 1972. "A Mathematical Model for Predicting Fire Spread in Wildland Fuels." *USDA Forest Service, Intermountain Forest and Range Experiment Station, Research Paper INT-115*.
- . 1983. *How to Predict the Spread and Intensity of Forest and Range Fires*. <http://www.treesearch.fs.fed.us/pubs/24635>.
- Sandberg, David V., Roger D. Ottmar, and Janice L. Peterson. 2002. "Wildland Fire in Ecosystems: Effects of Fire on Air." <http://www.treesearch.fs.fed.us/pubs/5247>.
- Scire, J. S., D. G. Strimaitis, and R. J. Yamartino. 2000. "A User's Guide for the CALPUFF Dispersion Model (Version 5)". User's guide. Concord, MA: EarthTech Inc.
- Skamarock, W. C., J. B. Klemp, J. Dudhia, D. O. Gill, D. M. Barker, M. G. Duda, X. Huang, W. Wang, and J. G. Powers. 2008. "A Description of the Advanced Research WRF Version 3". National Center for Atmospheric Research.
- Trentmann, J., M. O. Andreae, H. F. Graf, P. V. Hobbs, R. D. Ottmar, and T. Trautmann. 2002. "Simulation of a Biomass-burning Plume: Comparison of Model Results

- with Observations.” *Journal of Geophysical Research-Atmospheres* 107 (D1-D2) (January). doi:10.1029/2001JD000410.
- Urbanski, S. P. 2013. “Combustion Efficiency and Emission Factors for Wildfire-season Fires in Mixed Conifer Forests of the Northern Rocky Mountains, US.” *Atmos. Chem. Phys.* 13 (14) (July 30): 7241–7262. doi:10.5194/acp-13-7241-2013.
- Viney, NR. 1991. “A Review of Fine Fuel Moisture Modelling.” *International Journal of Wildland Fire* 1 (4) (January 1): 215–234.
- Ward, D. E., and C. C. Hardy. 1991. “Smoke Emissions from Wildland Fires.” *Environment International* 17 (2–3): 117–134. doi:10.1016/0160-4120(91)90095-8.
- Ward, D. E., and L. F. Radke. 1993. “Emissions Measurements from Vegetation Fires: A Comparative Evaluation of Methods and Results.” In , 53–76. <http://www.treearch.fs.fed.us/pubs/40604>.
- Wiedinmyer, C., S. K. Akagi, R. J. Yokelson, L. K. Emmons, J. A. Al-Saadi, J. J. Orlando, and A. J. Soja. 2011. “The Fire INventory from NCAR (FINN): a High Resolution Global Model to Estimate the Emissions from Open Burning.” *Geoscientific Model Development* 4 (3): 625–641. doi:10.5194/gmd-4-625-2011.
- Yokelson, R. J., I. R. Burling, J. B. Gilman, C. Warneke, C. E. Stockwell, J. de Gouw, S. K. Akagi, et al. 2013. “Coupling Field and Laboratory Measurements to Estimate the Emission Factors of Identified and Unidentified Trace Gases for Prescribed Fires.” *Atmospheric Chemistry and Physics* 13 (1): 89–116. doi:10.5194/acp-13-89-2013.
- Yokelson, R. J., J. G. Goode, D. E. Ward, R. A. Susott, R. E. Babbitt, D. D. Wade, I. Bertschi, D. W. T. Griffith, and W. M. Hao. 1999. “Emissions of Formaldehyde, Acetic Acid, Methanol, and Other Trace Gases from Biomass Fires in North Carolina Measured by Airborne Fourier Transform Infrared Spectroscopy.” *Journal of Geophysical Research: Atmospheres* 104 (D23): 30109–30125. doi:10.1029/1999JD900817.
- Yokelson, R. J., D. W. T. Griffith, and D. E. Ward. 1996. “Open-path Fourier Transform Infrared Studies of Large-scale Laboratory Biomass Fires.” *Journal of Geophysical Research-Atmospheres* 101 (D15) (September 20): 21067–21080. doi:10.1029/96JD01800.
- Yokelson, R. J., R. Susott, D. E. Ward, J. Reardon, and D. W. T. Griffith. 1997. “Emissions from Smoldering Combustion of Biomass Measured by Open-path Fourier Transform Infrared Spectroscopy.” *Journal of Geophysical Research-Atmospheres* 102 (D15) (August 20): 18865–18877. doi:10.1029/97JD00852.

Yokelson, R. J., S. P. Urbanski, E. L. Atlas, D. W. Toohy, E. C. Alvarado, J. D. Crouse, P. O. Wennberg, et al. 2007. "Emissions from Forest Fires Near Mexico City." *Atmospheric Chemistry and Physics* 7 (21): 5569–5584.

CHAPTER 2: POLLUTANT EMISSIONS FROM LOW INTENSITY PINE FOREST PRESCRIBED BURNS

2.1. ABSTRACT

Prescribed wildland fires are often used to improve ecosystem health and to minimize fuels to lower the potential for catastrophic wildfires. Emissions of pollutants from prescribed fires contribute to local and regional air quality issues and health impacts. Emissions of fine particulate matter (PM_{2.5}), CO, CO₂, CH₄, volatile organic compounds and nitrogen oxides (NO_x = NO + NO₂) are important pollutants associated with emissions from wildland fires. There remain large uncertainties in the actual emission rates of these pollutants for prescribed fires, particularly during smoldering combustion. The emission rate of any pollutant depends on the emission factors of the pollutant, fuel consumption per area burned and the total area burned. In this work, an instrumented tower was deployed within and immediately next to prescribed burns of longleaf pine litter and wiregrass in the Sandhill region, North Carolina. The purpose of the tower was to capture high time-resolution field observations of pollutant concentrations and derived emission factors from prescribed fires for these units including: particulate matter, black carbon, CO₂, CO, CH₄, NO_x, and NH₃. Additionally, we use modified combustion efficiency from the moment of ignition until the end of smoldering combustion to separate flaming from smoldering emissions. The emissions factors generally agreed well with similar work except for those of PM_{2.5} which were five times higher than previously reported. There was measurable variability between the emission factors of the two burns. By separately analyzing flaming and smoldering combustion, as well as

taking into account the differences in dead fuel moisture, live to dead fuel ratios, and small differences in surface meteorology, we develop a hypothesis for the sources of this variability.

2.2. INTRODUCTION

Wildland fires are globally the second largest contributors of total trace gases and the single largest source of fine carbonaceous particles in the troposphere (Akagi et al., 2011). The contribution by wildfires to the global and regional concentrations of CO, CO₂, CH₄ and particulate matter (PM), have generally been characterized based on season and geographic location (Wiedinmyer et al., 2011; Andreae and Merlet 2001). Prescribed fire, the use of fire to manage forest resources, reduce fire risk, and restore and maintain ecological health, contributes to this global and regional accumulation of trace gasses. Significant work has been done to characterize the contribution of non-methane organic compounds (NMOC) specific to prescribed burning in chaparral and oak savanna in the Southern United States (Yokelson et al., 2013). Little is known about the relative contribution of smoldering combustion during the prescription and smoldering combustion after the prescription ends (Burling et al., 2011; Bertschi et al., 2003). In the southeastern longleaf pine forests, prescribed fires are employed on intervals of 3-10 years in order to maintain high herb diversity and reduce the occurrence of high intensity fires (Keeley et al., 2009). In this region of the United States (US), prescribed burns made up 22 and 65% of the total area burned in 2011 and 2012, respectively (“NICC Wildland Fire Annual Report” 2012).

It has become common practice to report trace-gas and particle emissions from wildland fires in the form of emission factors (EF) (Urbanski 2013; Burling et al., 2011;

Yokelson et al., 2013; Akagi et al., 2013). Calculations of EF are computed using a carbon mass balance method to quantify trace-gas and particulate emissions per unit of dry vegetation consumed (Yokelson et al., 1999). Several studies (Burling et al., 2010; Burling et al., 2011; Christian et al., 2003; McMeeking et al., 2009; Yokelson et al., 1997) have found a strong correlation between EF and modified combustion efficiency (MCE) the relative combustion efficiency of the wildland fire, for many species. This is due to the relative availability of energy during the combustion process and resultant level of oxidation of the combustion cellulose byproducts. Because EF calculations link the trace-gas emissions to the amount of dry fuel consumed, they are useful inputs for modeling wildland fire emissions as only the location of the fire, the potential type of combustions (flaming vs. smoldering) and the amount and type of fuel is needed to determine emission rates. Literature on the relative influence of fuel moisture on the partitioning between flaming and smoldering combustion has emerged recently, shedding some light on fuel moisture role in influencing EFs. McMeeking et al. (2009) found MCE was inversely proportional to dead fuel moisture content. More recently, Chen et al. (2010) discovered that the EFs of NH₃ and CO increased with increasing dead fuel moisture content. Despite these initial insights into the effect of fuel moisture little is still understood about the sensitivity of these EFs to changes in fuel moisture (both live and dead).

Despite ever improving knowledge regarding EFs, the emission rate specific to smoldering combustion (Burling et al., 2011) as well as the influence that small differences in fuel moisture, surface wind speed, and the live to dead fuel ratios have on EFs is still not well characterized. The difficulty in obtaining this information has to do

with the difficulty in estimating the rate in fuel consumed per unit area, the total area burning at any given moment, as well as the influence of wind speed on combustion efficiency. Additionally, the spatial distribution of live fuels can be a difficult metric to determine and little is still known about the relative influencing of live fuels on combustion efficiency. Our study addresses these difficulty by using prescribed burn environments to better understand how the fire emissions factors (EF), are related to the modified combustion efficiency (MCE) of the fire. We further enrich this information from two research burns which shared the same surface fuel type, canopy cover, and similar surface meteorology by collecting near-source and in-source data for particulate, and trace gas emissions.

2.3. METHODS

The prescribed burns presented in this study occurred on February 16th, 2011 (units 18 and 19) and March 12th, 2011 (unit 27) in the Nature Conservancy's Calloway Forest, located in the Sandhills near Southern Pines, North Carolina (Figure 1).

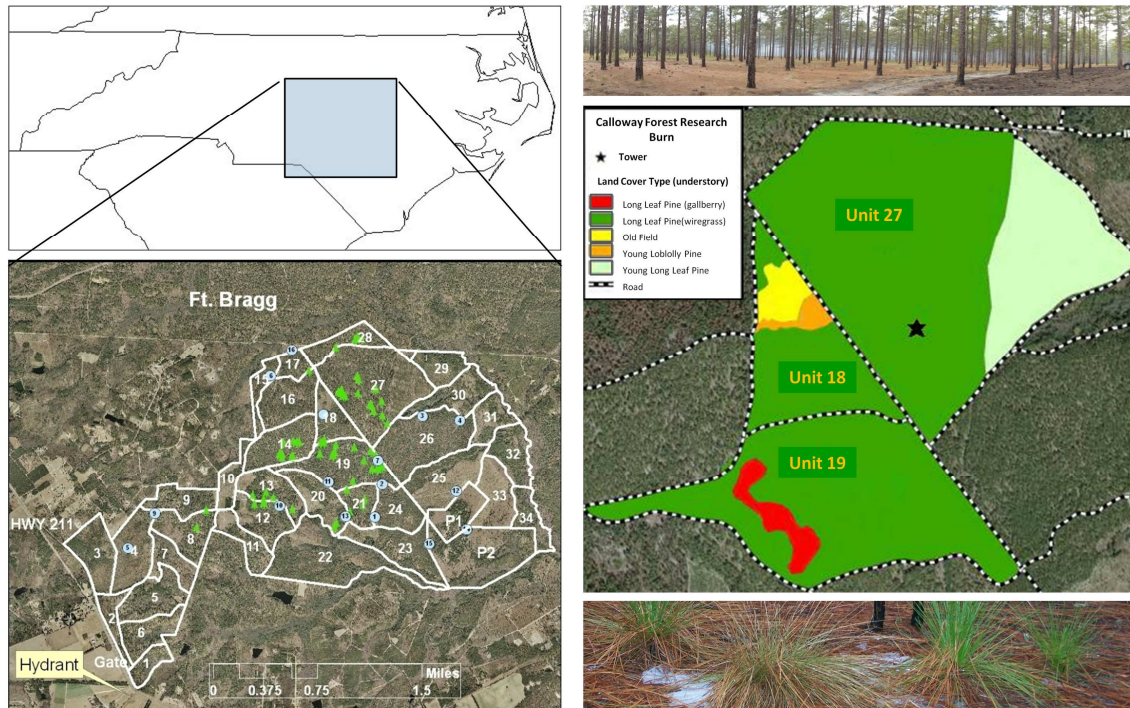


Figure 1 Counterclockwise from the top left corner, the blue square denotes the region of North Carolina, near Fort Bragg (lower left) where multiple prescribed burn (white outline) took place. Wire grass and longleaf pine litter (lower right) were the dominant surface fuels in the two burn units sampled in this study (bright green - middle right panel) of this study. The canopy fuels (not burned) are shown in the upper right corner and consisted predominantly of longleaf pine.

The prescribed burns were conducted by the North Carolina Chapter of The Nature Conservancy (TNC), who manages the land to return it back to full ecosystem health. Surface fuel type between the burn units did not vary greatly. Longleaf pine (*Pinus palustris* Mill.) needles and wiregrass (*Aristida beyrichiana* Trin. & Rupr.) were the dominant fuel types intermixed with turkey oak (*Quercus laevis* Walter).

2.3.1. Tower Instrumentation

A 30.5 m tower, operated by Washington State University (WSU), was instrumented with trace gas analysis equipment. Above canopy (25.6 m AGL), CO₂/H₂O

concentrations were captured at 10 Hz with an open path infrared gas analyzer (LI -7500, LI-COR, Lincoln, Nebraska). Also at this level was an inlet for a N₂O/CO analyzer (N₂O/CO-23d, Los Gatos Research, Mountain View, California) sampling at 10 Hz, an ammonia analyzer (G1103, Picarro, Sunnyvale, California) sampling at 3Hz, and a CH₄/CO₂ analyzer (G2301, Picarro, Sunnyvale, California) sampling at 10 Hz. Campbell (CSAT3, Campbell Scientific, Logan, Utah) and ATI (SATI-3S, Applied Technologies Inc., Longmont, Colorado) sonic anemometers, sampling at 10 Hz, were mounted at 4 levels on the tower (25.6, 19.7, 7.6, and 2.7 m AGL). An aspirated temperature profile was acquired from measurements taken at 8 levels along the tower (25.4, 19.3, 17.3, 13.3, 9.7, 7.2, 5.2, and 2.2 m AGL). At the base of the tower (2.9 m AGL), NO_x and NO concentrations (42, Thermo Environmental Instruments Inc. (TECO) Franklin, Massachusetts) as well as particulate black carbon (BC) (Aethelometer, AE-16, Magee Scientific, Berkeley, California) were monitored. Fine particulate matter (mean diameter ≤ 2.5 microns, PM_{2.5}) data were collected at approximately 2 m AGL (Environmental Beta-Attenuation Monitor, Met One Instruments, Grants Pass, Oregon). Particle bound polycyclic aromatic hydrocarbons (PAH) concentrations (PAS 2000CE, EcoChem Analytics, League City, Texas), sampled every 10 seconds, were taken 3 m AGL.

2.3.2. Unit 18 and 19

Units 18 and 19 had a combined area of 71 ha, mainly composed of longleaf pine with patches of turkey oak, gallberry (*Ilex coriacea* (Pursh) Chapm.) bushes, and young loblolly pine (*Pinus taeda* L.). The WSU tower was located approximately 500 m from the downwind edge of the burn unit. Figure 2 shows the array of the instruments for the first research burn on units 18 and 19. The ignition of this burn (hereafter referred to as

burn 1) occurred on February 16th, 2011 at 11:00 AM and lasted for 6 hours, ending at 5:00 PM when flaming combustion ceased. Trace gas sampling continued until 7:00 PM. Pre-burn and post-burn fuel loadings of 1-hr fuels were 8294 kg/ha and 1928 kg/ha, respectively. The average rate of spread was 0.14 m/s with a maximum flame height of 1.8 m; these were determined from video analyses using marked poles at 4 m intervals in one area of the burn. The fuel moisture content for 1-hr fuels was 35%. Skies were clear, the temperature ranged from 6 °C to 18 °C, and wind speeds varied between 1 and 3 m/s with flow from the south and southwest.

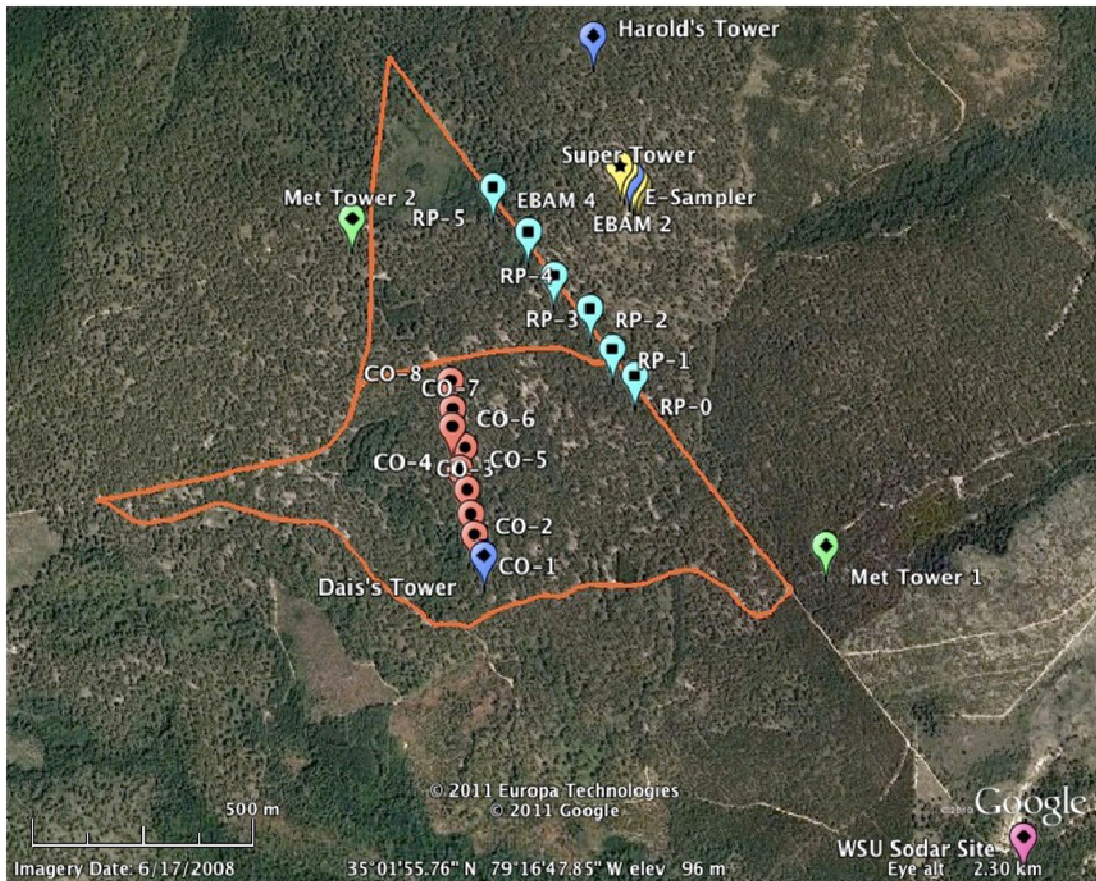


Figure 2 Burn units 18 and 19 (outlined in orange) are pictured here with the full suite of campaign instruments shown. The WSU tower is labeled “Super Tower” and denoted by a yellow marker in the upper right of the image.

2.3.3. Unit 27

Unit 27 had a total area of 91 ha. The WSU tower was located inside this burn unit, 500 m from the southwest edge of the unit (Figure 3). Several days prior to the burn, TNC fire crews blackened an area surrounding the tower. The ignition of this burn (hereafter referred to as burn 2) was on March 12th, 2001 at 11:10 AM and lasted for 4 hours ending at 3:00 PM when flaming combustion ceased. Trace gas sampling continued until midnight. Pre-burn and post-burn fuel loadings of 1-hr fuels were 13,019 kg/ha and 1927 kg/ha, respectively. This burn had a higher initial fuel loading by 1300 kg/ha as compared to burn 1. Burn 1 consumed 6400 kg/ha while burn 2 consumed 6200 kg/ha. The average rate of spread was 0.37 m/s with a maximum flame height of 1.5 m. The fuel moisture content for 1-hr fuels was 28%. Skies were clear, the temperature ranged from 10 °C to 19 °C, and wind speeds varied from 1 to 6 m/s with flow from the south and southeast.

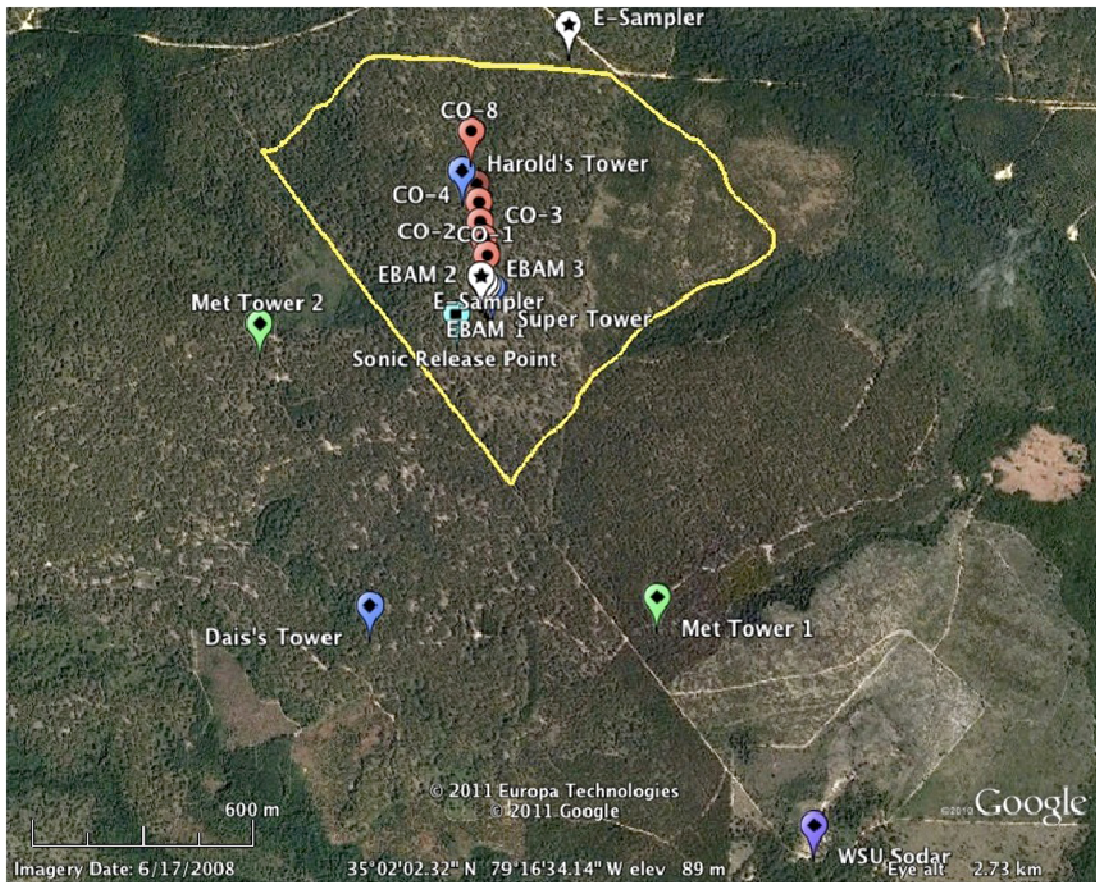


Figure 3. Unit 27 (outlined in yellow) is shown with the WSU tower (labeled “Super Tower”) in the southern quadrant.

2.4. ANALYSIS AND RESULTS

2.4.1. Meteorological Conditions

Surface temperatures varied between ~6 and 18 °C during burn 1 and were warmer by 4-6 °C during burn 2, while above canopy temperatures were similar for both burns (Figure 4).

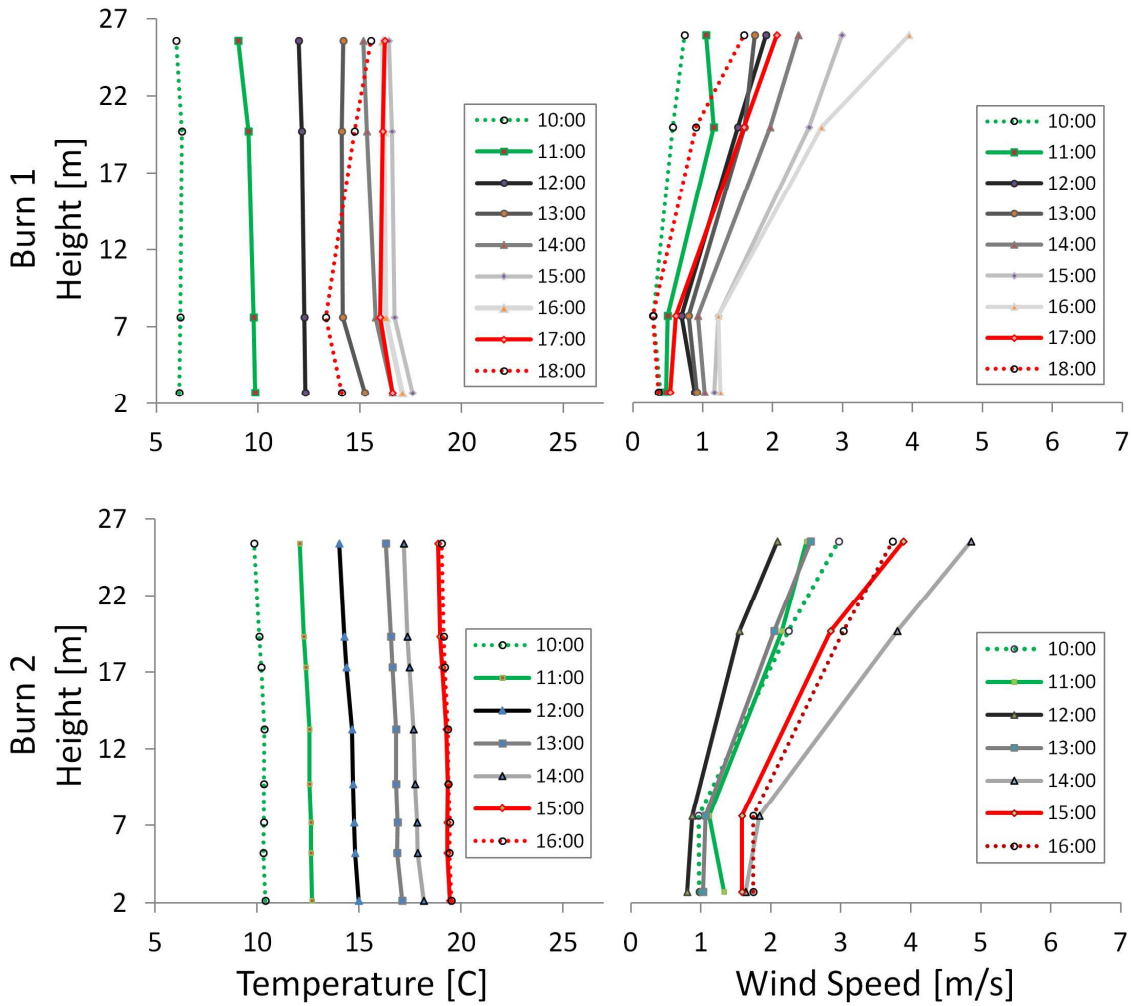


Figure 4 Vertical temperature (left) and wind speed (right) profiles for burns 1 (top) and 2 (bottom) shows an overall increase in magnitude.

The vertical profiles of wind speed were similar for both burns with burn 2 exhibiting slightly stronger afternoon gradients than burn 1. The surface wind speeds from burn 1 were on average 0.8 – 2.0 m/s slower than burn 2. The average above canopy wind speeds for both burns were comparable at roughly 2.8 m/s (Figure 5).

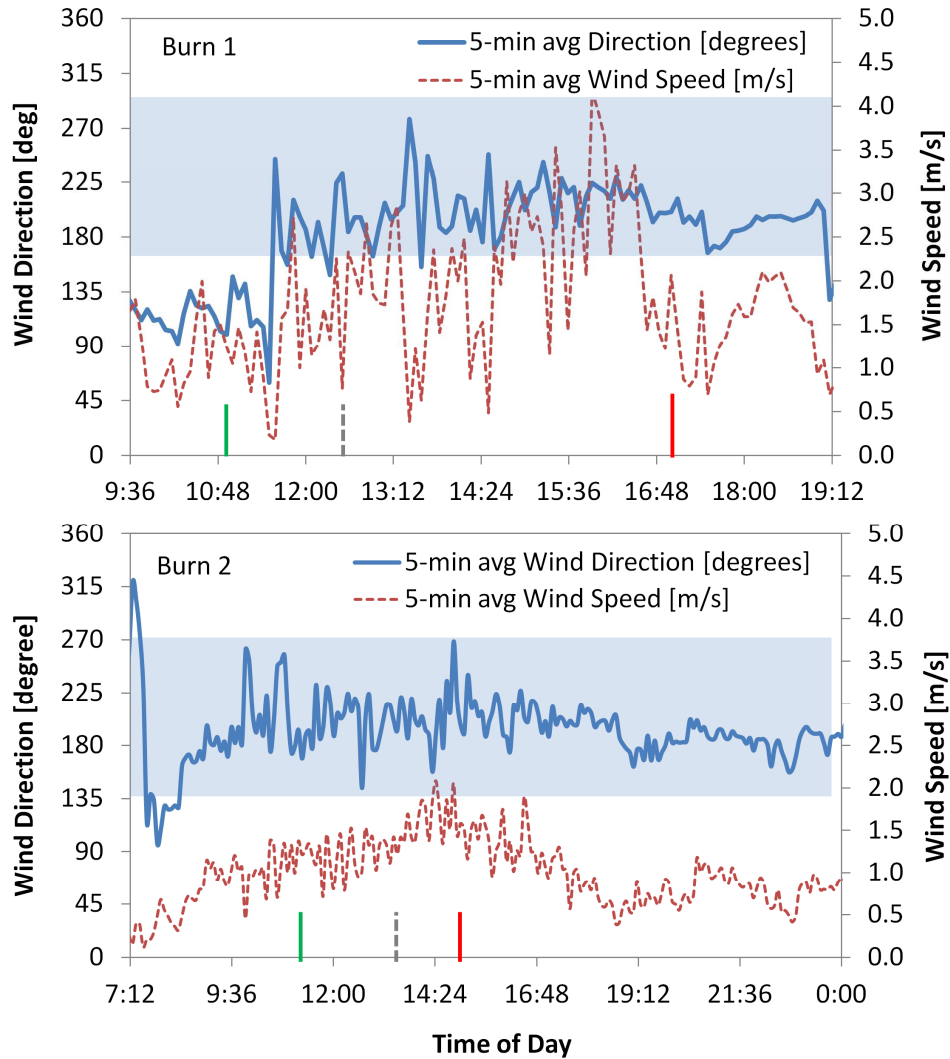


Figure 5 Wind speed and direction at the top of the canopy (25.7m AGL) for burn 1 (top) and burn 2 (bottom) were roughly constant for the duration of the prescription. The green and red bars denote the start and stop of the prescribed burn, while the grey dashed bar indicates the first smoke plume impact on the tower. The blue shaded area marks the range in wind direction that resulted in impact of the smoke plume on the tower.

Burn 1 showed more variability in wind speed at 1.0 m/s about the mean, compared to 0.25 m/s about the mean for burn 2. Burn 1 had wider variability in wind direction as well with winds generally originating out of the south but varying by 100 degrees. Burn

2 had a very steady wind direction out of the south at 180 degrees with only 25 degrees of variability.

2.4.2. Chemical Measurements

For the purpose of identifying emissions specifically from the combustion process, we were interested in the excess concentrations of a given species. The excess concentration ΔX of a species of interest X , were defined as $\Delta X = X_{\text{sample}} - X_{\text{background}}$. Background concentrations were identified as the minimum concentration at the start of the burning process. Thus, each species measured in each burn had its own background concentration (Table 1). Due to the sensitivity of the presented measurements, soil respiration was an observable phenomenon in the burn 1 CO_2 data and thus a diurnal trend of this process was estimated and used to represent the background concentration of CO_2 . This trend was not observed prior to burn 2.

Table 1. Background concentrations of the measured trace gasses and particulates for burn 1 and burn 2.

	Burn 1	Burn 2
	mg m⁻³	mg m⁻³
CO₂	$(-0.03)x + 686$	688
CO	0.14	0.17
CH₄	1.2	1.2
NO_x	0.004	0.002
BC	0	N/A
PAH	1.1E-05	4.0E-08
NO	5.9E-06	2.4E-06
PM 2.5	0.001	0.001
NH₃	0.005	0.002

Excess CO₂ concentrations were found to peak at concentrations more than 10 times greater in burn 2 (Figure 7) as compared to burn 1 (Figure 6).

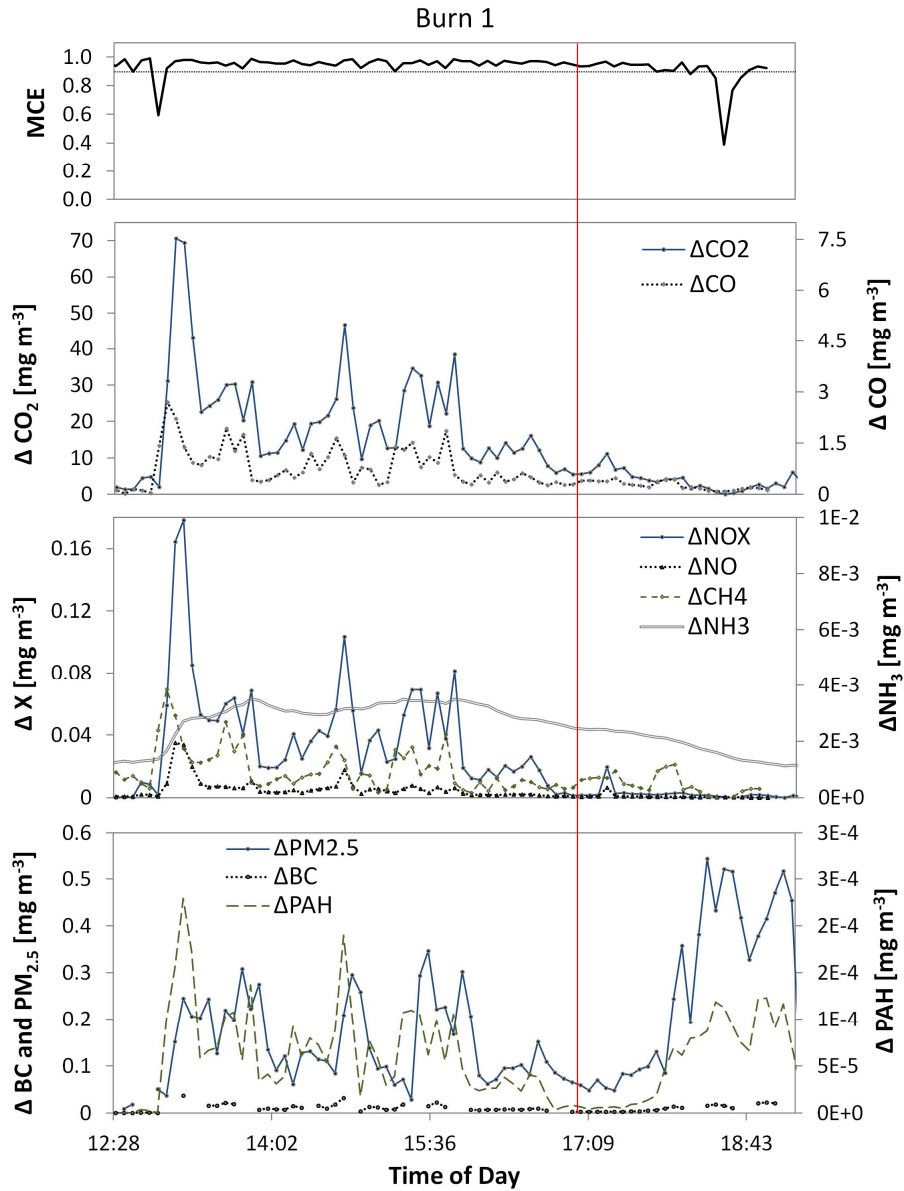


Figure 6 The 5-minute averaged time series of MCE and excess concentrations of CO, CO₂, NO_x, NO, CH₄, NH₃, PM_{2.5}, PAH, and BC (where applicable) are shown for burn 1. The time series starts when the smoke plume first encounters the tower and the red vertical line denotes the end of the prescribed burn.

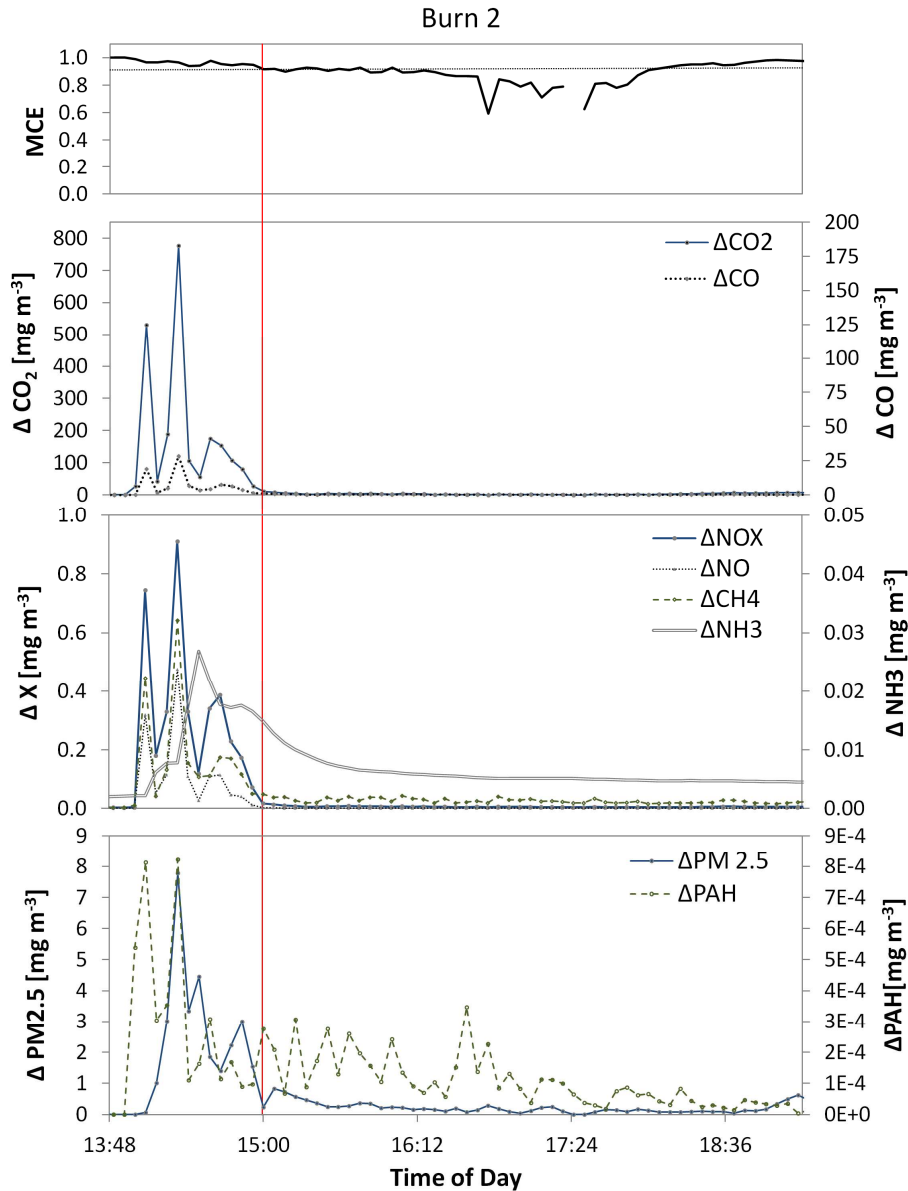


Figure 7 The excess concentrations for burn 2 were higher due to the in-source location of the sampling tower. The vertical red line denotes the end of the burn.

Concentrations of CO were 8 times higher in burn 2 as compared to burn 1. NO_x was elevated during the prescribed burn for both burn 1 and 2, but was 5 times higher in burn 2. Particulate matter appeared to peak during the prescribed burn for burn 2 but did not exhibit the same behavior in burn 1. Excess concentrations of NH₃ were almost 500 times higher in burn 2 as compared to burn 1. These higher concentrations in burn 2 as

compared to burn 1 simply reflect the proximity of the tower within the burn for burn 2 as opposed to downwind of the burn in burn 1.

The concentrations of CO₂, NO_x, and CH₄ demonstrated a higher correlation to CO during burn 2 compared to burn 1 (Figure 8). The CO to CO₂ correlation during burn 2 was R^2 of 0.99 and during burn 1 it was 0.51. In part, this may be due to the fact that the tower was downwind of the burn in the first burn and within the burn during the second case.

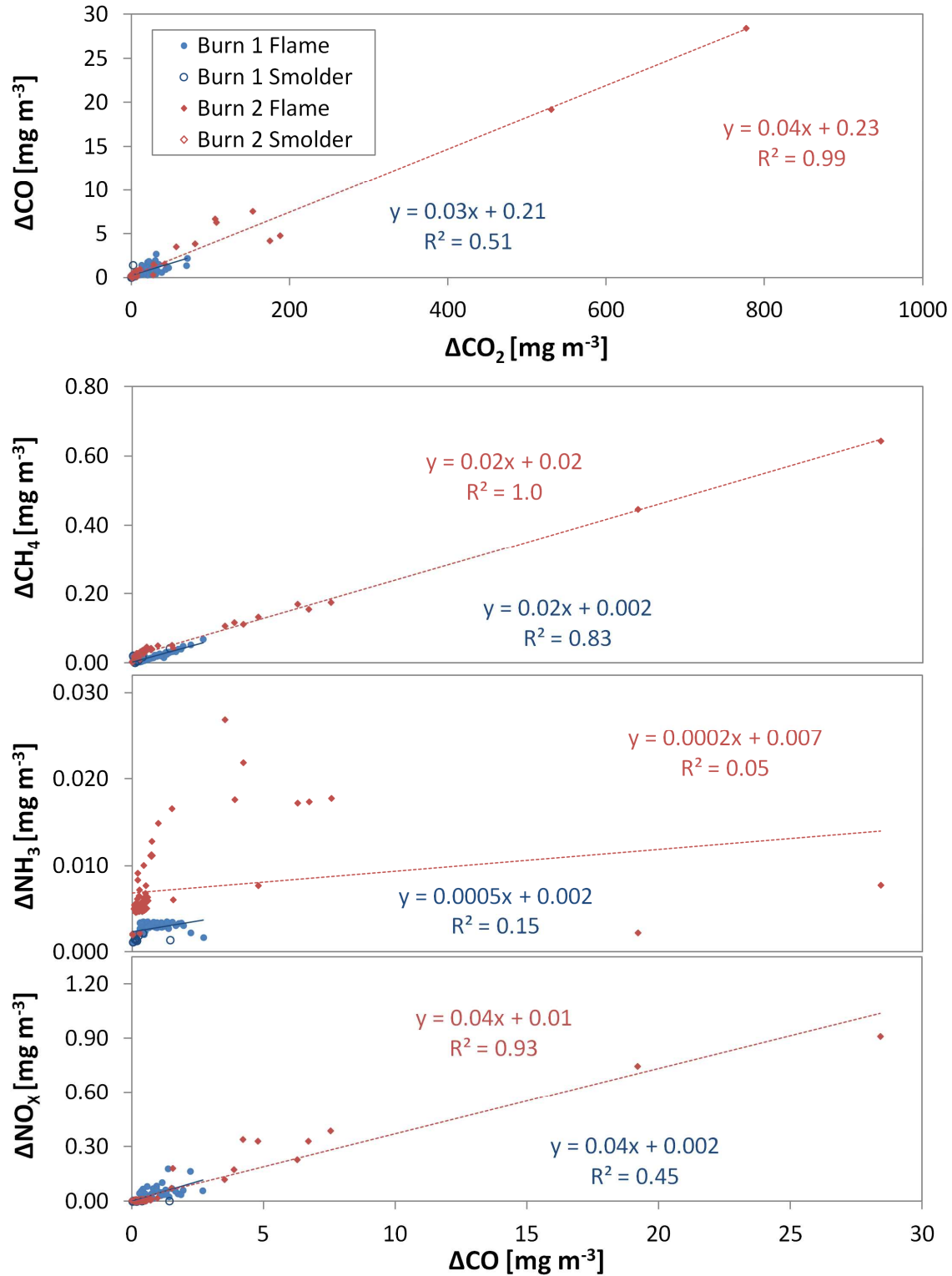


Figure 8 From top to bottom, excess concentrations of CO, CH₄, NH₃, and NO_x are plotted against CO₂ and CO for burns 1 (blue) and 2 (red). Trend lines and regression equations are shown for only flaming combustion.

Similarly, NO_x and CH₄ had R^2 values of 0.45 and 0.83, respectively, for burn 1 and 0.93 and 1.0, respectively, for burn 2. Concentrations of NH₃ showed little to no correlation with CO during the flaming period of either burn. This lack of correlation is not surprising given that NH₃ is more often an indicator of the amount of nitrogen in the vegetation and in previous studies has been found to correlate well with smoldering combustion (Dennis et al. 2002).

In order to relate excess concentrations to flaming and smoldering combustion we employed the MCE calculation (Ward and Radke 1993). MCE is the ratio of excess CO₂ to the sum of excess CO₂ and CO (as a proxy for total excess carbon) such that

$$\frac{\Delta CO_2}{\Delta CO_2 + \Delta CO} \quad (1)$$

where Δ denotes the excess concentration of each species. Similarly, we used the carbon mass balance method (Yokelson et al. 1999; Yokelson, Griffith, and Ward 1996) to calculate the emission factor (EF) of a species. An EF is the ratio of excess mass of a trace gas species emitted to the mass of fuel consumed. EF is calculated as

$$EF_X = 0.5(g_c g_{Fuel}^{-1}) \times 1000(gkg^{-1}) \times \frac{\Delta X}{\Delta C_{CO_2} + \Delta C_{CO} + \Delta C_{CH_4} + \Delta C_{PM_{2.5}}} \quad (2)$$

where ΔC_X is the excess concentration of carbon associated with species X. Carbon from PM_{2.5} was added to this carbon mass balance approach for a more complete accounting of total carbon emitted from the combustion process. We estimated that 50% of the particulate matter mass was carbon. This is low compared to Burling et al. (2011) and Ferek et al. (1998) who estimated a carbon mass fraction of 69% and 75% respectively. This underestimate on our part is due to the fact that Ferek and colleagues were looking

at PM₄ (particulate matter that is 4 μm or smaller) and thus were accounting for much larger particulate matter than was measured in this study. We acknowledge that we are not accounting for all of the carbon containing species emitted during biomass burning; however, according to Yokelson et al. (2007), neglecting other carbon containing species only changes the EF by 5%. Herein we follow Akagi et al. (2011) and consider emission factors associated with an MCE greater than 0.90 are associated with flaming combustion while those associated with MCE less than 0.90 are attributed to mainly smoldering combustion.

Time series of EFs and MCE for burns 1 (Figure 9) and 2 (Figure 10) show a significant increase in the production of particulates after the prescribed burn is over. Burn 2 shows an increase of NO_x, NH₃, and CH₄ at almost four times that of burn 1.

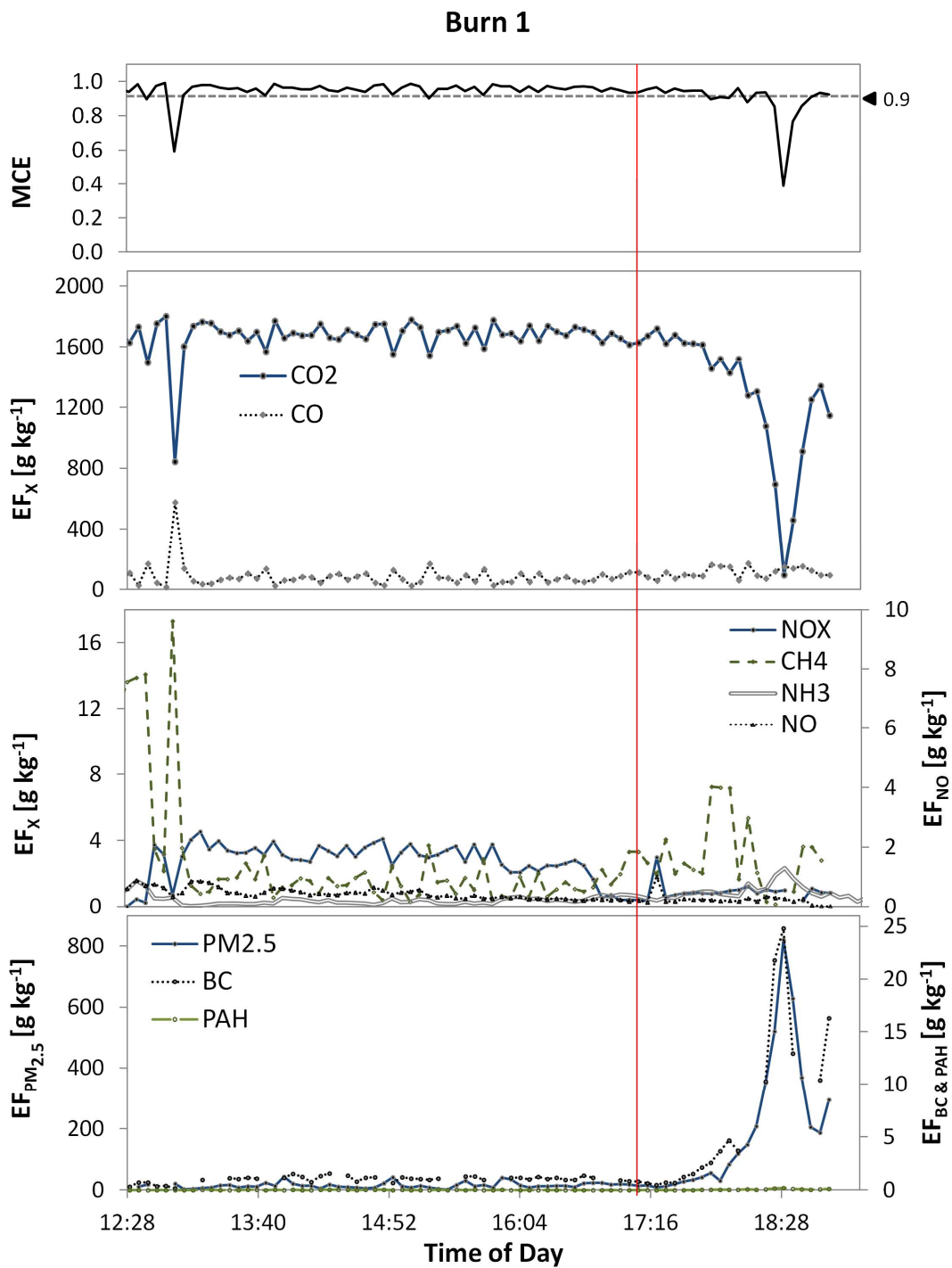


Figure 9 The time series of MCE and EFs for burn 1 are shown. The time series starts at the beginning of the burn and the red vertical line denotes the end of the prescribed burn. The gray dashed line in the MCE (top) plot denotes the threshold between flaming and smoldering combustion.

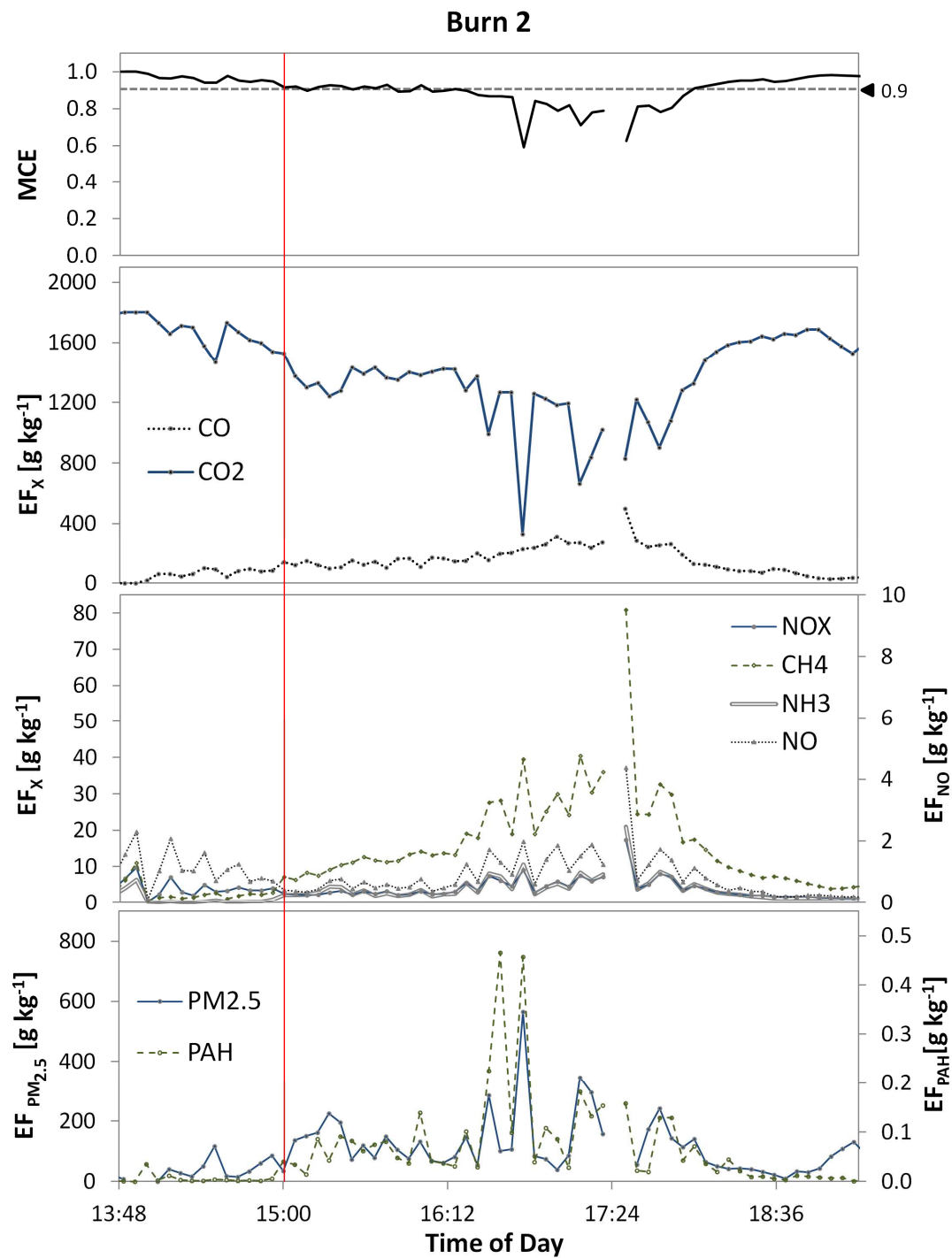


Figure 10 The time series of burn 2 is shown with the red vertical line denoting the end of the prescribed burn. The highest EFs of all gasses and particulates occur after the end of prescription except for CO₂.

Event averaged emission factors were separated based on the 0.90 threshold in MCE between flaming and smoldering combustion. The EFs of CO, CH₄, NH₃, and

PM_{2.5} all increased during smoldering combustion for both burns (Table 2). There was greater variability in the smoldering EF for CO₂ during burn 1 than during burn 2.

Table 2 The average and standard deviation of MCE and emissions factors (g kg⁻¹) are separated by flaming and smoldering combustion for both burn 1 (top) and burn 2 (bottom). The sample size (#) of each calculation is included.

Burn 1

	flaming			smoldering		
	#	avg	stdev	#	avg	stdev
MCE	72	0.99	0.02	9	0.82	0.08
CO ₂	72	1690	131	9	817	526
CO	72	56.3	40.3	9	230	159
CH ₄	71	4.3	6.4	8	53.1	131
NO _x	72	1.9	1.3	8	1.3	1.7
NO	72	0.35	0.22	9	1.68	0.00
NH ₃	72	0.39	0.35	9	2.74	4.91
PAH	71	0.01	0.01	9	0.06	0.07
PM 2.5	69	25.8	56.0	8	322	309
BC	56	1.2	2.3	7	9.5	10.4

Burn 2

	flaming			smoldering		
	#	avg	stdev	#	avg	stdev
MCE	171	0.97	0.02	24	0.71	0.25
CO ₂	171	1770	103	24	1185	317
CO	171	15.8	29.3	24	230	74.9
CH ₄	171	3.1	2.4	24	24	16
NO _x	171	0.9	1.2	24	5.2	3.3
NO	149	0.25	0.38	24	1.2	0.83
NH ₃	160	0.48	0.86	24	5.3	4.1
PAH	171	0.01	0.01	24	0.11	0.12
PM 2.5	96	39.5	40.6	23	153	123

Likewise, the variability in the smoldering EFs of CO, CH₄, and PM_{2.5} are also higher during burn 1. The greater variability in burn 1 could likely be due to the earlier timing

of this burn in the growing season or the smaller sample size of smoldering emissions from burn 1. The earlier timing would result in a mixture of live and dead fuel surface biomass that would be more dominated by dead fuels in burn 1 and less so in burn 2. This hypothesis would be further substantiated by noting that EF for NO_x and NH_3 are higher for burn 2, suggesting live plant activity increased between burns 1 and 2.

CO and CO_2 EF both correlate well with MCE having very little scatter in the data (Figure 11).

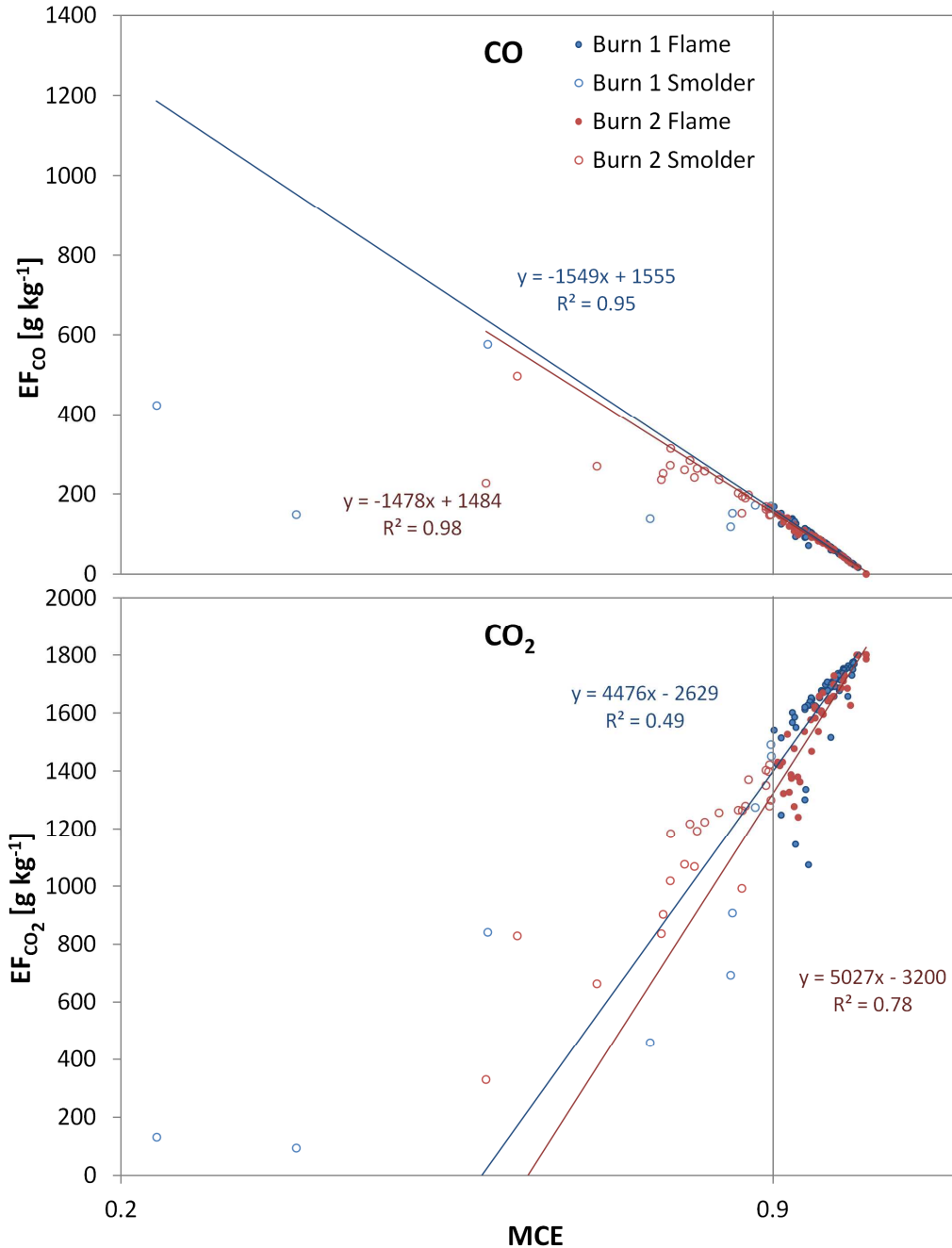


Figure 11 The relationship between emission factors (EF) and modified combustion efficiency (MCE) for CO (top) and CO₂ (bottom) are shown for both burn 2 (red) and burn 1 (blue). The regressions lines and corresponding equations are only representative of flaming combustion.

The EF of CO shows a strong negative correlation with MCE and the EF of CO₂ shows a strong positive correlation with MCE that mirrors the behavior of CO. CH₄ shows a low

to very low correlation while EFs of NO and NO_x show very little correlation with MCE for the second burn, and low correlations to MCE during the first burn (Figure 12).

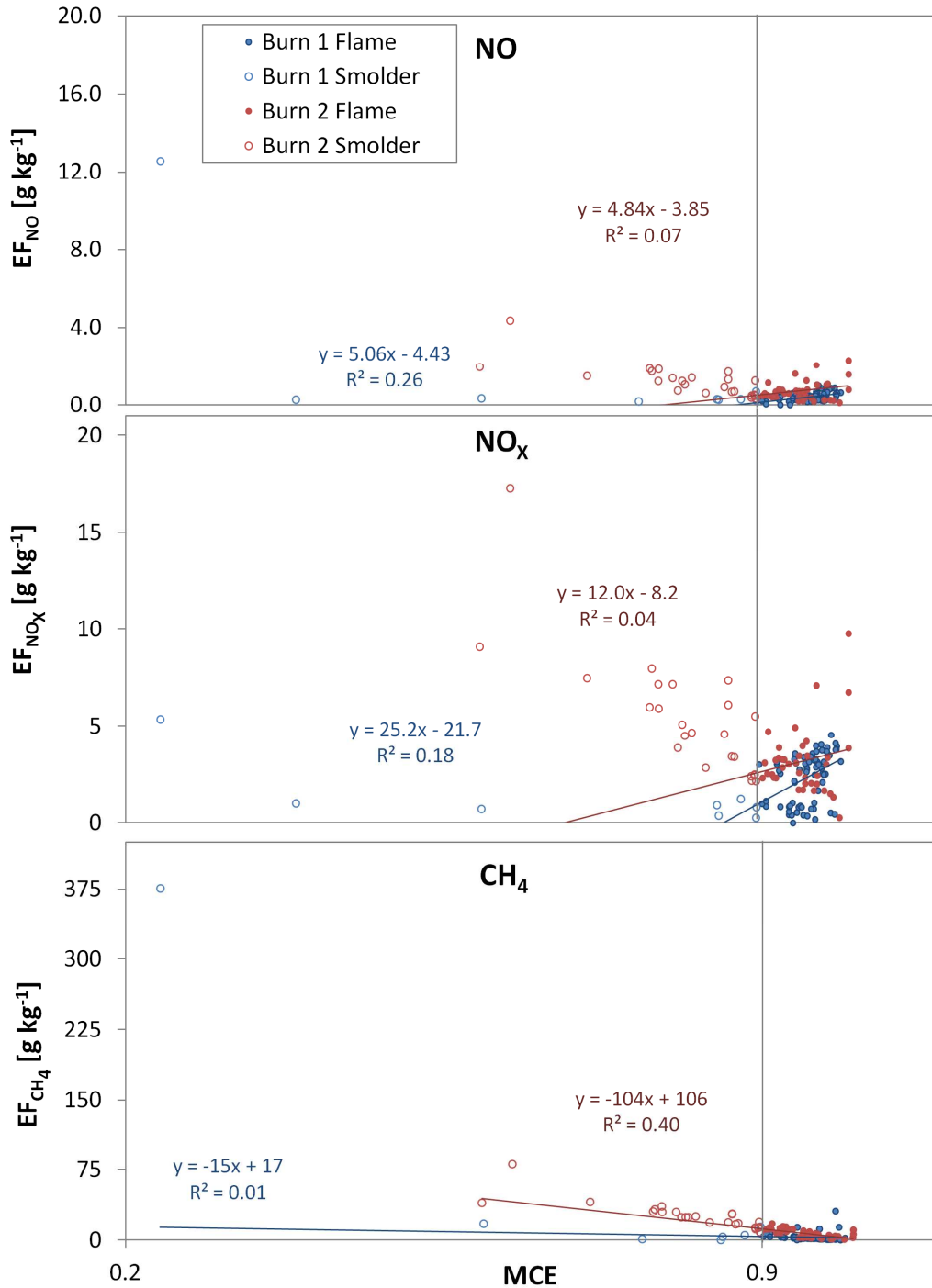


Figure 12 A comparison of EF to MCE for NO (top), NO_x (middle), and CH₄ (bottom) shows very poor correlation of NO and NO_x during burn 2 (red), and a slightly stronger correlation to MCE

during burn 1 (blue). The correlations of CH₄ have the opposite trend.

CH₄ appear to be negatively correlated overall to flaming combustion compared to NO and NO_x which are positively correlated during both burns. Burn 1 shows very moderate correlation between MCE and NO, and NO_x but poor correlation to CH₄. The EF of NH₃ shows a higher correlation with MCE during burn 2 than during burn 1, though both burns show poor overall correlation (Figure 13).

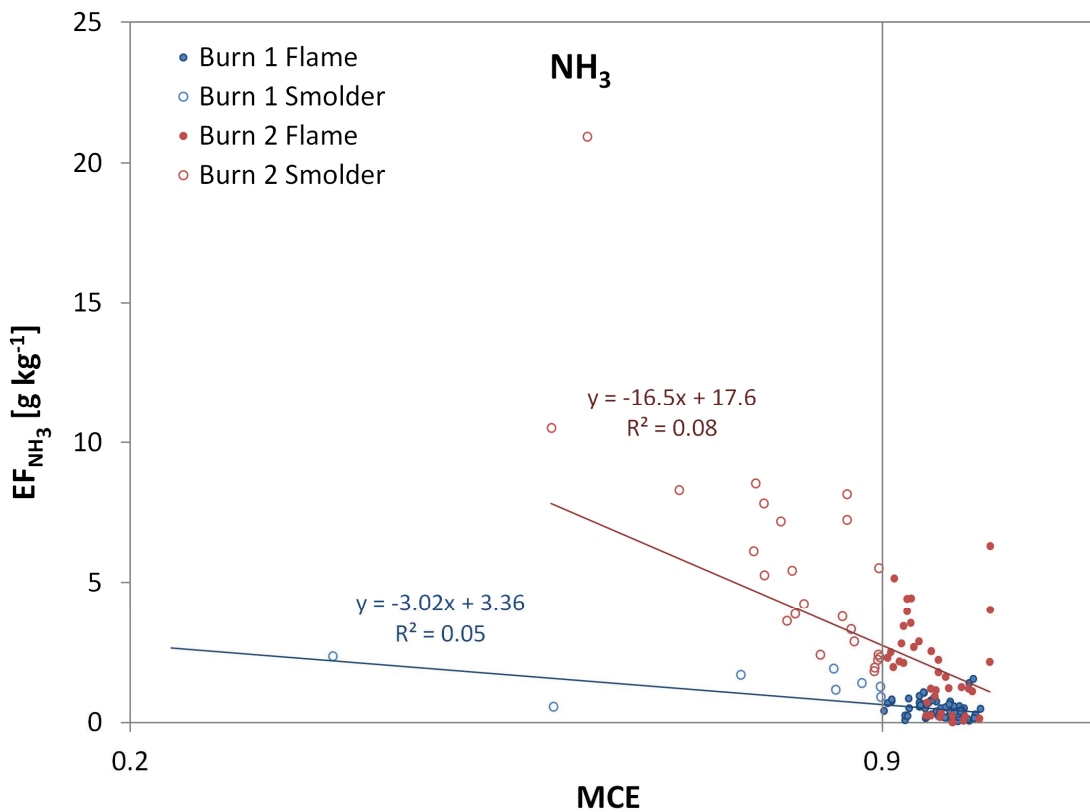


Figure 13 The EF of NH₃ compared to MCE during burn 1 (blue) and burn 2 (red). Overall, these correlations were very low.

In both burns 1 and 2, the EFs of PAH and PM_{2.5}, were very poorly correlated with MCE (Figure 14).

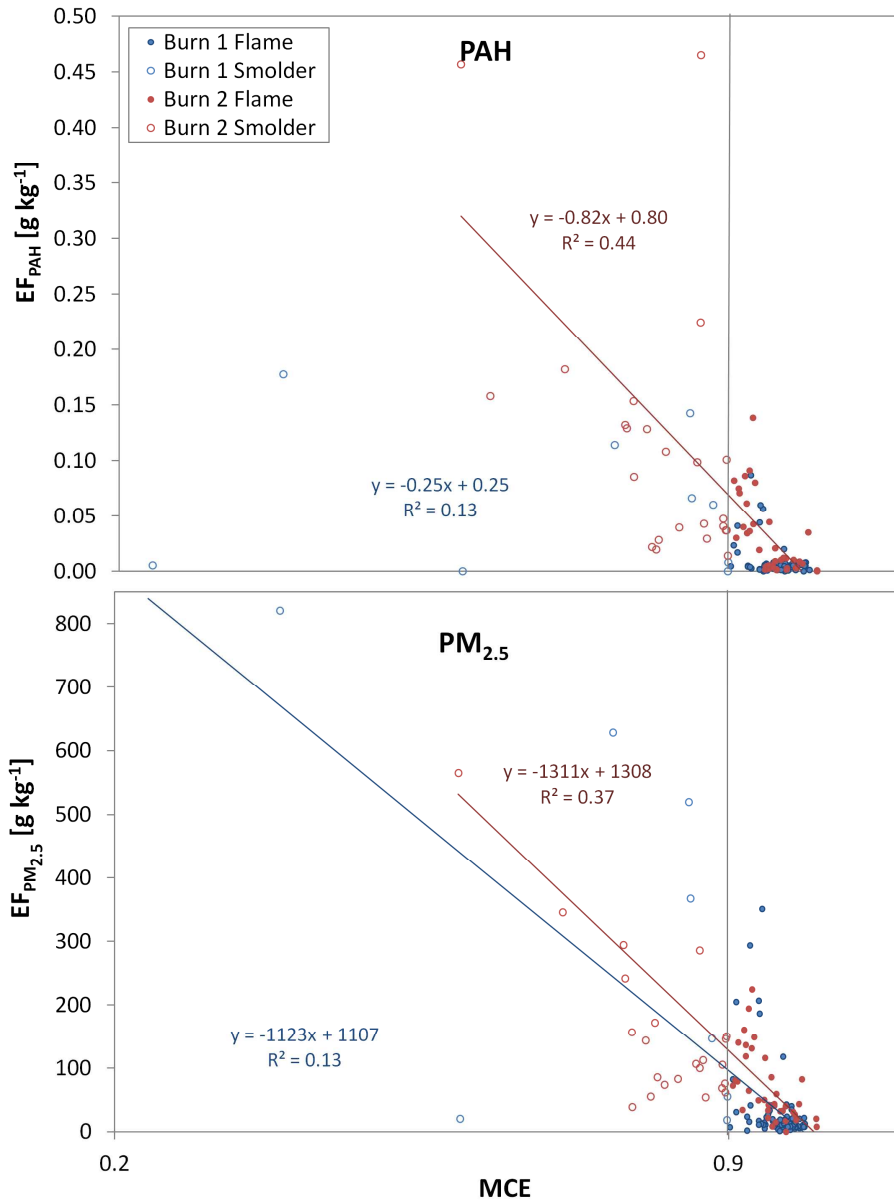


Figure 14 The EFs of PAH (top) and PM_{2.5} (bottom) are shown for burn 1 (blue) and burn 2 (red) along with regression lines and correlations to flaming combustion.

Black carbon was omitted from this portion of the analysis as instrument malfunctions produced unreliable results during burn 2.

2.5. DISCUSSION

Both prescribed burns presented in this study were conducted under the same canopy, in similar fuel type, and within the same prescription season. The burns were separated in time by 23 days. Both burns were conducted by the same TNC burn crew, and thus had similar burning technique as well as total fuel consumption. Surface wind speeds and temperature were higher for burn 2. Burn 1 had a 7 % higher dead fuel moisture and was two hours longer than burn 2 due to a need for slower ignition of the fuels. This need for slower ignition is further reflected by burn 1 having double the rate of spread as compared to burn 2. Given only this information, it would appear that burn 2 was more efficient than burn 1. However, burn 1 had higher overall average MCE for both flaming and smoldering, as compared to burn 2. One occurrence of smoldering combustion took place during burn 1, probably due to the slower ignition rate. Smoldering combustion didn't take place until after the prescribed burn was at an end in burn 2.

This is the first work of its kind to compare two near source surface burns under the same local canopy. Thus, it provides a unique look at the variability in EF that can be observed when there is little to no difference in surface fuels, canopy structure, surface meteorology, ignition pattern, and very little difference in fuel moisture. We were also generally able to separate the EFs associated with flaming and smoldering combustion as well as those associated with flaming and smoldering combustion during and after the prescribed burn took place. Other than Naeher et al. (2006), who looked at the evolution of CO and PM_{2.5}, we know of no other study which reports time series of excess trace gas concentrations during the full duration of a prescribed burn or wildfire.

Through further comparison of burns 1 and 2 we see that the EFs of $PM_{2.5}$ were higher during burn 1 and in general showed the greatest variability throughout this study. Another point of interest regarding $PM_{2.5}$ is the lower smoldering EF during burn 2 as compared with the lower dead fuel moisture content (28% for burn2 and 35% for burn 1). Fuel moisture directly influences the amount of energy needed during the combustion process and thus influences the overall energy balance. Specifically, given the same energy available for ignition, less energy per unit area is emitted from higher moisture fuels due to energy absorption by liquid water (Hardy et al. 2001; Sandberg et a., 2002). This difference in energy output directly impacts the overall combustion efficiency. Given this information one likely explanation for the lower $PM_{2.5}$ emissions during burn 2 (with lower overall MCE) would be that the lower efficiency burn was producing larger particles such as PM_{10} , which would not be obvious by just looking at concentrations of $PM_{2.5}$. If this hypothesis is true, it would imply that burn 1 was an overall higher efficiency burn than burn 2. A second explanation would be that less particulate matter was emitted overall. If this hypothesis were true, then this would imply that burn 2 was the higher efficiency burn. When we compare the gaseous EFs of burns 1 and 2 we see that burn 2 had an equivalent but slightly lower production of CO and a discernibly lower production of CH_4 and NO, than did burn 1. Decreased emissions of CO, CH_4 and NO during burn 2 imply a more efficient burn. This is further substantiated by noting that production of the oxygenated species (CO_2 and NO_x) was higher during burn 2. Thus far, the difference in emission factors implies that burn 2 was the more efficient burn however; this does not take into account the higher production of NH_3 during burn 2. Chen et al. (2010) found that an increase in the production of NH_3 and NO_x when fuels

were wetter, however the increase in production of NH_3 and NO_x in this study corresponds with the drier dead fuel moisture burn. Dennis et al. (2002) found that the EFs of nitrogen compounds are highly dependent on the amount of nitrogen in the fuel. This leads us to two possible explanations. The first, and least likely explanation for increased nitrogen, is that there was a major deposition event in the 23 days between the two prescribed burns, that was roughly equivalent exceeded the nitrogen deposited at this same site over the course of the last 2-3 years. The second, more plausible explanation is that active growth of the live fuels, and thus uptake of nitrogen from the soil, took place during the 23 days between these two burns. This increase in live fuel activity would not be reflected in the dead fuel moisture content by definition. An increase of live fuels would change the overall fuel moisture content significantly as they can have fuel moisture contents upwards of 400%. Information on the abundance of live fuels is needed to further substantiate this hypothesis. The ratio of live to dead surface fuels, the variability in moisture content of dead fuels, and differences in surface wind speeds and temperature may explain the majority of the variability we see within and between our two EF data sets. The calculations of MCE for burns 1 and 2 are the only data in strong disagreement with the hypothesis that burn 2 was more efficient than burn 1. It is possible that this disagreement could also be further explained through further knowledge of live to dead ratios. This is one of the first studies to report the average EFs known to be solely originating from smoldering combustion, based on time series of MCE. This separation allows for a better understanding of emission factors from smoldering combustion. In a much earlier laboratory study, Lobert et al. (1991) used the rate of

change in the concentration of CO to separate flaming and smoldering combustion in a time series.

2.5.1. Comparison with Other Studies

To compare emission factors from other works, we took a whole-event average for each burn (Table 3).

Table 3 Whole-event averages and standard deviations for MCE and trace-gas emission factors [g/kg dry fuel] are listed for both burns.

	Burn 1	Burn 2
MCE	0.93 (± 0.11)	0.96 (± 0.06)
CO₂	1552 (± 335)	1647 (± 244)
CO	93.8 (± 76.7)	53.4 (± 78.7)
CH₄	7.87 (± 42.4)	6.89 (± 9.14)
NO_x	2.25 (± 1.34)	1.76 (± 2.18)
NO	0.54 (± 1.37)	0.38 (± 0.59)
NH₃	0.88 (± 2.24)	1.41 (± 2.41)
PAH	0.01 (± 0.03)	0.02 (± 0.04)
PM_{2.5}	65.0 (± 143)	74.4 (± 74.9)

The emission factors of CH₄ and CO as well as MCE are compared with Urbanski (2013), who collated results from three studies that took place in the southeastern US. Urbanski (2013) reported a range of MCE between 0.90 and 0.96 with an average overall MCE of 0.933. Both burns fit within this window, with burn 2 at the upper end of this range. The emission factors of CH₄ and CO, for these three studies, had a range of 1-7 g kg⁻¹ and 49-113 g kg⁻¹, respectively. Our study found emission factors of CH₄ to be at the high end of this range and slightly exceeding any previously reported values. The emission factor of

CO fit within the range of the previous three studies. Recent work, which focused on prescribed fire emissions from mature longleaf pine, loblolly pine turkey oak, and sparkleberry (*Vaccinium arboretum* Marsh.) in South Carolina (Akagi et al. 2013), found lower overall emission factors of CO₂ and NH₃, but higher overall emission factors of CO and CH₄. Yokelson et al. (2013) reported emission factors for CH₄, NH₃, and PM_{2.5} for a pine forest understory that were about 2, 2, and 5 times lower respectively than this work (Figure 15).

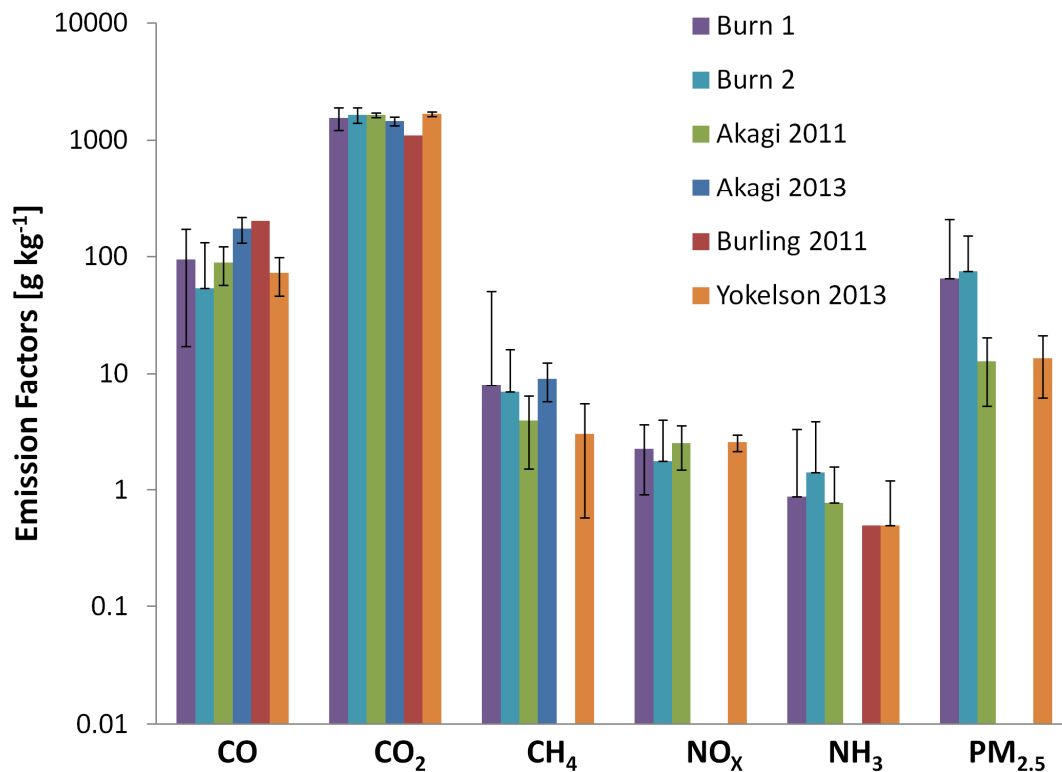


Figure 15 Emission factors of CO, CO₂, CH₄, NO_x, NH₃, and PM_{2.5} from this study are compared with results from similar pine understory measurements.

To compare our results with those looking specifically at residual smoldering combustion (Burling et al. 2011) we refer back to (Table 2) and find that we agree well for the emission factors of CO₂, CO, and CH₄. However, our emission factors of NH₃ are 5-10 times higher. Since NH₃ is highly dependent on the nitrogen content of the fuel (Dennis

et al. 2002; Dignon and Penner 1991), this could explain the elevated levels present in our results.

The PM_{2.5} sensor was located at ground level while all other carbon-containing trace gas instruments were located at the top of the canopy. Due to the difference in location, it could be argued that the excess PM_{2.5} concentrations were abnormally high due to gradients in concentration that might exist between the surface and the top of the canopy. However, even if the overall excess concentrations were reduced by 50%, the overall EF of PM_{2.5} would still be 3 times higher than that reported in other studies (Akagi et al. 2011; Yokelson et al. 2013). This difference is dominantly due to the amount of PM_{2.5} produced during smoldering combustion. If smoldering combustion was removed from the analysis, our PM_{2.5} EF would match other studies well. Thus, though the displacement of the instruments means that potentially different volumes of air are sampled, the EF calculations of PM_{2.5}, from flaming combustion, still match well with those reported in the literature. This gives us confidence that the difference in height between the two sampling locations is not the reason for our elevated PM_{2.5} EFs.

2.6. CONCLUSIONS

We have presented a unique data set, collected over two days in the winter of 2011, which allowed for comparing two low intensity prescribed burns that shared the same fuel type, canopy, and ignition techniques. This data set provides a detailed view of the high variability of trace gases and fine particulates at and very near the source of the fire. Our results show the strong variability present in EFs potentially due to small differences in surface meteorology, fuel moisture content, and the overall ratio of dead to live fuel.

The time resolution and sampling techniques allowed for separation of the trace gas and particles results between flaming and smoldering combustion as well as the onset of smoldering combustion. Overall, our results agree well with similar studies which focus on prescribed fires in the southeastern United States and with those that look at smoldering combustion. However, we observed overall higher emission factors of PM_{2.5}.

2.7. REFERENCES

- Akagi, S. K., J. S. Craven, J. W. Taylor, G. R. McMeeking, R. J. Yokelson, I. R. Burling, S. P. Urbanski, et al. 2012. “Evolution of Trace Gases and Particles Emitted by a Chaparral Fire in California.” *Atmospheric Chemistry and Physics* 12 (3): 1397–1421. doi:10.5194/acp-12-1397-2012.
- Akagi, S. K., R. J. Yokelson, I. R. Burling, S. Meinardi, I. Simpson, D. R. Blake, G. R. McMeeking, et al. 2013. “Measurements of Reactive Trace Gases and Variable O-3 Formation Rates in Some South Carolina Biomass Burning Plumes.” *Atmospheric Chemistry and Physics* 13 (3): 1141–1165. doi:10.5194/acp-13-1141-2013.
- Akagi, S. K., R. J. Yokelson, C. Wiedinmyer, M. J. Alvarado, J. S. Reid, T. Karl, J. D. Crounse, and P. O. Wennberg. 2011. “Emission Factors for Open and Domestic Biomass Burning for Use in Atmospheric Models.” *Atmospheric Chemistry and Physics* 11 (9): 4039–4072. doi:10.5194/acp-11-4039-2011.
- Andreae, Meinrat O., and P. Merlet. 2001. “Emission of Trace Gases and Aerosols from Biomass Burning.” *Global Biogeochemical Cycles* 15 (4): 955–966.
- Arizona Department of Environmental Quality. 2003. “Simple Approach Smoke Estimation Model (SASEM), Version 4.0”. Arizona Department of Environmental Quality. <http://www.azdeq.gov/environ/air/smoke/download/sasemi.pdf>.
- Bertschi, I., R. J. Yokelson, D. E. Ward, R. E. Babbitt, R. A. Susott, J. G. Goode, and W. M. Hao. 2003. “Trace Gas and Particle Emissions from Fires in Large Diameter and Belowground Biomass Fuels.” *Journal of Geophysical Research-Atmospheres* 108 (D13) (February 15). doi:10.1029/2002JD002100.
- Breyfogle, S., and S. Ferguson. 1996. “User Assessment of Smoke-Dispersion Models for Wildland Biomass Burning”. General Technical Report PNW-GTR-379. Pacific Northwest Research Station: USDA, Forest Service.

- Bunting, S. C., B. M. Kilgore, and C. L. Bushey. 1987. *Guidelines for Prescribed Burning Sagebrush-grass Rangelands in the Northern Great Basin*. <http://www.treesearch.fs.fed.us/pubs/25027>.
- Burling, I. R., R. J. Yokelson, S. K. Akagi, S. P. Urbanski, C. E. Wold, D. W. T. Griffith, T. J. Johnson, J. Reardon, and D. R. Weise. 2011. "Airborne and Ground-based Measurements of the Trace Gases and Particles Emitted by Prescribed Fires in the United States." *Atmospheric Chemistry and Physics* 11 (23): 12197–12216. doi:10.5194/acp-11-12197-2011.
- Burling, I. R., R. J. Yokelson, D. W. T. Griffith, T. J. Johnson, P. Veres, J. M. Roberts, C. Warneke, et al. 2010. "Laboratory Measurements of Trace Gas Emissions from Biomass Burning of Fuel Types from the Southeastern and Southwestern United States." *Atmospheric Chemistry and Physics* 10 (22): 11115–11130. doi:10.5194/acp-10-11115-2010.
- Chen, L.-W. A., P. Verburg, A. Shackelford, D. Zhu, R. Susfalk, J. C. Chow, and J. G. Watson. 2010. "Moisture Effects on Carbon and Nitrogen Emission from Burning of Wildland Biomass." *Atmos. Chem. Phys.* 10 (14) (July 20): 6617–6625. doi:10.5194/acp-10-6617-2010.
- Christian, T. J., B. Kleiss, R. J. Yokelson, R. Holzinger, P. J. Crutzen, W. M. Hao, B. H. Saharjo, and D. E. Ward. 2003. "Comprehensive Laboratory Measurements of Biomass-burning Emissions: 1. Emissions from Indonesian, African, and Other Fuels." *Journal of Geophysical Research-Atmospheres* 108 (D23) (December 4). doi:10.1029/2003JD003704.
- Clark, T. L., J. L. Coen, and D. Latham. 2004. "Description of a Coupled Atmosphere-fire Model." *International Journal of Wildland Fire* 13 (1): 49–63. doi:10.1071/WF03043.
- Clark, T. L., M. A. Jenkins, J. L. Coen, and D. R. Packham. 1996. "A Coupled Atmosphere-fire Model: Role of the Convective Froude Number and Dynamic Fingering at the Fireline." *International Journal of Wildland Fire* 6 (4) (December): 177–190. doi:10.1071/WF9960177.
- Coen, J. L. 2005. "Simulation of the Big Elk Fire Using Coupled Atmosphere-fire Modeling." *International Journal of Wildland Fire* 14 (1): 49–59. doi:10.1071/WF04047.
- Coen, J. L., M. Cameron, J. Michalakes, E. G. Patton, P. J. Riggan, and K. M. Yedinak. 2013. "WRF-Fire: Coupled Weather-Wildland Fire Modeling with the Weather Research and Forecasting Model." *Journal of Applied Meteorology and Climatology* 52 (1) (January): 16–38. doi:10.1175/JAMC-D-12-023.1.
- Crosby, JS. 1949. "Vertical Wind Currents and Fire Behavior." *Fire Control Notes* 10 (2): 12–14.

- Cunningham, Philip, and Michael J. Reeder. 2009. "Severe Convective Storms Initiated by Intense Wildfires: Numerical Simulations of Pyro-convection and Pyro-tornadogenesis." *Geophysical Research Letters* 36 (June 26). doi:10.1029/2009GL039262.
- Dennis, A., M. Fraser, S. Anderson, and D. Allen. 2002. "Air Pollutant Emissions Associated with Forest, Grassland, and Agricultural Burning in Texas." *Atmospheric Environment* 36 (23) (August): 3779–3792. doi:10.1016/S1352-2310(02)00219-4.
- Dignon, J., and J. E. Penner. 1991. In *Global Biomass Burning: Atmospheric, Climatic, and Biospheric Implications*, by Joel S. Levine. MIT Press.
- Eidsmoe, G. 2007. "Investigation Report: Guejito Fire". Investigation CA-MVU-010484. Guejito Creek drainage: California Department of Forestry and Fire Protection. http://www.fire.ca.gov/fire_protection/downloads/redsheets/CA-MVU-010484_Complete.pdf.
- Ferek, R. J., J. S. Reid, P. V. Hobbs, C. R. Blake, and C. Liou. 1998. "Emission Factors of Hydrocarbons, Halocarbons, Trace Gases and Particles from Biomass Burning in Brazil." *Journal of Geophysical Research: Atmospheres* 103 (D24): 32107–32118. doi:10.1029/98JD00692.
- Freitas, S. R., K. M. Longo, R. Chatfield, D. Latham, M. A. F. Silva Dias, M. O. Andreae, E. Prins, J. C. Santos, R. Gielow, and J. A. Carvalho Jr. 2007. "Including the Sub-grid Scale Plume Rise of Vegetation Fires in Low Resolution Atmospheric Transport Models." *Atmos. Chem. Phys.* 7 (13) (July 2): 3385–3398. doi:10.5194/acp-7-3385-2007.
- Gilbert, M. 2008. "Investigation Report: Witch Fire". Investigation 07-CDF-570. Highway 78 west of Santa Ysabel, San Diego County: California Department of Forestry and Fire Protection. http://www.fire.ca.gov/fire_protection/downloads/redsheets/CA-MVU-010432_Complete.pdf.
- Goodrick, S. L., G. L. Achtemeier, N. K. Larkin, Y. Liu, and T. M. Strand. 2013. "Modelling Smoke Transport from Wildland Fires: a Review." *International Journal of Wildland Fire* 22 (1): 83–94.
- Goodrick, Scott L., Gary L. Achtemeier, Narasimhan K. Larkin, Yongqiang Liu, and Tara M. Strand. 2013. "Modelling Smoke Transport from Wildland Fires: a Review." *International Journal of Wildland Fire* 22 (1): 83–94.
- Haines, D. A. 1988. "A Lower Atmospheric Severity Index for Wildland Fires." *National Weather Digest* 13 (2): 23–27.

- Hardy, C., R. Ottmar, J. Peterson, J. Core, and P. Seamon, ed. 2001. "Smoke Management Guide for Prescribed and Wildland Fire". National Wildfire Coordination Group. <http://www.nwcg.gov/pms/pubs/SMG/SMG-72.pdf>.
- Hayes, GL. 1941. "Influences of Altitude and Aspect on Daily Variations in Factors of Fire Danger." *US Department of Agriculture, Circular 591* (Washington DC).
- Jain, R., J. Vaughan, K. Heitkamp, C. Ramos, C. Claiborn, M. Schreuder, M. Schaaf, and B. Lamb. 2007. "Development of the ClearSky Smoke Dispersion Forecast System for Agricultural Field Burning in the Pacific Northwest." *Atmospheric Environment* 41 (32) (October): 6745–6761. doi:10.1016/j.atmosenv.2007.04.058.
- Jenkins, M. A. 2004. "Investigating the Haines Index Using Parcel Model Theory." *International Journal of Wildland Fire* 13 (3): 297–309. doi:10.1071/WF03055.
- Jolly, W. M. 2007. "Sensitivity of a Surface Fire Spread Model and Associated Fire Behaviour Fuel Models to Changes in Live Fuel Moisture." *International Journal of Wildland Fire* 16 (4): 503–509.
- Keeley, J. E., G. H. Aplet, N. L. Christensen, S. G. Conard, E. A. Johnson, P. N. Omi, D. L. Peterson, and T. W. Swetnam. 2009. "Ecological Foundations for Fire Management in North American Forest and Shrubland Ecosystems". United States Department of Agriculture, Forest Service, Pacific Northwest Research Station, Portland, OR. <http://www.treesearch.fs.fed.us/pubs/32483>.
- Kilgore, B. M., and G. A. Curtis. 1987. *Guide to Understory Burning in Ponderosa Pine-larch-fir Forests in the Intermountain West*. <http://www.treesearch.fs.fed.us/pubs/32954>.
- Kochanski, A., M. A. Jenkins, J. Mandel, J. Beezley, and S. Krueger. 2013. "Real Time Simulation of 2007 Santa Ana Fires." *Forest Ecology and Management* 294 (April 15): 136–149. doi:10.1016/j.foreco.2012.12.014.
- Kochanski, A., M. A. Jenkins, R. Sun, S. Krueger, S. Abedi, and J. Charney. 2013. "The Importance of Low-level Environmental Vertical Wind Shear to Wildfire Propagation: Proof of Concept." *Journal of Geophysical Research: Atmospheres*: n/a–n/a. doi:10.1002/jgrd.50436.
- Lavdas, L. G. 1996. "Program VSMOKE: Users Manual". General Technical Report GTR-SRS-006. Southeastern Research Station: USDA, Forest Service.
- Lobert, J. M., D. H. Scharffe, W. Hao, T. A. Kuhlbusch, R. Seuwen, P. Warneck, and P. J. Crutzen. 1991. "Experimental Evaluation of Biomass Burning Emissions: Nitrogen and Carbon Containing Compounds." In *Global Biomass Burning*, edited by J. S. Levine, 289–304. MIT Press.
- McMeeking, Gavin R., Sonia M. Kreidenweis, Stephen Baker, Christian M. Carrico, Judith C. Chow, Jeffrey L. Collett, Wei Min Hao, et al. 2009. "Emissions of Trace

- Gases and Aerosols During the Open Combustion of Biomass in the Laboratory.” *Journal of Geophysical Research-Atmospheres* 114 (October 14). doi:10.1029/2009JD011836.
- Naeher, Luke P, Gary L Achtemeier, Jeff S Glitzenstein, Donna R Streng, and David Macintosh. 2006. “Real-time and Time-integrated PM2.5 and CO from Prescribed Burns in Chipped and Non-chipped Plots: Firefighter and Community Exposure and Health Implications.” *Journal of Exposure Science & Environmental Epidemiology* 16 (4) (July): 351–361. doi:10.1038/sj.jes.7500497.
- NCAR. 2012. *Weather Research and Forecasting Model* (version 3.4). http://www.mmm.ucar.edu/wrf/users/download/get_source.html.
- Nelson, R. M. 2003. “Power of the Fire - a Thermodynamic Analysis.” *International Journal of Wildland Fire* 12 (1): 51–65. doi:10.1071/WF02032.
- Nelson, Rm. 1993. “Byram Derivation of the Energy Criterion for Forest and Wildland Fires.” *International Journal of Wildland Fire* 3 (3) (September): 131–138. doi:10.1071/WF9930131.
- “NICC Wildland Fire Annual Report.” 2012. NIFC. <http://www.predictiveservices.nifc.gov/intelligence/intelligence.htm>.
- Pharo, J. A., L. G. Lavadas, and P. M. Bailey. 1976. “Smoke Transport and Dispersion”. General Technical Report SE-10. Southern Forestry Smoke Management Guidebook. Southeastern Research Station: USDA, Forest Service.
- Potter, B. E. 2002. “A Dynamics Based View of Atmosphere-fire Interactions.” *International Journal of Wildland Fire* 11 (3-4): 247–255. doi:10.1071/WF02008.
- . 2012a. “Atmospheric Interactions with Wildland Fire Behaviour – I. Basic Surface Interactions, Vertical Profiles and Synoptic Structures.” *International Journal of Wildland Fire* 21 (7): 779–801.
- . 2012b. “Atmospheric Interactions with Wildland Fire Behaviour – II. Plume and Vortex Dynamics.” *International Journal of Wildland Fire* 21 (7): 802–817.
- Reifsnyder, W. E. 1954. “Atmospheric Stability and Forest Fire Behavior”. PhD dissertation, New Haven, CT: Yale University.
- Rothermel, R. C. 1972. “A Mathematical Model for Predicting Fire Spread in Wildland Fuels.” *USDA Forest Service, Intermountain Forest and Range Experiment Station, Research Paper* INT-115.
- . 1983. *How to Predict the Spread and Intensity of Forest and Range Fires*. <http://www.treearch.fs.fed.us/pubs/24635>.

- Sandberg, David V., Roger D. Ottmar, and Janice L. Peterson. 2002. "Wildland Fire in Ecosystems: Effects of Fire on Air." <http://www.treesearch.fs.fed.us/pubs/5247>.
- Scire, J. S., D. G. Strimaitis, and R. J. Yamartino. 2000. "A User's Guide for the CALPUFF Dispersion Model (Version 5)". User's guide. Concord, MA: EarthTech Inc.
- Skamarock, W. C., J. B. Klemp, J. Dudhia, D. O. Gill, D. M. Barker, M. G. Duda, X. Huang, W. Wang, and J. G. Powers. 2008. "A Description of the Advanced Research WRF Version 3". National Center for Atmospheric Research.
- Trentmann, J., M. O. Andreae, H. F. Graf, P. V. Hobbs, R. D. Ottmar, and T. Trautmann. 2002. "Simulation of a Biomass-burning Plume: Comparison of Model Results with Observations." *Journal of Geophysical Research-Atmospheres* 107 (D1-D2) (January). doi:10.1029/2001JD000410.
- Urbanski, S. P. 2013. "Combustion Efficiency and Emission Factors for Wildfire-season Fires in Mixed Conifer Forests of the Northern Rocky Mountains, US." *Atmos. Chem. Phys.* 13 (14) (July 30): 7241–7262. doi:10.5194/acp-13-7241-2013.
- Viney, NR. 1991. "A Review of Fine Fuel Moisture Modelling." *International Journal of Wildland Fire* 1 (4) (January 1): 215–234.
- Ward, D. E., and C. C. Hardy. 1991. "Smoke Emissions from Wildland Fires." *Environment International* 17 (2–3): 117–134. doi:10.1016/0160-4120(91)90095-8.
- Ward, D. E., and L. F. Radke. 1993. "Emissions Measurements from Vegetation Fires: A Comparative Evaluation of Methods and Results." In , 53–76. <http://www.treesearch.fs.fed.us/pubs/40604>.
- Wiedinmyer, C., S. K. Akagi, R. J. Yokelson, L. K. Emmons, J. A. Al-Saadi, J. J. Orlando, and A. J. Soja. 2011. "The Fire INventory from NCAR (FINN): a High Resolution Global Model to Estimate the Emissions from Open Burning." *Geoscientific Model Development* 4 (3): 625–641. doi:10.5194/gmd-4-625-2011.
- Yokelson, R. J., I. R. Burling, J. B. Gilman, C. Warneke, C. E. Stockwell, J. de Gouw, S. K. Akagi, et al. 2013. "Coupling Field and Laboratory Measurements to Estimate the Emission Factors of Identified and Unidentified Trace Gases for Prescribed Fires." *Atmospheric Chemistry and Physics* 13 (1): 89–116. doi:10.5194/acp-13-89-2013.
- Yokelson, R. J., J. G. Goode, D. E. Ward, R. A. Susott, R. E. Babbitt, D. D. Wade, I. Bertschi, D. W. T. Griffith, and W. M. Hao. 1999. "Emissions of Formaldehyde, Acetic Acid, Methanol, and Other Trace Gases from Biomass Fires in North Carolina Measured by Airborne Fourier Transform Infrared Spectroscopy." *Journal of Geophysical Research: Atmospheres* 104 (D23): 30109–30125. doi:10.1029/1999JD900817.

- Yokelson, R. J., D. W. T. Griffith, and D. E. Ward. 1996. "Open-path Fourier Transform Infrared Studies of Large-scale Laboratory Biomass Fires." *Journal of Geophysical Research-Atmospheres* 101 (D15) (September 20): 21067–21080. doi:10.1029/96JD01800.
- Yokelson, R. J., R. Susott, D. E. Ward, J. Reardon, and D. W. T. Griffith. 1997. "Emissions from Smoldering Combustion of Biomass Measured by Open-path Fourier Transform Infrared Spectroscopy." *Journal of Geophysical Research-Atmospheres* 102 (D15) (August 20): 18865–18877. doi:10.1029/97JD00852.
- Yokelson, R. J., S. P. Urbanski, E. L. Atlas, D. W. Toohey, E. C. Alvarado, J. D. Crouse, P. O. Wennberg, et al. 2007. "Emissions from Forest Fires Near Mexico City." *Atmospheric Chemistry and Physics* 7 (21): 5569–5584.

CHAPTER 3: AN ANALYSIS OF SENSITIVITY TO AMBIENT ATMOSPHERIC STABILITY ON FIRE BEHAVIOR AND SMOKE PLUME RISE USING WRF-FIRE

3.1. ABSTRACT

This sensitivity analysis of WRF-Fire, a fully coupled fire-atmosphere model, applied in large eddy simulation mode, seeks to quantify the influence of resolved atmospheric flow upon fire behavior. Specifically, the influence of ambient atmospheric stability on fire-line rate-of-spread (ROS), a new metric of fire area termed rate-of-growth (ROG), and smoke plume rise are investigated under neutral to unstable atmospheric stability for an ideal grass fire. The neutral stability case had a lower plume height as compared to the unstable case, a slower ROS, and a slower ROG; while the unstable case showed a higher, though oscillating, ROG for the same time period. These results are attributed to surface heating and the resulting turbulent mixing associated with different ambient atmospheric stability conditions that may only be apparent if one uses a two-way coupled fire-atmosphere model.

3.2. INTRODUCTION

Prescribed fire practices have evolved over the last 30+ years to include consideration of atmospheric stability for the sake of down-wind smoke management (Hardy et al. 2001). These fires are often conducted in a narrow window of temperature and humidity that influence fine-fuel moisture content in order to control fire behavior while also taking combustion efficiency and emission factors into account (Bunting et al., 1987; Kilgore and Curtis 1987; Rothermel 1983). On diurnal time scales, higher moistures typically occur from midnight to the mid-morning hours when fine dead fuels

retain the signature of night-time relative humidity. Moisture content of both live and dead fuels has been a long-discussed topic for its influence of fire behavior (Jolly 2007; Viney 1991). However, little is known about how the morning to mid-day atmospheric stability (largely the transition from stable to neutral to unstable) influences fire behavior.

For prescribed fires, estimates of the smoke plume dynamics and resulting plume rise, from numerical models, are largely based on specification of the generic atmospheric stability class that best suits the timing of the burn, as well as generalized assumptions of the fire heat flux and size (Breyfogle and Ferguson 1996). In large part, this simplified approach is due to both the added computational expense of further detail as well as the lack of available detailed data to drive more complex approaches (Goodrick et al., 2013).

Fire behavior and smoke plume dynamics share intimate linkages between the fire and the atmosphere which can only be investigated with the use of a coupled fire-atmosphere model. New model platforms have recently become available which dynamically couple the fire and atmosphere systems (Clark et al., 1996; Clark et al., 2004; Coen 2005). In the mid 2000s, Coen and colleagues developed a new coupled fire-atmosphere model using the Weather Research and Forecasting (WRF) mesoscale model with an empirical fire behavior model developed by Rothermel (1972). The most recent detailed descriptions of this new coupled model, hereafter referred to as WRF-Fire, can be found in (Coen et al., (2013), and at http://www.mmm.ucar.edu/research/wildfire/wrf/wrf_fire.html.

Our objective is to investigate the role that ambient atmospheric stability plays in influencing fire-line rate of spread (ROS), rate of growth (ROG), and plume rise using

WRF-Fire. This study represents the first use of a fully coupled model to investigate the role of stability and will provide the basis for improvements in prescribing fire behavior and plume rise for use in larger scale air quality models.

3.3. METHODS

Atmospheric stability derives from the buoyant convective dynamics in the atmospheric boundary layer, the layer of our atmosphere directly influenced by turbulent mixing from heating and cooling of the Earth's surface. For the purposes of this study, stability is measured in terms of the vertical temperature profile, relative to the dry adiabatic lapse rate and in terms of the Obuhkov length. In this work, a plume is defined as the mass of pyrogenic pollutants released from a forest fire and plume rise refers to the height above ground level (AGL) of the plume center of mass. ROS is defined as the rate of change in position, along the dominant wind direction, of the furthest extent of the combustion zone. Likewise, ROG is defined as the rate of change in overall fire area per unit time. In the following sections, the model setup, numerical experiments, analysis methods, and results are presented.

3.3.1. WRF-Fire model setup

The 2012 release of WRF-Fire, contained in WRF V3.4 (NCAR 2012) was used in large eddy simulation (LES) mode to quantify ROS, ROG, and plume rise for an ideal fire. LES uses spatial filtering and sub-grid scale models to solve the Navier Stokes equations. This approach allows for the resolution of turbulent flows, which make up the atmospheric boundary layer. The model time step was set at 1/16 second to capture turbulent dynamics. While this time step is smaller than one may expect, fires cause fast

moving vertical flows with strong heat fluxes. The steep temporal and spatial gradients of flow features associated with fire require small model time steps to resolve the flow.

The model domain was 228 x 80 cells in the x and y directions, respectively, with a horizontal cell size of 35 m x 35 m (Figure 1).

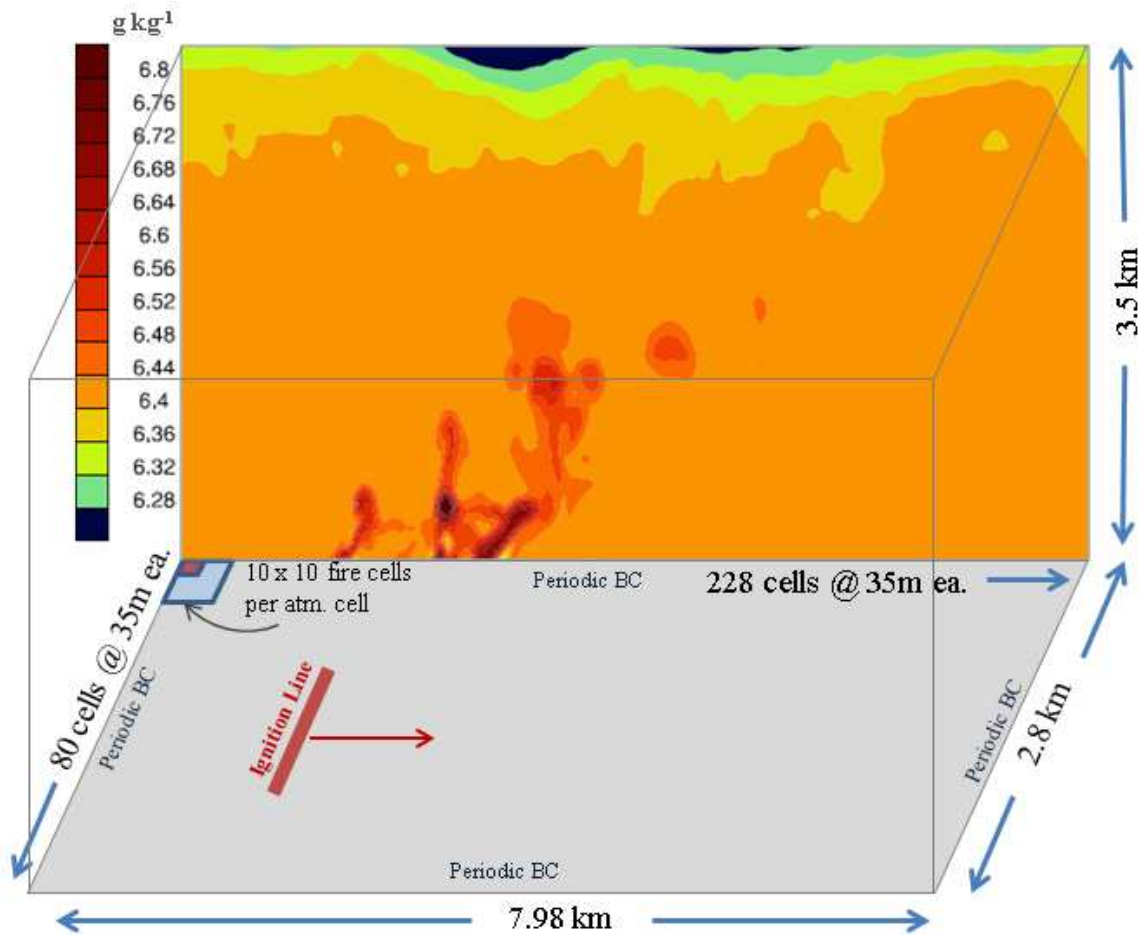


Figure 1 A schematic of the idealized model domain is shown above. The back panel of the schematic shows an example of the water vapor released in the model during the combustion process.

The fire grid was 3.5 m x 3.5 m (10 times finer than the atmosphere grid) on a side and extended the full length of the atmosphere grid. The vertical extent of the simulated domain was 3.5 km, having a hyperbolic stretched vertical grid with z_scale factor of 2.25, and a total of 50 vertical levels. The vertical height of the grid cell closest to the

surface was 6.3 m. The boundary conditions were periodic (looped) on both the x and y domain edges. Due to the use of periodic boundary conditions, any tracer that is released in the domain during a simulation will recirculate back to its approximate (x,y) -location of emission after 13 minutes. Thus, emissions from the ignition of a fire, such as water vapor, will interfere with the background environment after this window of time passes. Because of this interference, we limit our analysis to 13 minutes from the ignition of the fire.

The only two WRF microphysics schemes used during these simulations were the Monin-Obukhov scheme, which references look-up tables based on similarity theory, and a surface thermal diffusion scheme that only depends on soil temperature for surface layer thermal diffusion properties (Skamarock et al. 2008). Incoming solar radiation, cloud formation, and precipitation were ignored.

We used a 3rd order Runge-Kutta time integration scheme. Turbulence was parameterized with a 1.5 order Turbulent Kinetic Energy (TKE) closure. Upper level Rayleigh damping was turned off. The horizontal and vertical diffusion coefficients were both set at $1.0 \text{ m}^2 \text{ s}^{-1}$. The model was run in non-hydrostatic mode. Isotropic vertical and horizontal diffusion coefficients were used. The horizontal and vertical momentum advection orders were set to 5th and 3rd, respectively. The horizontal and vertical scalar advection orders were also set to 5th and 3rd, respectively. There were 6 sound steps per time step. The surface drag coefficient was set at 0.005 to represent tall grass. The Smagorinsky coefficient was set to 0.18 and the TKE coefficient was 0.10. Surface heat flux was varied between the two stability cases and is discussed more below.

3.3.2. Two cases: idealized stability regimes

We focused on two atmospheric stability regimes, neutral and unstable, having dimensionless Obukhov stability (z/L) values of -0.03 and -0.18 respectively. The neutral and unstable idealized scenarios were initialized using a vertical log wind profile and realistic vertical water vapor profile. There were no y -direction winds, and the surface pressure was set to 921 mb. The surface heat fluxes determined the atmospheric stability of the system after spin-up (Figure 2a). For the neutral stability case, the surface heat flux was set to zero, while the unstable case had a surface heat flux of 100 W m^{-2} . For both cases, a low thermal inversion was included in the initial vertical temperature profile as a representation of morning-time CBL conditions during the transition from neutral to unstable conditions. The potential temperature profiles, after spin-up and just before ignition confirm that the surface layer developed neutral and unstable conditions (Figure 2)

2) The wind speed profiles were slower above the surface layer for the neutral case and thus this will need to be taken into account when interpreting results. The water vapor profiles were virtually identical for both stability cases and had very little vertical variability.

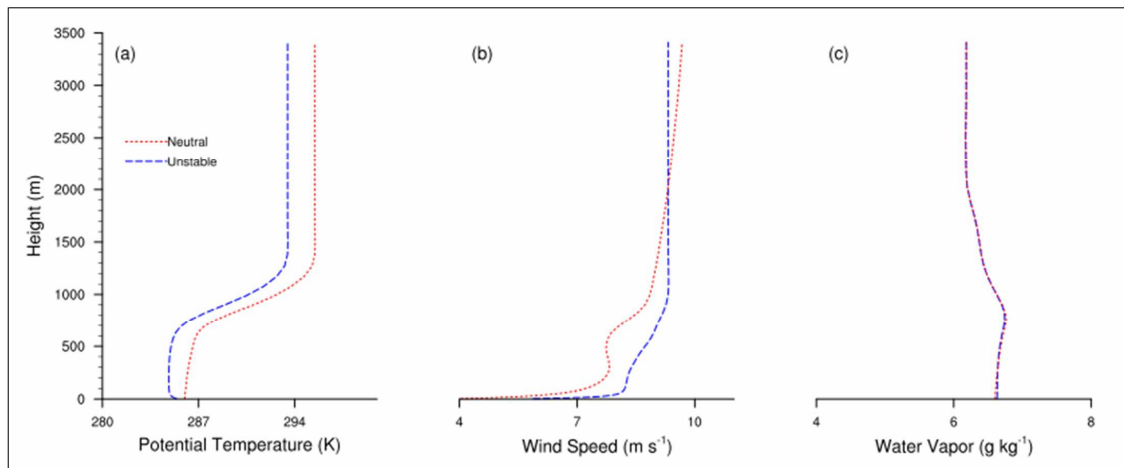


Figure 2 The potential temperature(a), wind speed(b), and water vapor(c) profiles just after turbulence spin up and before ignition are shown here.

The WRF surface vegetation was defined to be mixed shrub and grassland (FUELMAP - USGS 9) having a soil moisture of 15% and a roughness height of 6 cm. Turbulence was initiated via a combination of surface roughness, surface heat flux, a temporary heat bubble, and shear stress from the initial condition vertical profiles. The onset of turbulence occurred at 3 minutes for both the unstable and neutral cases. Both cases were considered to have fully developed turbulent structure, resembling the structure of a daytime CBL, when the change in the standard deviation of the average surface winds as well as the surface momentum flux were steady (Figure 3).

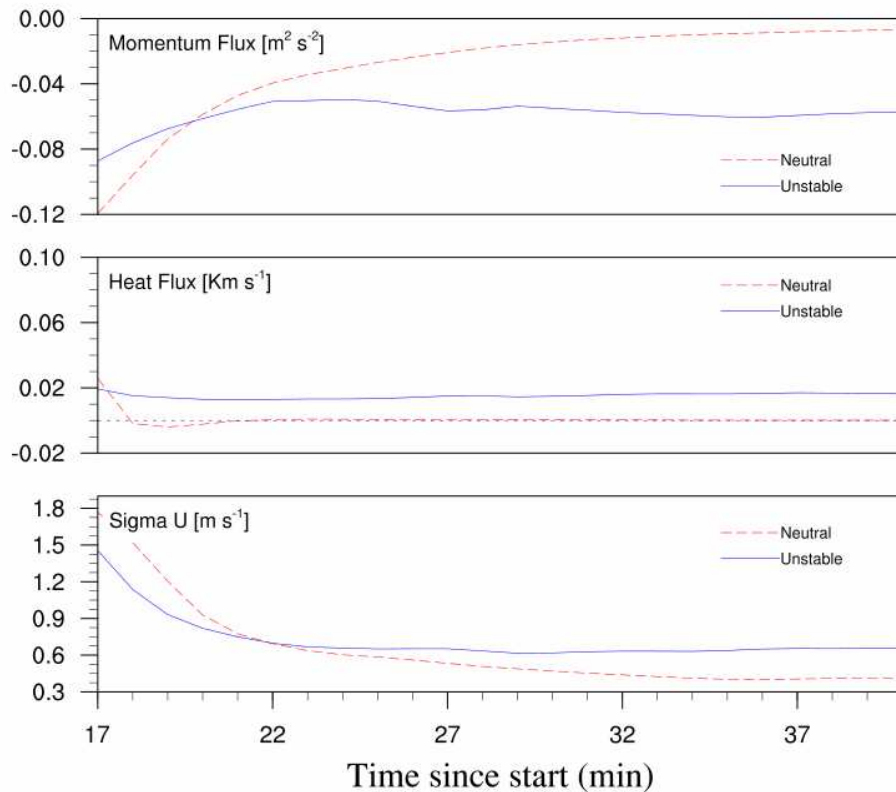


Figure 3 Time series of surface momentum and heat fluxes as well as the standard deviation of U-direction winds show stable behavior after 37 minutes from the start of the simulation.

For the control case, ignition of a 300 m long line-fire, having an ignition radius of 12 m, began at 42 minutes after the start of the simulation, when turbulence was fully developed.

Fire-line ignition timing was varied to capture the range of influence of turbulent surface winds on ROS and plume rise. For both stability cases, the ignition timing was delayed by 1, 3, 5, 7, and 10 minutes resulting in six replications for each case (including the control cases). The ignition occurred instantaneously and was centered along the y -axis, 1.5 km from the inlet (left most) edge of the model domain. The fuel category for the fire model is tall grass (Anderson category 3) with a height of 0.762 m and an initial mass loading of 0.674 kg m^{-2} . The heat of combustion of completely dry tall grass was set at $17.4 \times 10^6 \text{ J kg}^{-1}$ and its dead-fuel moisture of extinction was 25%. The fuel-moisture content was set at 10%.

3.3.3. Analysis Methods

Plume rise and fire-line forward ROS were calculated using the available standard outputs of water vapor mixing ratio and fire area respectively. For the scope of this work, we assumed that fire-line forward ROS was the rate-of-change in the furthest x -direction extent of fire area. Thus, this forward ROS value is assumed to be an x -direction rate of lateral motion of the fire area that does not give insight into the y -direction motion of the fire line (ROS of the flanks of the fire-line). This assumption seems reasonable given the dominant x -direction winds and log profile vertical wind shear. As an example of what the shape of the surface fire looks like, an arced shape for the advancing flame front (from left to right) can be seen in the surface (yellow-red area) plot of fire emitted total heat flux in Figure 1.

WRF-Fire does not model smoke emissions resulting from biomass burning. Thus, water vapor concentrations, higher than background, were used as a proxy for the presence and location of the pyrogenic plume. An example of this excess water vapor can be seen in the vertical slice (contours) of the model domain illustrated in Figure 1.

To track plume dynamics, we sampled the volume defined by 27 y-axis cells along the center of the domain so that only the region directly upwind, at, and downwind of the fire area were used. This means that water vapor travelling parallel to the fire, but outside this central sampling region, was not used in the following calculations. The height of the center-of-mass of the vapor plume (H) was estimated as

$$H = \frac{\sum z \bar{Q} dz}{\sum \bar{Q} dz} \quad (1)$$

where \bar{Q} is the averaged perturbation of water-vapor concentration along the y axis, described on an x - z plane; z is the height AGL of each vertical cell center; and dz represents the thickness of each vertical cell.

A new metric of fire area, termed Rate of Growth (ROG) was used to further investigate fire behavior beyond the traditional ROS measure.

$$\text{ROG}(t) = \frac{A_f(t) - A_f(t-1)}{\Delta t} \quad (2)$$

ROG is defined as the change in overall fire area (A_f) per unit time (Δt). This variable was calculated using the fire area variable corresponding with the finer fire mesh already calculated by WRF-Fire.

3.4. RESULTS

3.4.1. Fire-line ROS

Figure 4 shows average forward ROS (solid and dashed lines) and standard deviation (pattern-filled area) for the six neutral case (blue) and six unstable case (red) replications.

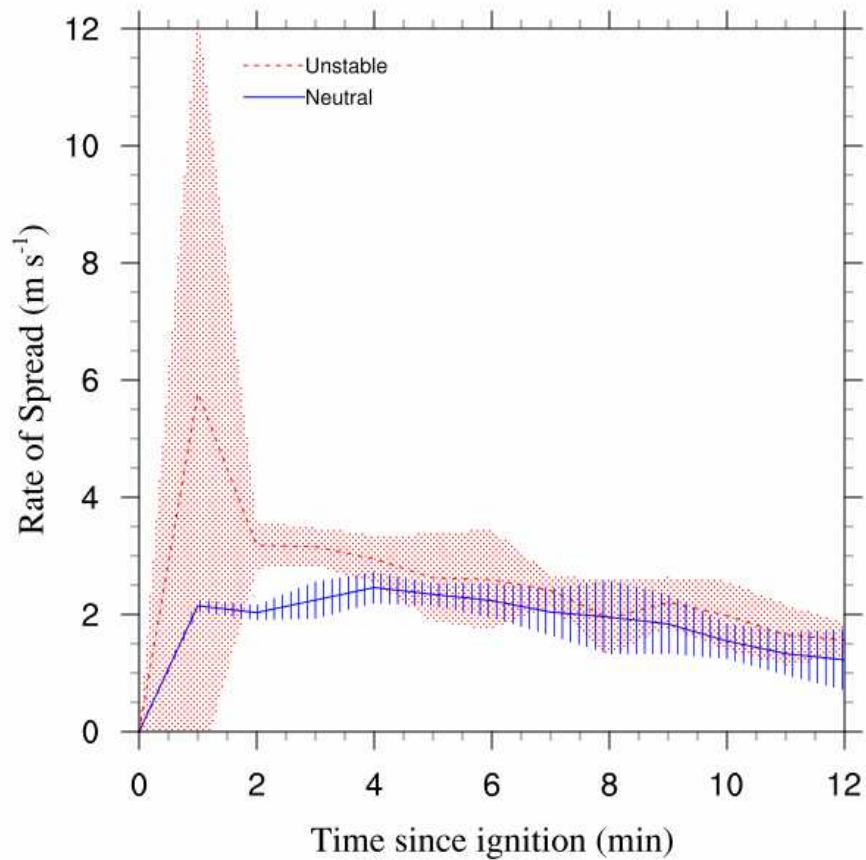


Figure 4 The solid and dashed lines denote the average forward ROS for the neutral (blue) case and unstable (red) case respectively. The shaded areas denote the standard deviation for the unstable (red dots) and neutral (blue lines) cases.

At around 1 minute after ignition, on average the unstable case has a 3.5 m s^{-1} higher forward ROS than the neutral case. Two minutes after ignition, the neutral case average remains lower by between $0.25\text{-}1.0 \text{ m s}^{-1}$ except for one instance, 8 minutes after ignition,

when the two ROS are the same. After 4 minutes have passed, the average forward ROS and standard deviation, for both cases, converges to show no statistical difference between the two cases. The difference in ROS for the first 4 minutes may likely be due to the difference in vertical wind profile seen in Figure 2. The unstable and neutral case both show a slowing of the forward ROS starting approximately four minutes after ignition. The variability of the forward ROS for the neutral case is slightly more uniform among the replications with standard deviation ranging between 0.2 and 1.25 m s⁻¹ and with an average standard deviation of 0.3 m s⁻¹. The unstable case standard deviation has a range of 0.25 – 6.5 m s⁻¹ with an average standard deviation of 0.5 m s⁻¹.

The difference in fire area between the two cases is significantly different (Figure 5) with the unstable case growing to 1.7 times the size of the neutral case by the end of the 12 minutes of simulation time.

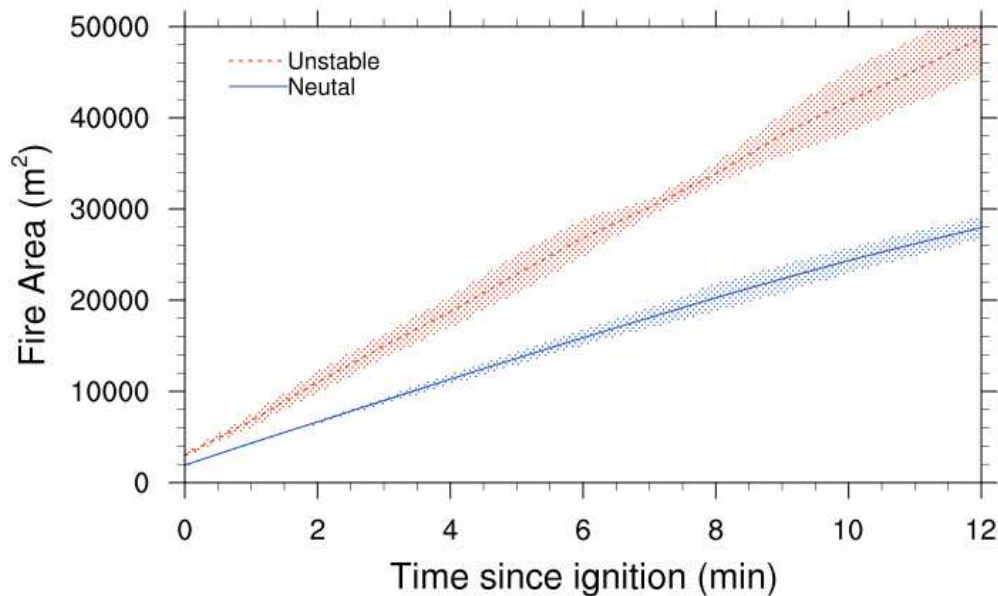


Figure 5 The dashed red line denotes the average fire area for the unstable case and the solid blue line denote the average fire area for the neutral case. The patterned areas show the standard deviation for the unstable (red) and neutral (blue) cases.

Results from ROG for the full suite of 12 simulations (Figure 6) shows that there is a slight decreasing trend in ROG for the neutral cases, having an initial ROG of $40 \text{ m}^2 \text{ s}^{-1}$ and a final ROG of $30 \text{ m}^2 \text{ s}^{-1}$.

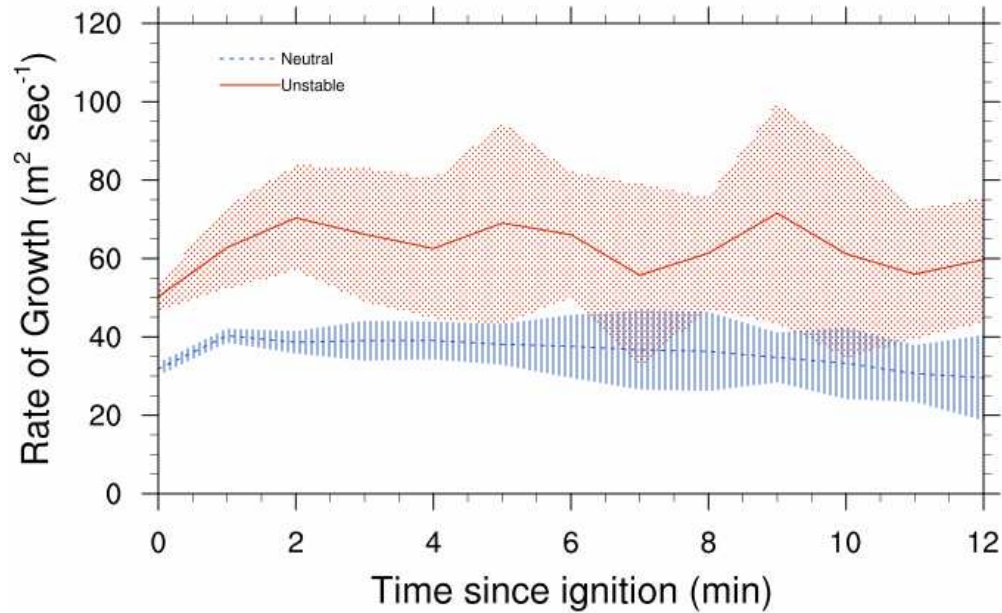


Figure 6 A Rate of Growth (ROG) time series is shown for the unstable (red) and neutral (blue) cases with the shaded red and blue areas denoting the standard deviation of the two cases respectively.

The ROG for the unstable case was more variable ($10\text{-}25 \text{ m}^2 \text{ s}^{-1}$ for the unstable case versus $5\text{-}10 \text{ m}^2 \text{ s}^{-1}$ for the neutral case) but shows an overall constant rate during the simulation of $65 \text{ m}^2 \text{ s}^{-1}$.

3.4.2. Plume Rise

The plume center line (solid lines) for the neutral case (blue) remained below or at the thermal inversion (grey dashed line) until the plume has traveled 400 m downwind of the flaming front (Figure 7).

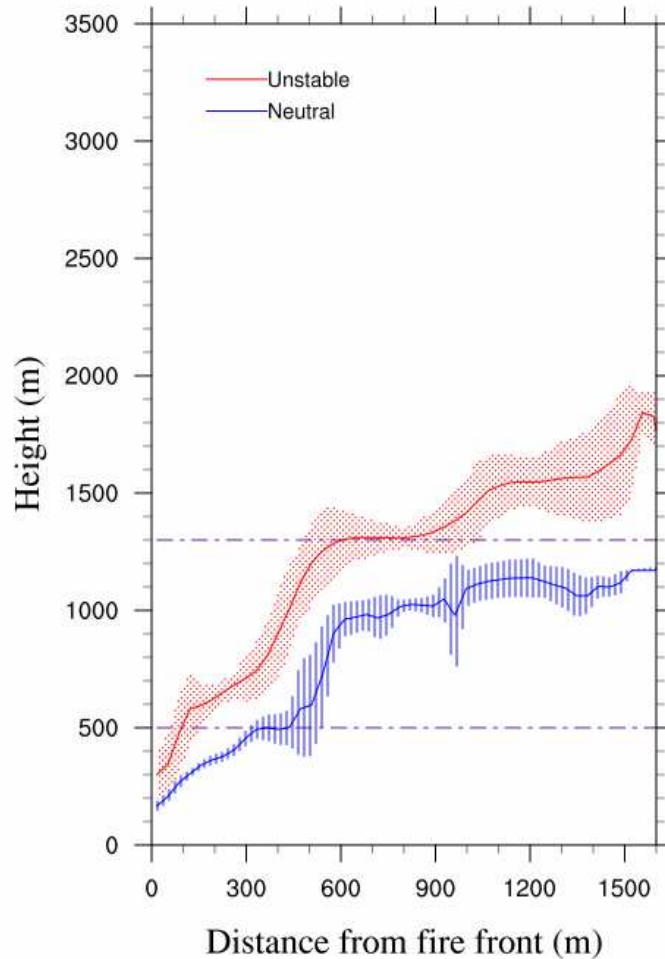


Figure 7 The solid lines represent the average plume centerline for the unstable (red) and neutral (blue) stability cases. The shaded areas represent the standard deviations for the unstable (red dots) and neutral (blue lines) cases. The gray dashed lines denote the top and bottom of the thermal inversion at 1.3km and 0.5 km AGL respectively. The bottom gray dashed line is also defined as the top of the CBL.

The unstable case (red) pushes through this thermal inversion at 100 m downwind of the flaming front. Both plume rise above the inversion layer with final plume height, 13 minutes after ignition, resting at 1150 m for the neutral case and increasing to 1650 m for the unstable case. The standard deviations (pattern-filled areas) for both cases are roughly equivalent.

3.5. DISCUSSION

The average ROS for the unstable case was significantly higher than that of the neutral case for the first 4 minutes of the simulations with the largest difference in average ROS (3.5 m s^{-1}) occurring one minute from the start of the simulation. In the neutral case, there was no background surface heat flux, while the unstable case had a background surface heat flux of 100 W m^{-2} . The lack of background surface heating in the neutral case would lead to less energetic vertical motion with surface flows being dominated by background wind speeds predominantly parallel to the surface before ignition occurred. Conversely, the unstable case is subject to a uniform surface heating that would amplify vertical mixing and surface turbulent kinetic energy.

The total fire area 12 minutes after ignition for the unstable case was almost twice the size of that for the neutral case even though surface winds were virtually identical. This suggests that surface heating and the associated effect on atmospheric stability may be a strong forcing mechanism for fire behavior above and beyond the usual metrics of surface wind speed and fuel characteristics. We speculate that the results of these findings would likely be enhanced in an environment with topographic relief present. Specifically terrain features would likely magnify the vertical motion that dominates the background surface flow before ignition of a fire even takes place.

The ROG metric, introduced in this work, yields insight into the overall growth of the fire with the unstable case showing constant growth while the neutral case has a decreasing trend in ROG. This behavior could not have been teased out of solely looking at the ROS, and thus yields new insights into the overall fire activity. The measurable differences in ROG lend potential insights into the influence that atmospheric stability

has on the overall growth of a fire under no versus slight surface heating conditions. Recall that in Figure 5 the change in fire area was discernibly different for the two cases. The difference in rate, the trend of these rates, and the overall variability in these rates would not have been obvious without further looking at the ROG. This study suggests that atmospheric stability plays an important role in the ROG of prescribed fires.

The 500 m lower plume rise for the neutral case can also be attributed to the lack of background surface heating and thus damped vertical motion at the surface. The neutral plume remained below the thermal inversion (0.5 km AGL) for an extra 300 m downwind as compared to the unstable plume. This is likely due to the lack of surface heating in the neutral case. Though the difference in overall plume rise between the two cases can be considered significant, the dominant forcing of plume rise for both cases appears to be the location of the thermal inversion which denotes the top of the CBL. More specifically, though both plumes rise above the CBL, this thermal inversion layer appears to be the dominant damping mechanism which results in differences in plume rise height between the two cases. Two minutes after ignition, the ROG for the neutral burn begins to decrease. This decrease in growth rate, along with the lack of background surface heating could both be factors in the lower plume rise for the neutral case.

3.6. SUMMARY AND CONCLUSIONS

The purpose of the study was to investigate the impact of surface heating and associated lower-level atmospheric stability in a turbulent boundary layer while at the same time purposefully ignoring the role of moisture content of the fuels and changes in CBL humidity. We found that head-fire ROS was little influenced and was not an informative metric for understanding overall fire behavior. A fire area metric called rate

of growth (ROG) was introduced that subsequently showed significantly different behavior that suggested the neutral stability case was energetically decreasing with time while the unstable case produced a constant (though variable) growth environment. The authors know of no data sets available for which to compare these findings. The neutral stability case produced lower overall plume heights, which settled out within the thermal inversion layer. The unstable case pushed through this inversion layer and continued to rise an additional 400 m, suggesting that the vertical momentum for this case was high enough to overcome complete damping during ascent through an inversion.

Jenkins (2004) used a parcel model to determine that near adiabatic lapse rates (neutral conditions) and deeper boundary layers characterized the largest vertical ascent. She also found that the presence of a thermal inversion above the boundary layer significantly damped out vertical ascent. Our findings show a larger vertical ascent with the transition from neutral to unstable conditions in the boundary layer. Though the presence of a thermal inversion above the boundary layer did appear to influence the final height of both smoke plumes, the plume for the unstable case lifted above the top of the thermal inversion layer (above 1300 m AGL).

For this analysis, the limitations in using water vapor as a tracer for smoke plumes meant that we were limited to a distance of 1.6 km downwind of the fire for our analysis. The neutral plume has reached its steady state location by this distance; however, the unstable plume is still rising and its final height is not known. Due to the limitations of using periodic boundary conditions, we had to make the assumption that simulating 13 minutes of an idealized fire was sufficient to develop relationships between atmospheric

stability and the resulting fire dynamics. Given the scope and scale of this study, these limitations seem reasonable

For future work, quantifying the role of surface heating on ROS and plume centerline is needed to either assert or refute the hypothesis that surface heating dominantly influenced plume rise. The relative importance of the surface heating from the surface fire versus that of the background conditions also needs to be investigated. Further work looking at the relative importance of the CBL thermal inversion location is currently underway.

3.7. REFERENCES

- Akagi, S. K., J. S. Craven, J. W. Taylor, G. R. McMeeking, R. J. Yokelson, I. R. Burling, S. P. Urbanski, et al. 2012. “Evolution of Trace Gases and Particles Emitted by a Chaparral Fire in California.” *Atmospheric Chemistry and Physics* 12 (3): 1397–1421. doi:10.5194/acp-12-1397-2012.
- Akagi, S. K., R. J. Yokelson, I. R. Burling, S. Meinardi, I. Simpson, D. R. Blake, G. R. McMeeking, et al. 2013. “Measurements of Reactive Trace Gases and Variable O-3 Formation Rates in Some South Carolina Biomass Burning Plumes.” *Atmospheric Chemistry and Physics* 13 (3): 1141–1165. doi:10.5194/acp-13-1141-2013.
- Akagi, S. K., R. J. Yokelson, C. Wiedinmyer, M. J. Alvarado, J. S. Reid, T. Karl, J. D. Crouse, and P. O. Wennberg. 2011. “Emission Factors for Open and Domestic Biomass Burning for Use in Atmospheric Models.” *Atmospheric Chemistry and Physics* 11 (9): 4039–4072. doi:10.5194/acp-11-4039-2011.
- Andreae, Meinrat O., and P. Merlet. 2001. “Emission of Trace Gases and Aerosols from Biomass Burning.” *Global Biogeochemical Cycles* 15 (4): 955–966.
- Arizona Department of Environmental Quality. 2003. “Simple Approach Smoke Estimation Model (SASEM), Version 4.0”. Arizona Department of Environmental Quality.
<http://www.azdeq.gov/enviro/air/smoke/download/sasemi.pdf>.
- Bertschi, I., R. J. Yokelson, D. E. Ward, R. E. Babbitt, R. A. Susott, J. G. Goode, and W. M. Hao. 2003. “Trace Gas and Particle Emissions from Fires in Large Diameter and Belowground Biomass Fuels.” *Journal of Geophysical Research-Atmospheres* 108 (D13) (February 15). doi:10.1029/2002JD002100.
- Breyfogle, S., and S. Ferguson. 1996. “User Assessment of Smoke-Dispersion Models for Wildland Biomass Burning”. General Technical Report PNW-GTR-379. Pacific Northwest Research Station: USDA, Forest Service.
- Bunting, S. C., B. M. Kilgore, and C. L. Bushey. 1987. *Guidelines for Prescribed Burning Sagebrush-grass Rangelands in the Northern Great Basin*.
<http://www.treesearch.fs.fed.us/pubs/25027>.
- Burling, I. R., R. J. Yokelson, S. K. Akagi, S. P. Urbanski, C. E. Wold, D. W. T. Griffith, T. J. Johnson, J. Reardon, and D. R. Weise. 2011. “Airborne and Ground-based Measurements of the Trace Gases and Particles Emitted by Prescribed Fires in the United States.” *Atmospheric Chemistry and Physics* 11 (23): 12197–12216. doi:10.5194/acp-11-12197-2011.

- Burling, I. R., R. J. Yokelson, D. W. T. Griffith, T. J. Johnson, P. Veres, J. M. Roberts, C. Warneke, et al. 2010. "Laboratory Measurements of Trace Gas Emissions from Biomass Burning of Fuel Types from the Southeastern and Southwestern United States." *Atmospheric Chemistry and Physics* 10 (22): 11115–11130. doi:10.5194/acp-10-11115-2010.
- Chen, L.-W. A., P. Verburg, A. Shackelford, D. Zhu, R. Susfalk, J. C. Chow, and J. G. Watson. 2010. "Moisture Effects on Carbon and Nitrogen Emission from Burning of Wildland Biomass." *Atmos. Chem. Phys.* 10 (14) (July 20): 6617–6625. doi:10.5194/acp-10-6617-2010.
- Christian, T. J., B. Kleiss, R. J. Yokelson, R. Holzinger, P. J. Crutzen, W. M. Hao, B. H. Saharjo, and D. E. Ward. 2003. "Comprehensive Laboratory Measurements of Biomass-burning Emissions: 1. Emissions from Indonesian, African, and Other Fuels." *Journal of Geophysical Research-Atmospheres* 108 (D23) (December 4). doi:10.1029/2003JD003704.
- Clark, T. L., J. L. Coen, and D. Latham. 2004. "Description of a Coupled Atmosphere-fire Model." *International Journal of Wildland Fire* 13 (1): 49–63. doi:10.1071/WF03043.
- Clark, T. L., M. A. Jenkins, J. L. Coen, and D. R. Packham. 1996. "A Coupled Atmosphere-fire Model: Role of the Convective Froude Number and Dynamic Fingering at the Fireline." *International Journal of Wildland Fire* 6 (4) (December): 177–190. doi:10.1071/WF9960177.
- Coen, J. L. 2005. "Simulation of the Big Elk Fire Using Coupled Atmosphere-fire Modeling." *International Journal of Wildland Fire* 14 (1): 49–59. doi:10.1071/WF04047.
- Coen, J. L., M. Cameron, J. Michalakes, E. G. Patton, P. J. Riggan, and K. M. Yedinak. 2013. "WRF-Fire: Coupled Weather-Wildland Fire Modeling with the Weather Research and Forecasting Model." *Journal of Applied Meteorology and Climatology* 52 (1) (January): 16–38. doi:10.1175/JAMC-D-12-023.1.
- Crosby, JS. 1949. "Vertical Wind Currents and Fire Behavior." *Fire Control Notes* 10 (2): 12–14.
- Cunningham, Philip, and Michael J. Reeder. 2009. "Severe Convective Storms Initiated by Intense Wildfires: Numerical Simulations of Pyro-convection and Pyro-tornadogenesis." *Geophysical Research Letters* 36 (June 26). doi:10.1029/2009GL039262.
- Dennis, A., M. Fraser, S. Anderson, and D. Allen. 2002. "Air Pollutant Emissions Associated with Forest, Grassland, and Agricultural Burning in Texas." *Atmospheric Environment* 36 (23) (August): 3779–3792. doi:10.1016/S1352-2310(02)00219-4.

- Dignon, J., and J. E. Penner. 1991. In *Global Biomass Burning: Atmospheric, Climatic, and Biospheric Implications*, by Joel S. Levine. MIT Press.
- Eidsmoe, G. 2007. "Investigation Report: Guejito Fire". Investigation CA-MVU-010484. Guejito Creek drainage: California Department of Forestry and Fire Protection. http://www.fire.ca.gov/fire_protection/downloads/redsheets/CA-MVU-010484_Complete.pdf.
- Ferek, R. J., J. S. Reid, P. V. Hobbs, C. R. Blake, and C. Liou. 1998. "Emission Factors of Hydrocarbons, Halocarbons, Trace Gases and Particles from Biomass Burning in Brazil." *Journal of Geophysical Research: Atmospheres* 103 (D24): 32107–32118. doi:10.1029/98JD00692.
- Freitas, S. R., K. M. Longo, R. Chatfield, D. Latham, M. A. F. Silva Dias, M. O. Andreae, E. Prins, J. C. Santos, R. Gielow, and J. A. Carvalho Jr. 2007. "Including the Sub-grid Scale Plume Rise of Vegetation Fires in Low Resolution Atmospheric Transport Models." *Atmos. Chem. Phys.* 7 (13) (July 2): 3385–3398. doi:10.5194/acp-7-3385-2007.
- Gilbert, M. 2008. "Investigation Report: Witch Fire". Investigation 07-CDF-570. Highway 78 west of Santa Ysabel, San Diego County: California Department of Forestry and Fire Protection. http://www.fire.ca.gov/fire_protection/downloads/redsheets/CA-MVU-010432_Complete.pdf.
- Goodrick, S. L., G. L. Achtemeier, N. K. Larkin, Y. Liu, and T. M. Strand. 2013. "Modelling Smoke Transport from Wildland Fires: a Review." *International Journal of Wildland Fire* 22 (1): 83–94.
- Goodrick, Scott L., Gary L. Achtemeier, Narasimhan K. Larkin, Yongqiang Liu, and Tara M. Strand. 2013. "Modelling Smoke Transport from Wildland Fires: a Review." *International Journal of Wildland Fire* 22 (1): 83–94.
- Haines, D. A. 1988. "A Lower Atmospheric Severity Index for Wildland Fires." *National Weather Digest* 13 (2): 23–27.
- Hardy, C., R. Ottmar, J. Peterson, J. Core, and P. Seamon, ed. 2001. "Smoke Management Guide for Prescribed and Wildland Fire". National Wildfire Coordination Group. <http://www.nwcg.gov/pms/pubs/SMG/SMG-72.pdf>.
- Hayes, G. L. 1941. "Influences of Altitude and Aspect on Daily Variations in Factors of Fire Danger." *US Department of Agriculture, Circular 591* (Washington DC).
- Jain, R., J. Vaughan, K. Heitkamp, C. Ramos, C. Claiborn, M. Schreuder, M. Schaaf, and B. Lamb. 2007. "Development of the ClearSky Smoke Dispersion Forecast System for Agricultural Field Burning in the Pacific Northwest." *Atmospheric Environment* 41 (32) (October): 6745–6761. doi:10.1016/j.atmosenv.2007.04.058.

- Jenkins, M. A. 2004. "Investigating the Haines Index Using Parcel Model Theory." *International Journal of Wildland Fire* 13 (3): 297–309. doi:10.1071/WF03055.
- Jolly, W. M. 2007. "Sensitivity of a Surface Fire Spread Model and Associated Fire Behaviour Fuel Models to Changes in Live Fuel Moisture." *International Journal of Wildland Fire* 16 (4): 503–509.
- Keeley, J. E., G. H. Aplet, N. L. Christensen, S. G. Conard, E. A. Johnson, P. N. Omi, D. L. Peterson, and T. W. Swetnam. 2009. "Ecological Foundations for Fire Management in North American Forest and Shrubland Ecosystems". United States Department of Agriculture, Forest Service, Pacific Northwest Research Station, Portland, OR. <http://www.treesearch.fs.fed.us/pubs/32483>.
- Kilgore, B. M., and G. A. Curtis. 1987. *Guide to Understory Burning in Ponderosa Pine-larch-fir Forests in the Intermountain West*. <http://www.treesearch.fs.fed.us/pubs/32954>.
- Kochanski, A., M. A. Jenkins, J. Mandel, J. Beezley, and S. Krueger. 2013. "Real Time Simulation of 2007 Santa Ana Fires." *Forest Ecology and Management* 294 (April 15): 136–149. doi:10.1016/j.foreco.2012.12.014.
- Kochanski, A., M. A. Jenkins, R. Sun, S. Krueger, S. Abedi, and J. Charney. 2013. "The Importance of Low-level Environmental Vertical Wind Shear to Wildfire Propagation: Proof of Concept." *Journal of Geophysical Research: Atmospheres*: n/a–n/a. doi:10.1002/jgrd.50436.
- Lavdas, L. G. 1996. "Program VSMOKE: Users Manual". General Technical Report GTR-SRS-006. Southeastern Research Station: USDA, Forest Service.
- Lobert, J. M., D. H. Scharffe, W. Hao, T. A. Kuhlbusch, R. Seuwen, P. Warneck, and P. J. Crutzen. 1991. "Experimental Evaluation of Biomass Burning Emissions: Nitrogen and Carbon Containing Compounds." In *Global Biomass Burning*, edited by J. S. Levine, 289–304. MIT Press.
- McMeeking, Gavin R., Sonia M. Kreidenweis, Stephen Baker, Christian M. Carrico, Judith C. Chow, Jeffrey L. Collett, Wei Min Hao, et al. 2009. "Emissions of Trace Gases and Aerosols During the Open Combustion of Biomass in the Laboratory." *Journal of Geophysical Research-Atmospheres* 114 (October 14). doi:10.1029/2009JD011836.
- Naeher, Luke P, Gary L Achtemeier, Jeff S Glitzenstein, Donna R Streng, and David Macintosh. 2006. "Real-time and Time-integrated PM_{2.5} and CO from Prescribed Burns in Chipped and Non-chipped Plots: Firefighter and Community Exposure and Health Implications." *Journal of Exposure Science & Environmental Epidemiology* 16 (4) (July): 351–361. doi:10.1038/sj.jes.7500497.
- NCAR. 2012. *Weather Research and Forecasting Model* (version 3.4). http://www.mmm.ucar.edu/wrf/users/download/get_source.html.

- Nelson, R. M. 2003. "Power of the Fire - a Thermodynamic Analysis." *International Journal of Wildland Fire* 12 (1): 51–65. doi:10.1071/WF02032.
- Nelson, Rm. 1993. "Byram Derivation of the Energy Criterion for Forest and Wildland Fires." *International Journal of Wildland Fire* 3 (3) (September): 131–138. doi:10.1071/WF9930131.
- "NICC Wildland Fire Annual Report." 2012. NIFC.
<http://www.predictiveservices.nifc.gov/intelligence/intelligence.htm>.
- Pharo, J. A., L. G. Lavadas, and P. M. Bailey. 1976. "Smoke Transport and Dispersion". General Technical Report SE-10. Southern Forestry Smoke Management Guidebook. Southeastern Research Station: USDA, Forest Service.
- Potter, B. E. 2002. "A Dynamics Based View of Atmosphere-fire Interactions." *International Journal of Wildland Fire* 11 (3-4): 247–255. doi:10.1071/WF02008.
- . 2012a. "Atmospheric Interactions with Wildland Fire Behaviour – I. Basic Surface Interactions, Vertical Profiles and Synoptic Structures." *International Journal of Wildland Fire* 21 (7): 779–801.
- . 2012b. "Atmospheric Interactions with Wildland Fire Behaviour – II. Plume and Vortex Dynamics." *International Journal of Wildland Fire* 21 (7): 802–817.
- Reifsnyder, W. E. 1954. "Atmospheric Stability and Forest Fire Behavior". PhD dissertation, New Haven, CT: Yale University.
- Rothermel, R. C. 1972. "A Mathematical Model for Predicting Fire Spread in Wildland Fuels." *USDA Forest Service, Intermountain Forest and Range Experiment Station, Research Paper INT-115*.
- . 1983. *How to Predict the Spread and Intensity of Forest and Range Fires*.
<http://www.treesearch.fs.fed.us/pubs/24635>.
- Sandberg, David V., Roger D. Ottmar, and Janice L. Peterson. 2002. "Wildland Fire in Ecosystems: Effects of Fire on Air." <http://www.treesearch.fs.fed.us/pubs/5247>.
- Scire, J. S., D. G. Strimaitis, and R. J. Yamartino. 2000. "A User's Guide for the CALPUFF Dispersion Model (Version 5)". User's guide. Concord, MA: EarthTech Inc.
- Skamarock, W. C., J. B. Klemp, J. Dudhia, D. O. Gill, D. M. Barker, M. G. Duda, X. Huang, W. Wang, and J. G. Powers. 2008. "A Description of the Advanced Research WRF Version 3". National Center for Atmospheric Research.
- Trentmann, J., M. O. Andreae, H. F. Graf, P. V. Hobbs, R. D. Ottmar, and T. Trautmann. 2002. "Simulation of a Biomass-burning Plume: Comparison of Model Results

- with Observations.” *Journal of Geophysical Research-Atmospheres* 107 (D1-D2) (January). doi:10.1029/2001JD000410.
- Urbanski, S. P. 2013. “Combustion Efficiency and Emission Factors for Wildfire-season Fires in Mixed Conifer Forests of the Northern Rocky Mountains, US.” *Atmos. Chem. Phys.* 13 (14) (July 30): 7241–7262. doi:10.5194/acp-13-7241-2013.
- Viney, NR. 1991. “A Review of Fine Fuel Moisture Modelling.” *International Journal of Wildland Fire* 1 (4) (January 1): 215–234.
- Ward, D. E., and C. C. Hardy. 1991. “Smoke Emissions from Wildland Fires.” *Environment International* 17 (2–3): 117–134. doi:10.1016/0160-4120(91)90095-8.
- Ward, D. E., and L. F. Radke. 1993. “Emissions Measurements from Vegetation Fires: A Comparative Evaluation of Methods and Results.” In , 53–76. <http://www.treearch.fs.fed.us/pubs/40604>.
- Wiedinmyer, C., S. K. Akagi, R. J. Yokelson, L. K. Emmons, J. A. Al-Saadi, J. J. Orlando, and A. J. Soja. 2011. “The Fire INventory from NCAR (FINN): a High Resolution Global Model to Estimate the Emissions from Open Burning.” *Geoscientific Model Development* 4 (3): 625–641. doi:10.5194/gmd-4-625-2011.
- Yokelson, R. J., I. R. Burling, J. B. Gilman, C. Warneke, C. E. Stockwell, J. de Gouw, S. K. Akagi, et al. 2013. “Coupling Field and Laboratory Measurements to Estimate the Emission Factors of Identified and Unidentified Trace Gases for Prescribed Fires.” *Atmospheric Chemistry and Physics* 13 (1): 89–116. doi:10.5194/acp-13-89-2013.
- Yokelson, R. J., J. G. Goode, D. E. Ward, R. A. Susott, R. E. Babbitt, D. D. Wade, I. Bertschi, D. W. T. Griffith, and W. M. Hao. 1999. “Emissions of Formaldehyde, Acetic Acid, Methanol, and Other Trace Gases from Biomass Fires in North Carolina Measured by Airborne Fourier Transform Infrared Spectroscopy.” *Journal of Geophysical Research: Atmospheres* 104 (D23): 30109–30125. doi:10.1029/1999JD900817.
- Yokelson, R. J., D. W. T. Griffith, and D. E. Ward. 1996. “Open-path Fourier Transform Infrared Studies of Large-scale Laboratory Biomass Fires.” *Journal of Geophysical Research-Atmospheres* 101 (D15) (September 20): 21067–21080. doi:10.1029/96JD01800.
- Yokelson, R. J., R. Susott, D. E. Ward, J. Reardon, and D. W. T. Griffith. 1997. “Emissions from Smoldering Combustion of Biomass Measured by Open-path Fourier Transform Infrared Spectroscopy.” *Journal of Geophysical Research-Atmospheres* 102 (D15) (August 20): 18865–18877. doi:10.1029/97JD00852.

Yokelson, R. J., S. P. Urbanski, E. L. Atlas, D. W. Toohy, E. C. Alvarado, J. D. Crouse, P. O. Wennberg, et al. 2007. "Emissions from Forest Fires Near Mexico City." *Atmospheric Chemistry and Physics* 7 (21): 5569–5584.

CHAPTER 4: DEVELOPMENT OF A PLUME RISE ANALYSIS TECHNIQUE FOR LARGE WILDLAND FIRES USING WRF-SFIRE

4.1. ABSTRACT

Assumptions about the vertical distribution and dispersion of smoke from wildland fires are large sources of uncertainty in regional air quality models. These assumptions can be avoided altogether with the use of a coupled fire-atmosphere model. We use WRF-Sfire, a coupled fire-atmosphere model capable of spanning multiple spatial scales, and introduce the use of an inert tracer to track plume rise for the Witch and Guejito fires in southern California during 2007. By using a center-of-mass approach, we are able to resolve the centerline of the smoke plumes resulting from these fires. Our analysis agrees reasonably well with MISR satellite observations. This approach provides a foundation for linking WRF-Sfire simulations to a regional air quality model.

4.2. INTRODUCTION

At regional scales, smoke produced from wildland fires can pose risks to air quality (Hardy et al. 2001) and climate (Cunningham and Reeder 2009). Yet smoke transport, particularly plume rise, remains a large uncertainty in regional air quality models. At the regional scale, smoke plumes resulting from wildland fires, are largely modeled with the use of Eulerian grid and puff models which make assumptions or use simple stack plume rise algorithms to assign the initial vertical distribution of pollutants (Goodrick et al. 2013). Recently, the emergence of coupled fire-atmosphere models has made it possible to avoid these assumptions. The difficulty in using coupled fire-atmosphere models is twofold in that the spatial scales of interest are highly variable,

from the meter to the 100s of kilometers scale (Freitas et al., 2007), and there are currently no coupled fire-atmosphere models which also model pollutant production due to the combustion process.

We employ the use of a coupled fire-atmosphere model called WRF-Sfire, in which the Rothermel (1972) fire behavior model is coupled with the Weather Research and Forecasting (WRF) model (NCAR 2012). More information about WRF-Sfire can be found in (Kochanski et al., 2013). Through the use of a coupled fire-atmosphere model, and the introduction of an inert tracer, we are able to avoid making assumptions about vertical distribution of pollutants, size and heat release of the fire, as well as the dispersion characteristics of the local atmosphere. We apply a vertical column center-of-mass integration approach to determine the plume height of an inert tracer. This approach is evaluated for the Witch and Guejito fires, which burned in southern California during the autumn of 2007 and which were previously simulated using WRF-Sfire (Kochanski et al., 2013). Our work will contribute to future assessment and improvement of wildland fire plume rise calculations currently used in regional air quality models.

4.3. METHODS

All WRF-Sfire simulations were conducted by Kochanski and colleagues (2013). The Witch/Guejito WRF-Sfire simulation was configured with four nested domains, having horizontal grid sizes of 32, 8, 2, and 0.5 km (Figure 1).

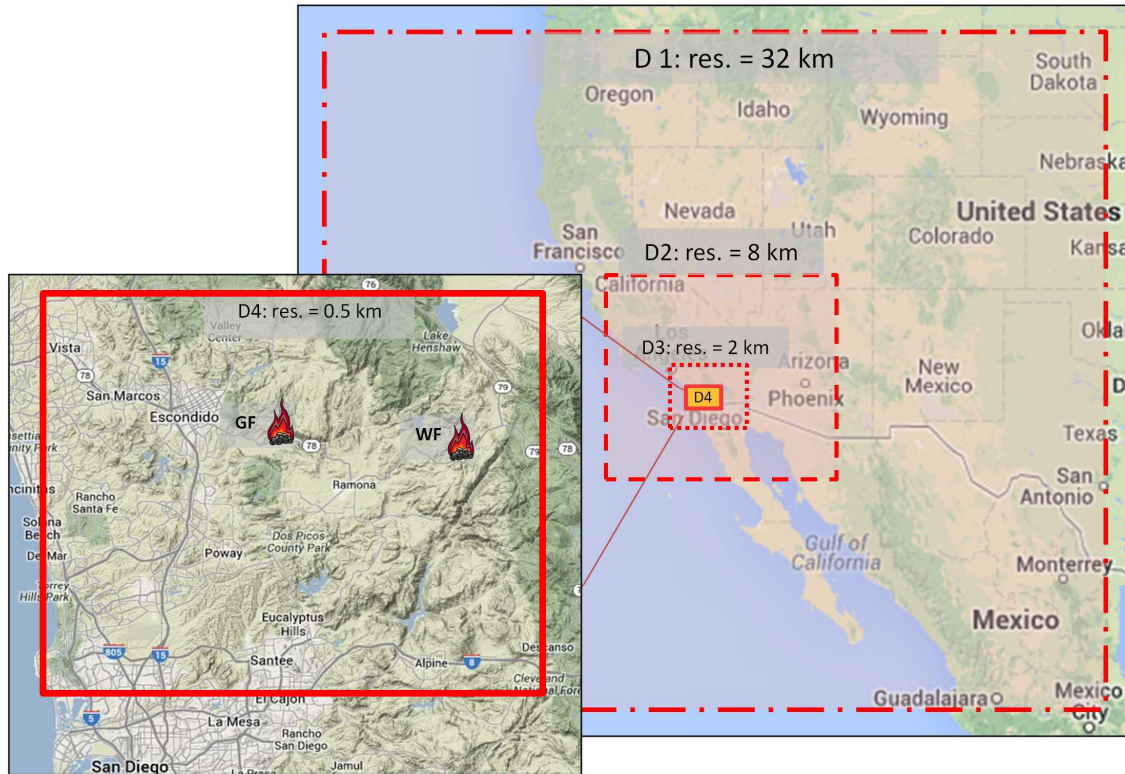


Figure 1 Model domain locations for the domains 1-4 (D1-D4) were centered over southern California. The Witch Fire (WF) and Guejito Fire (GF) locations are shown on the D4 inset at left.

The vertical dimension extended up to 15.4 km and was defined by a vertically stretched grid where the surface layer thickness was roughly 20 m and the top-most vertical layer was roughly 2000 m thick. The fire domain was located in the finest resolution domain and had a refinement ratio of 25, thus making the horizontal fire-grid cell size 20 m on a side. Outputs from the model were saved every 10 minutes. Further details of this setup can be found in Kochanski et al. (2013)

For the Witch/Guejito WRF-Sfire simulation, two tracers (dry $PM_{2.5}$ and PM_{10}), which were meant to generically represent primary particulate matter (PM), were added to the model. These tracers are inert scalars that are emitted at a rate proportional to the fuel consumption rate and thus, the heat release rate of the fire. A single tracer generically referred to as PM, which was the sum of $PM_{2.5}$ and PM_{10} , was used for this

work. Concentrations of background PM were also present in the simulation (to be used for other purposes) and thus all the particulate matter in the modeling domain does not correspond to that which was specifically released from the fire. To filter out the PM having a non-fire origin, we used a threshold column concentration of $20 \mu\text{g m}^{-3}$, below which no PM concentrations would be considered.

To track plume dynamics, we sampled the vertical distribution of the PM tracer concentrations for each x - y location in the domain volume such as those shown in Figure

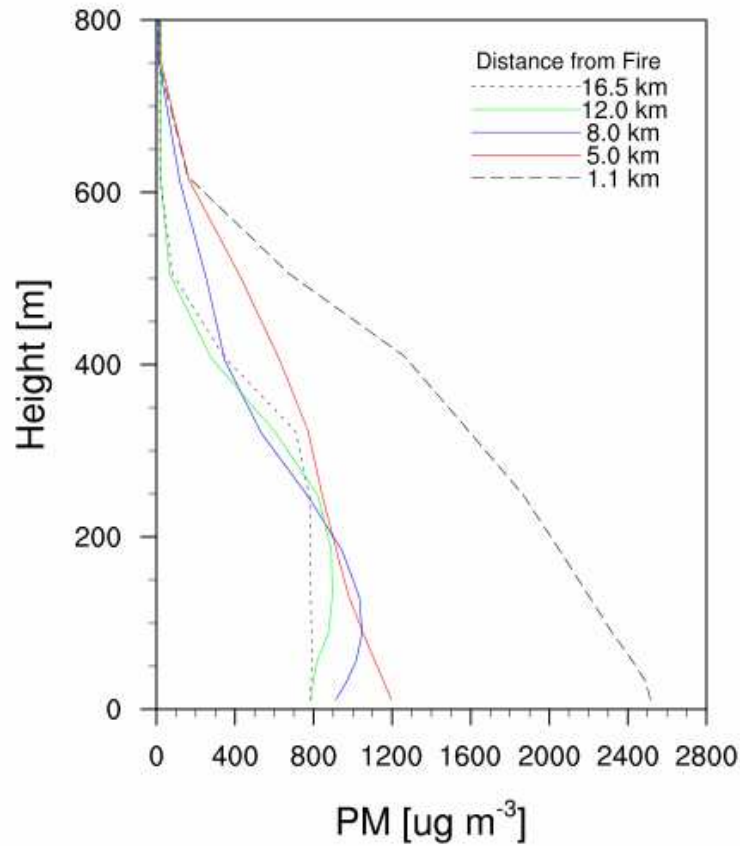


Figure 2 Column vertical profiles of PM are shown for 1.1 (black dash), 5.0 (red), 8.0 (blue), 12.0 (green), and 16.5 (grey dots) km downwind from the fire.

The height of the center-of-mass of the vapor plume (H) was estimated as

$$H = \frac{\sum zC\Delta z}{\sum C\Delta z} \quad (1)$$

where C is the concentration of the tracer along the z axis, described on an x - y plane; z is the height AGL of each vertical cell center; and Δz represents the thickness of each vertical cell.

4.3.1. Case Studies

Combined, the Witch and Guejito fires burned 79.7 ha, making these the largest fires in California for 2007. These fires took place during a strong Santa Ana wind event where strong and extremely dry down-slope winds, originating from the Great Basin and Mohave desert regions, made their way to the Pacific coast, warming as they descend in altitude.

The Witch fire was first discovered on October 21st, 2007 at 12:29 pm near State Highway 78 and Santa Ysabel. The specific origin of the fire was at Latitude 33° 04' 59.1" and Longitude -117° 41' 38.9". The cause of the fire was thought to be due to arcing between power lines. Fifteen minutes before the fire was first discovered, the Julian (16 km east of the fire origin) Remote Automated Weather Station (RAWS) reported a relative humidity of 16%, ambient temperature of 14 °C, and winds coming from the east at 10.7 m/s and gusting to 19.2 m/s (Gilbert 2008). These conditions reflected severe fire weather across southern California and thus a red flag warning.

The Guejito fire was first discovered on October 22nd, 2007 at 1:00 am in the Guejito Creek drainage, on the south side of State Highway 78 and 402 m west of Bandy Canyon Rd. (33° 05' 37.3", -116° 57' 41.9") in southern California. The cause of the fire was thought to be due to arcing between power lines. A weather station at the Ramona

Airport showed that at the time of first discovery, the ambient temperature was 22 °C, the relative humidity was 6%, 15.6 m/s winds were from the ENE and were gusting up to 19.7 m/s (Eidsmoe 2007).

4.4. RESULTS

Plume-center heights were calculated for each grid column with fire PM present for each 10-minute interval of the innermost domain (62.5 x 52.5 km), during the simulation. These plume heights were averaged over 6-hr time intervals representing nighttime (10:00pm – 4:00am) and daytime (10:00am – 4:00pm) conditions. These 6-hr averages are shown in Figure 1, where the top row (Figure 2, A 1-3) represents the nighttime hours between October 21st and 22nd, 2007; the middle row (Figure 2, B 1-3) represents the daytime hours during October 22nd; and the bottom row (Figure 2, C 1-3) represents the nighttime hours between October 22nd and 23rd.

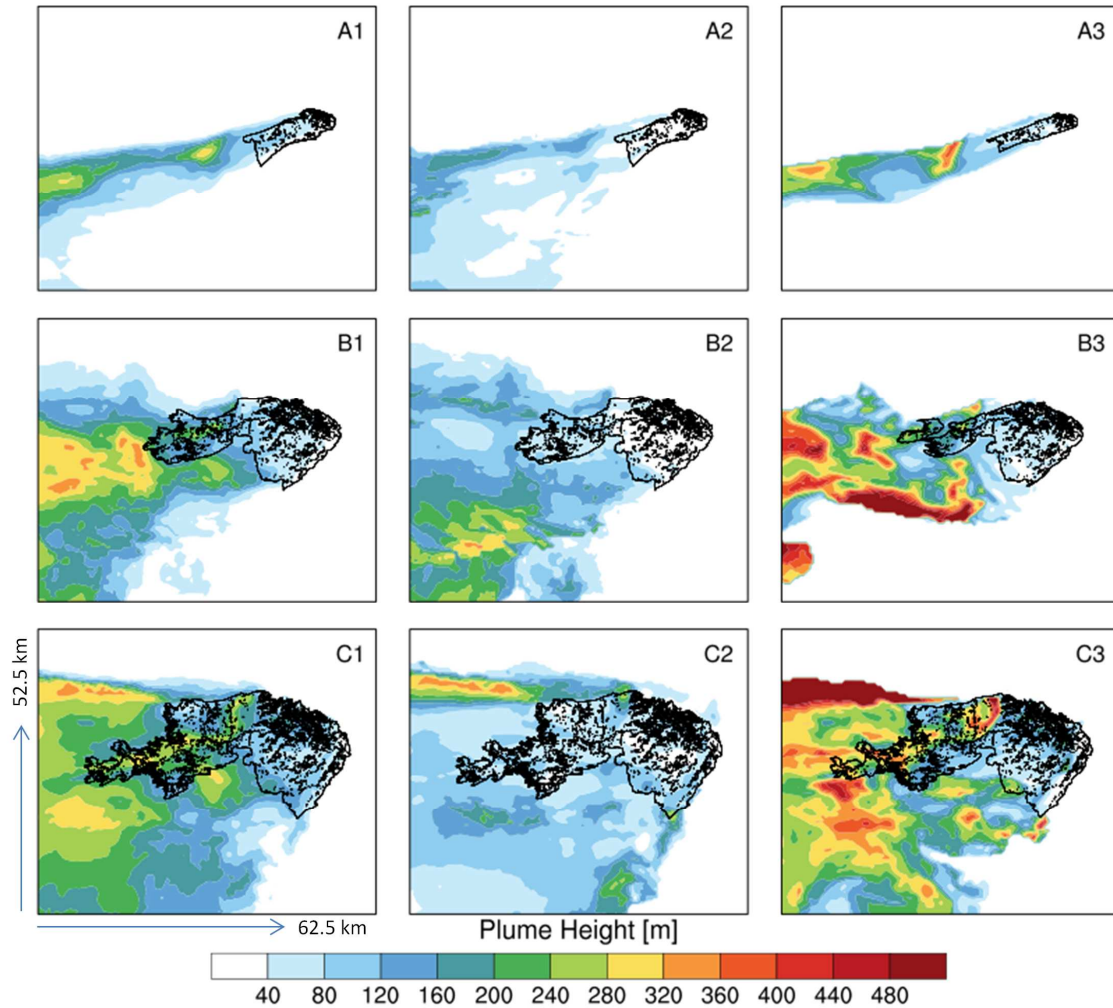


Figure 3 The rows of this panel, from left to right, represent the 6-hr averaged plume height (1), the 6-hr standard deviation of the plume height (2), and a single instance 3 hours into the 6-hr time frame (3). The rows depict three time frames, the first night (A), daytime (B), and the second night (C) during the simulation. The fire area, at the end of each time period, is shown as a black outline in each plot. The domain is 62.5 x 52.5 km.

The left most column of Figure 2 (A-C 1) depicts the 6-hr averaged plume height and associated final fire area for this time period. The middle column of this figure (A-C 2) shows the standard deviation in the 6-hr average of plume height along with the final fire area for the time period. The right most column of Figure 2 (A-C 3) shows a single snapshot of the plume height at 3 hours into the beginning of each 6-hr averaged time

period. The 6-hr average plume height never exceeded 360 m above ground level (AGL). However, in the case of the overnight 6-hr average for October 22-23 (Figure 2, C1), the standard deviation of the average exceeded the magnitude of the average itself in the upper left corner of the domain. The snap shots (Figure 2, A-C 3) show the strong variability in instantaneous plume height. At times, as is the case with Figure 2 C3, multiple plume peaks can be seen moving through the domain.

The 6-hr averaged ambient vertical temperature near the fire shows elevated surface temperatures over night (Figure 4, A1 and C1) as compared to the daytime profiles (Figure 4, B1). However, the daytime temperature profile showed the largest variability (blue shaded area) above the surface. The 6-hr averaged vertical wind speed profiles (Figure 4, A-C 2) show a very strong surface jet around 500 m above the ground with the strongest overall magnitudes as well as variability occurring during the daytime hours (B2).

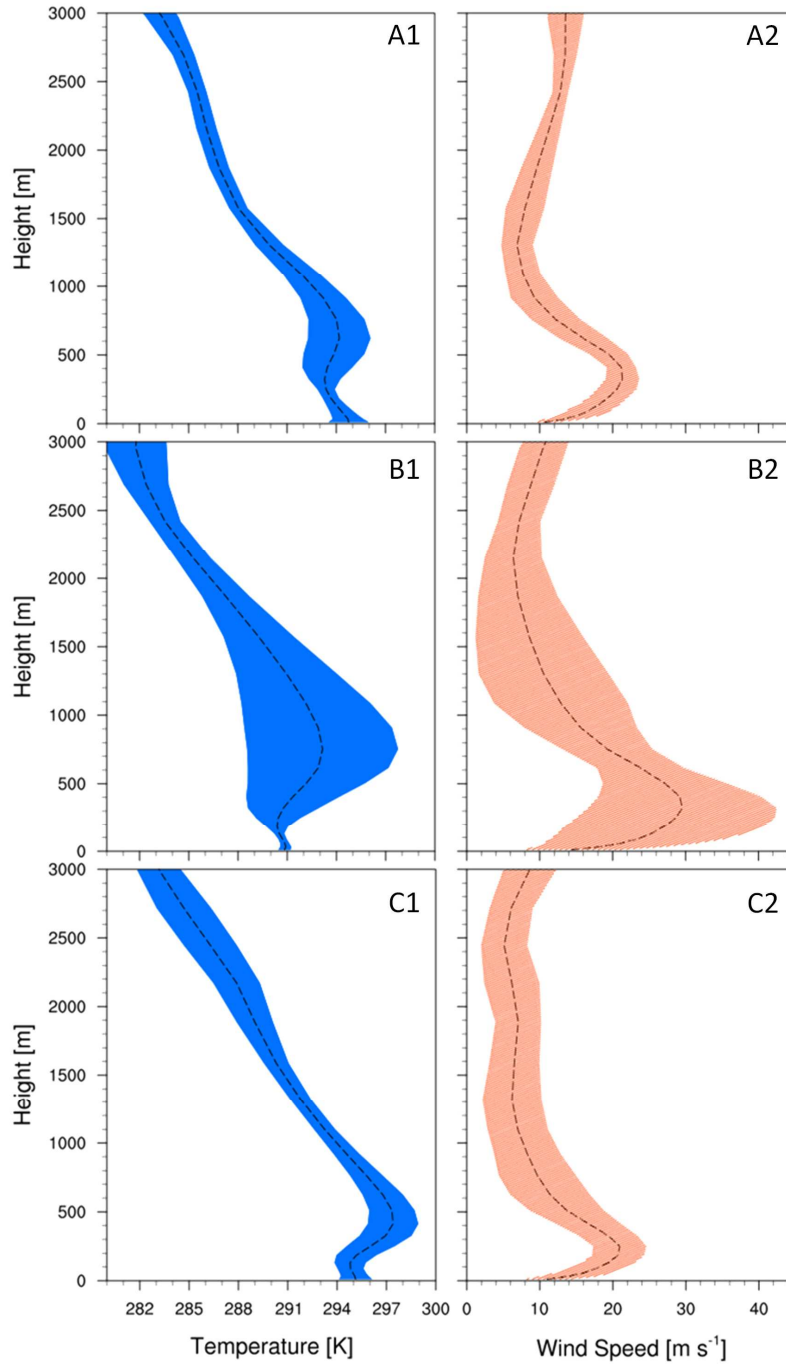


Figure 4 The panel depicts 6-hr averaged vertical profiles (black dashed line) of temperature (1) and wind speed (2) for first nighttime period (A), the daytime (B), and the following nighttime (C) during the simulation. The shaded areas represent the standard deviation of the 6-hr average for temperature (blue) and wind speed (orange).

For comparison with satellite retrievals, we also present data (Herron-Thorpe and Leung, personal communication, WSU), representing MISR plume rise calculations in the vicinity of the Witch and Guejito fires during the time period of our simulation (Table 1). MISR is a high-resolution visual imager carried on the Terra satellite, which has a sun-synchronous Earth orbit. Use of stereoscopic techniques with MISR data provides the basis for plume rise estimates for large wildland fires.

Table 1 The eight unique median plume height measures, taken using MISR retrievals during the same time period as our simulations, give estimates of the average plume height occurring in the vicinity of the Witch and Guejito fires.

Longitude	Latitude	Date	Time	Median Plume Height AGL [m]
-118.67	34.574	10/21/2007	18:39:31	540
-118.671	34.076	10/21/2007	18:39:31	455
-117.441	33.244	10/21/2007	18:39:52	943
-116.562	32.623	10/21/2007	18:39:52	684
-117.068	32.334	10/21/2007	18:40:13	691
-116.901	32.035	10/21/2007	18:40:13	367
-116.62	31.799	10/21/2007	18:40:13	829
-116.492	31.578	10/23/2007	18:27:49	963

4.5. DISCUSSION

The 6-hr averaged plume heights were generally about 100 m lower than those reported from MISR retrievals. However, as the standard deviation of the 6-hr averaged

plume height shows (Figure 3, A-C 2), there was tremendous variability in this average, with the lower predictions from MISR falling within one standard deviation of the mean simulated plume height. There is potential error associated with comparing these data to the available MISR data since it is unknown where (downwind of the fire) the median plume height was reached.

Mapping the instantaneous plume heights (like those shown in Figure 3, A-C 3) also illustrates the non-Gaussian horizontal spread of plume. At times, this method was able to capture multiple plume rise peaks that could correspond to more than one plume updraft core, which is known to occur in wildland fires (Goodrick et al. 2013).

We are making several assumptions in the use of this method, which are important to review in the context of the results presented. WRF-Sfire was setup with a stretched vertical grid. Thus, even if no vertical diffusion was modeled, there would be an appearance of vertical diffusion as the tracers rise and distribute into larger and larger cells. To be sure that the stretched vertical grid is not innately lowering the plume rise, through dilution, there would need to be comparisons made with simulations having evenly spaced vertical resolution. We are also making the assumption that there is only one peak per vertical column (Figure 5) in our integration scheme. Though for the majority of cases this may be true, there may arise situations in which two individual concentration peaks occur in the column of air (Figure 5).

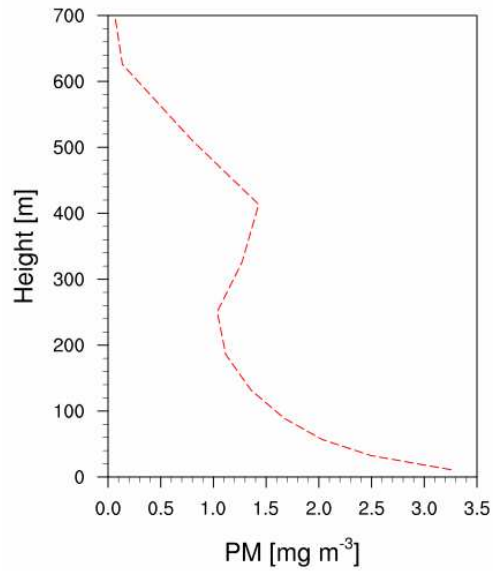


Figure 5 Example of vertical column PM concentration profiles that shows a double peak.

Using the presented method, these two separate plumes would appear as one plume that is at the median between these two points. Finally, the use of a numerical filter to remove background PM may skew or completely remove low-level PM concentrations originating from the fire. Likewise, the concentration of PM was defined as proportional to the heat release of the fire. The filtering of low concentrations may cause us to completely miss sections of the plume which have become diluted or emitted at a very low rate from the fire (Figure 6).

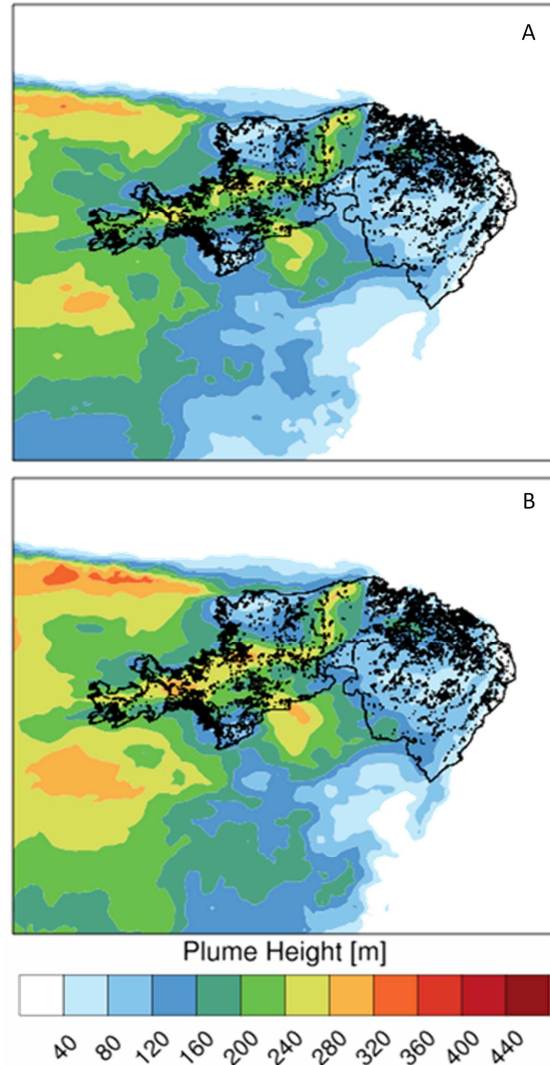


Figure 6 Panel A is a 6-hr averaged plume rise using a $20 \mu\text{g m}^{-3}$ filter on the PM data. Panel B is the same 6-hr time period with a $10 \mu\text{g m}^{-3}$ filter on the PM data.

Differences resulting from using different filter quantities can be seen in Figure 3. Of particular note is the overall rise in plume height throughout the domain with the lower PM filter in place. The proportionality of PM to wildland fire heat release is not a physical representation of the behavior of PM or any other trace gas associated with the fire. Because of these possible low quantities of emissions, associated with low heat release, it may be that as PM rises, through a stretched grid, we are further

underestimating the total mass of pollutant present in the plume, and thus further lowering our overall plume rise estimate. Further work, looking at how this proportionality influences plume height, is obviously warranted.

4.6. SUMMARY AND CONCLUSIONS

We demonstrated the use of a column center-of-mass approach on an inert tracer as a means of estimating plume height for the Witch and Guejito fires in southern California, from October 21-23, 2007. We found that our 6-hr averages of plume rise were low but within one standard deviation of the plume heights estimated using MISR data. Instantaneous measures of plume heights agreed well with MISR data, but still trended low. Further work will need to be done to look at how well plume rise is estimated as a function of downwind distance from the fire. We also captured the non-Gaussian horizontal distribution of the plume with this technique.

This approach is unique in its use of a coupled fire-atmosphere model. Additionally, its use does not require one to make assumptions about, injection height, fire area, or dispersion coefficients. Nor are assumptions made as to the Gaussian distribution of the plume.

Future work has been suggested which would make this approach more robust, possibly account for the low plume height estimates, and lead to the use of this technique as a tool for assessing the accuracy of wildland fire plume rise estimates in operational smoke transport models.

4.7. REFERENCES

- Akagi, S. K., J. S. Craven, J. W. Taylor, G. R. McMeeking, R. J. Yokelson, I. R. Burling, S. P. Urbanski, et al. 2012. “Evolution of Trace Gases and Particles Emitted by a Chaparral Fire in California.” *Atmospheric Chemistry and Physics* 12 (3): 1397–1421. doi:10.5194/acp-12-1397-2012.
- Akagi, S. K., R. J. Yokelson, I. R. Burling, S. Meinardi, I. Simpson, D. R. Blake, G. R. McMeeking, et al. 2013. “Measurements of Reactive Trace Gases and Variable O-3 Formation Rates in Some South Carolina Biomass Burning Plumes.” *Atmospheric Chemistry and Physics* 13 (3): 1141–1165. doi:10.5194/acp-13-1141-2013.
- Akagi, S. K., R. J. Yokelson, C. Wiedinmyer, M. J. Alvarado, J. S. Reid, T. Karl, J. D. Crounse, and P. O. Wennberg. 2011. “Emission Factors for Open and Domestic Biomass Burning for Use in Atmospheric Models.” *Atmospheric Chemistry and Physics* 11 (9): 4039–4072. doi:10.5194/acp-11-4039-2011.
- Andreae, Meinrat O., and P. Merlet. 2001. “Emission of Trace Gases and Aerosols from Biomass Burning.” *Global Biogeochemical Cycles* 15 (4): 955–966.
- Arizona Department of Environmental Quality. 2003. “Simple Approach Smoke Estimation Model (SASEM), Version 4.0”. Arizona Department of Environmental Quality.
<http://www.azdeq.gov/environ/air/smoke/download/sasemi.pdf>.
- Bertschi, I., R. J. Yokelson, D. E. Ward, R. E. Babbitt, R. A. Susott, J. G. Goode, and W. M. Hao. 2003. “Trace Gas and Particle Emissions from Fires in Large Diameter and Belowground Biomass Fuels.” *Journal of Geophysical Research-Atmospheres* 108 (D13) (February 15). doi:10.1029/2002JD002100.
- Breyfogle, S., and S. Ferguson. 1996. “User Assessment of Smoke-Dispersion Models for Wildland Biomass Burning”. General Technical Report PNW-GTR-379. Pacific Northwest Research Station: USDA, Forest Service.
- Bunting, S. C., B. M. Kilgore, and C. L. Bushey. 1987. *Guidelines for Prescribed Burning Sagebrush-grass Rangelands in the Northern Great Basin*.
<http://www.treesearch.fs.fed.us/pubs/25027>.
- Burling, I. R., R. J. Yokelson, S. K. Akagi, S. P. Urbanski, C. E. Wold, D. W. T. Griffith, T. J. Johnson, J. Reardon, and D. R. Weise. 2011. “Airborne and Ground-based Measurements of the Trace Gases and Particles Emitted by Prescribed Fires in the United States.” *Atmospheric Chemistry and Physics* 11 (23): 12197–12216. doi:10.5194/acp-11-12197-2011.

- Burling, I. R., R. J. Yokelson, D. W. T. Griffith, T. J. Johnson, P. Veres, J. M. Roberts, C. Warneke, et al. 2010. "Laboratory Measurements of Trace Gas Emissions from Biomass Burning of Fuel Types from the Southeastern and Southwestern United States." *Atmospheric Chemistry and Physics* 10 (22): 11115–11130. doi:10.5194/acp-10-11115-2010.
- Chen, L.-W. A., P. Verburg, A. Shackelford, D. Zhu, R. Susfalk, J. C. Chow, and J. G. Watson. 2010. "Moisture Effects on Carbon and Nitrogen Emission from Burning of Wildland Biomass." *Atmos. Chem. Phys.* 10 (14) (July 20): 6617–6625. doi:10.5194/acp-10-6617-2010.
- Christian, T. J., B. Kleiss, R. J. Yokelson, R. Holzinger, P. J. Crutzen, W. M. Hao, B. H. Saharjo, and D. E. Ward. 2003. "Comprehensive Laboratory Measurements of Biomass-burning Emissions: 1. Emissions from Indonesian, African, and Other Fuels." *Journal of Geophysical Research-Atmospheres* 108 (D23) (December 4). doi:10.1029/2003JD003704.
- Clark, T. L., J. L. Coen, and D. Latham. 2004. "Description of a Coupled Atmosphere-fire Model." *International Journal of Wildland Fire* 13 (1): 49–63. doi:10.1071/WF03043.
- Clark, T. L., M. A. Jenkins, J. L. Coen, and D. R. Packham. 1996. "A Coupled Atmosphere-fire Model: Role of the Convective Froude Number and Dynamic Fingering at the Fireline." *International Journal of Wildland Fire* 6 (4) (December): 177–190. doi:10.1071/WF9960177.
- Coen, J. L. 2005. "Simulation of the Big Elk Fire Using Coupled Atmosphere-fire Modeling." *International Journal of Wildland Fire* 14 (1): 49–59. doi:10.1071/WF04047.
- Coen, J. L., M. Cameron, J. Michalakes, E. G. Patton, P. J. Riggan, and K. M. Yedinak. 2013. "WRF-Fire: Coupled Weather-Wildland Fire Modeling with the Weather Research and Forecasting Model." *Journal of Applied Meteorology and Climatology* 52 (1) (January): 16–38. doi:10.1175/JAMC-D-12-023.1.
- Crosby, JS. 1949. "Vertical Wind Currents and Fire Behavior." *Fire Control Notes* 10 (2): 12–14.
- Cunningham, Philip, and Michael J. Reeder. 2009. "Severe Convective Storms Initiated by Intense Wildfires: Numerical Simulations of Pyro-convection and Pyro-tornadogenesis." *Geophysical Research Letters* 36 (June 26). doi:10.1029/2009GL039262.
- Dennis, A., M. Fraser, S. Anderson, and D. Allen. 2002. "Air Pollutant Emissions Associated with Forest, Grassland, and Agricultural Burning in Texas." *Atmospheric Environment* 36 (23) (August): 3779–3792. doi:10.1016/S1352-2310(02)00219-4.

- Dignon, J., and J. E. Penner. 1991. In *Global Biomass Burning: Atmospheric, Climatic, and Biospheric Implications*, by Joel S. Levine. MIT Press.
- Eidsmoe, G. 2007. "Investigation Report: Guejito Fire". Investigation CA-MVU-010484. Guejito Creek drainage: California Department of Forestry and Fire Protection. http://www.fire.ca.gov/fire_protection/downloads/redsheets/CA-MVU-010484_Complete.pdf.
- Ferek, R. J., J. S. Reid, P. V. Hobbs, C. R. Blake, and C. Liou. 1998. "Emission Factors of Hydrocarbons, Halocarbons, Trace Gases and Particles from Biomass Burning in Brazil." *Journal of Geophysical Research: Atmospheres* 103 (D24): 32107–32118. doi:10.1029/98JD00692.
- Freitas, S. R., K. M. Longo, R. Chatfield, D. Latham, M. A. F. Silva Dias, M. O. Andreae, E. Prins, J. C. Santos, R. Gielow, and J. A. Carvalho Jr. 2007. "Including the Sub-grid Scale Plume Rise of Vegetation Fires in Low Resolution Atmospheric Transport Models." *Atmos. Chem. Phys.* 7 (13) (July 2): 3385–3398. doi:10.5194/acp-7-3385-2007.
- Gilbert, M. 2008. "Investigation Report: Witch Fire". Investigation 07-CDF-570. Highway 78 west of Santa Ysabel, San Diego County: California Department of Forestry and Fire Protection. http://www.fire.ca.gov/fire_protection/downloads/redsheets/CA-MVU-010432_Complete.pdf.
- Goodrick, S. L., G. L. Achtemeier, N. K. Larkin, Y. Liu, and T. M. Strand. 2013. "Modelling Smoke Transport from Wildland Fires: a Review." *International Journal of Wildland Fire* 22 (1): 83–94.
- Goodrick, Scott L., Gary L. Achtemeier, Narasimhan K. Larkin, Yongqiang Liu, and Tara M. Strand. 2013. "Modelling Smoke Transport from Wildland Fires: a Review." *International Journal of Wildland Fire* 22 (1): 83–94.
- Haines, D. A. 1988. "A Lower Atmospheric Severity Index for Wildland Fires." *National Weather Digest* 13 (2): 23–27.
- Hardy, C., R. Ottmar, J. Peterson, J. Core, and P. Seamon, ed. 2001. "Smoke Management Guide for Prescribed and Wildland Fire". National Wildfire Coordination Group. <http://www.nwcg.gov/pms/pubs/SMG/SMG-72.pdf>.
- Hayes, G. L. 1941. "Influences of Altitude and Aspect on Daily Variations in Factors of Fire Danger." *US Department of Agriculture, Circular 591* (Washington DC).
- Jain, R., J. Vaughan, K. Heitkamp, C. Ramos, C. Claiborn, M. Schreuder, M. Schaaf, and B. Lamb. 2007. "Development of the ClearSky Smoke Dispersion Forecast System for Agricultural Field Burning in the Pacific Northwest." *Atmospheric Environment* 41 (32) (October): 6745–6761. doi:10.1016/j.atmosenv.2007.04.058.

- Jenkins, M. A. 2004. "Investigating the Haines Index Using Parcel Model Theory." *International Journal of Wildland Fire* 13 (3): 297–309. doi:10.1071/WF03055.
- Jolly, W. M. 2007. "Sensitivity of a Surface Fire Spread Model and Associated Fire Behaviour Fuel Models to Changes in Live Fuel Moisture." *International Journal of Wildland Fire* 16 (4): 503–509.
- Keeley, J. E., G. H. Aplet, N. L. Christensen, S. G. Conard, E. A. Johnson, P. N. Omi, D. L. Peterson, and T. W. Swetnam. 2009. "Ecological Foundations for Fire Management in North American Forest and Shrubland Ecosystems". United States Department of Agriculture, Forest Service, Pacific Northwest Research Station, Portland, OR. <http://www.treesearch.fs.fed.us/pubs/32483>.
- Kilgore, B. M., and G. A. Curtis. 1987. *Guide to Understory Burning in Ponderosa Pine-larch-fir Forests in the Intermountain West*. <http://www.treesearch.fs.fed.us/pubs/32954>.
- Kochanski, A., M. A. Jenkins, J. Mandel, J. Beezley, and S. Krueger. 2013. "Real Time Simulation of 2007 Santa Ana Fires." *Forest Ecology and Management* 294 (April 15): 136–149. doi:10.1016/j.foreco.2012.12.014.
- Kochanski, A., M. A. Jenkins, R. Sun, S. Krueger, S. Abedi, and J. Charney. 2013. "The Importance of Low-level Environmental Vertical Wind Shear to Wildfire Propagation: Proof of Concept." *Journal of Geophysical Research: Atmospheres*: n/a–n/a. doi:10.1002/jgrd.50436.
- Lavdas, L. G. 1996. "Program VSMOKE: Users Manual". General Technical Report GTR-SRS-006. Southeastern Research Station: USDA, Forest Service.
- Lobert, J. M., D. H. Scharffe, W. Hao, T. A. Kuhlbusch, R. Seuwen, P. Warneck, and P. J. Crutzen. 1991. "Experimental Evaluation of Biomass Burning Emissions: Nitrogen and Carbon Containing Compounds." In *Global Biomass Burning*, edited by J. S. Levine, 289–304. MIT Press.
- McMeeking, Gavin R., Sonia M. Kreidenweis, Stephen Baker, Christian M. Carrico, Judith C. Chow, Jeffrey L. Collett, Wei Min Hao, et al. 2009. "Emissions of Trace Gases and Aerosols During the Open Combustion of Biomass in the Laboratory." *Journal of Geophysical Research-Atmospheres* 114 (October 14). doi:10.1029/2009JD011836.
- Naeher, Luke P, Gary L Achtemeier, Jeff S Glitzenstein, Donna R Streng, and David Macintosh. 2006. "Real-time and Time-integrated PM_{2.5} and CO from Prescribed Burns in Chipped and Non-chipped Plots: Firefighter and Community Exposure and Health Implications." *Journal of Exposure Science & Environmental Epidemiology* 16 (4) (July): 351–361. doi:10.1038/sj.jes.7500497.
- NCAR. 2012. *Weather Research and Forecasting Model* (version 3.4). http://www.mmm.ucar.edu/wrf/users/download/get_source.html.

- Nelson, R. M. 2003. "Power of the Fire - a Thermodynamic Analysis." *International Journal of Wildland Fire* 12 (1): 51–65. doi:10.1071/WF02032.
- Nelson, Rm. 1993. "Byram Derivation of the Energy Criterion for Forest and Wildland Fires." *International Journal of Wildland Fire* 3 (3) (September): 131–138. doi:10.1071/WF9930131.
- "NICC Wildland Fire Annual Report." 2012. NIFC.
<http://www.predictiveservices.nifc.gov/intelligence/intelligence.htm>.
- Pharo, J. A., L. G. Lavadas, and P. M. Bailey. 1976. "Smoke Transport and Dispersion". General Technical Report SE-10. Southern Forestry Smoke Management Guidebook. Southeastern Research Station: USDA, Forest Service.
- Potter, B. E. 2002. "A Dynamics Based View of Atmosphere-fire Interactions." *International Journal of Wildland Fire* 11 (3-4): 247–255. doi:10.1071/WF02008.
- . 2012a. "Atmospheric Interactions with Wildland Fire Behaviour – I. Basic Surface Interactions, Vertical Profiles and Synoptic Structures." *International Journal of Wildland Fire* 21 (7): 779–801.
- . 2012b. "Atmospheric Interactions with Wildland Fire Behaviour – II. Plume and Vortex Dynamics." *International Journal of Wildland Fire* 21 (7): 802–817.
- Reifsnyder, W. E. 1954. "Atmospheric Stability and Forest Fire Behavior". PhD dissertation, New Haven, CT: Yale University.
- Rothermel, R. C. 1972. "A Mathematical Model for Predicting Fire Spread in Wildland Fuels." *USDA Forest Service, Intermountain Forest and Range Experiment Station, Research Paper INT-115*.
- . 1983. *How to Predict the Spread and Intensity of Forest and Range Fires*.
<http://www.treesearch.fs.fed.us/pubs/24635>.
- Sandberg, David V., Roger D. Ottmar, and Janice L. Peterson. 2002. "Wildland Fire in Ecosystems: Effects of Fire on Air." <http://www.treesearch.fs.fed.us/pubs/5247>.
- Scire, J. S., D. G. Strimaitis, and R. J. Yamartino. 2000. "A User's Guide for the CALPUFF Dispersion Model (Version 5)". User's guide. Concord, MA: EarthTech Inc.
- Skamarock, W. C., J. B. Klemp, J. Dudhia, D. O. Gill, D. M. Barker, M. G. Duda, X. Huang, W. Wang, and J. G. Powers. 2008. "A Description of the Advanced Research WRF Version 3". National Center for Atmospheric Research.
- Trentmann, J., M. O. Andreae, H. F. Graf, P. V. Hobbs, R. D. Ottmar, and T. Trautmann. 2002. "Simulation of a Biomass-burning Plume: Comparison of Model Results

- with Observations.” *Journal of Geophysical Research-Atmospheres* 107 (D1-D2) (January). doi:10.1029/2001JD000410.
- Urbanski, S. P. 2013. “Combustion Efficiency and Emission Factors for Wildfire-season Fires in Mixed Conifer Forests of the Northern Rocky Mountains, US.” *Atmos. Chem. Phys.* 13 (14) (July 30): 7241–7262. doi:10.5194/acp-13-7241-2013.
- Viney, NR. 1991. “A Review of Fine Fuel Moisture Modelling.” *International Journal of Wildland Fire* 1 (4) (January 1): 215–234.
- Ward, D. E., and C. C. Hardy. 1991. “Smoke Emissions from Wildland Fires.” *Environment International* 17 (2–3): 117–134. doi:10.1016/0160-4120(91)90095-8.
- Ward, D. E., and L. F. Radke. 1993. “Emissions Measurements from Vegetation Fires: A Comparative Evaluation of Methods and Results.” In , 53–76. <http://www.treearch.fs.fed.us/pubs/40604>.
- Wiedinmyer, C., S. K. Akagi, R. J. Yokelson, L. K. Emmons, J. A. Al-Saadi, J. J. Orlando, and A. J. Soja. 2011. “The Fire INventory from NCAR (FINN): a High Resolution Global Model to Estimate the Emissions from Open Burning.” *Geoscientific Model Development* 4 (3): 625–641. doi:10.5194/gmd-4-625-2011.
- Yokelson, R. J., I. R. Burling, J. B. Gilman, C. Warneke, C. E. Stockwell, J. de Gouw, S. K. Akagi, et al. 2013. “Coupling Field and Laboratory Measurements to Estimate the Emission Factors of Identified and Unidentified Trace Gases for Prescribed Fires.” *Atmospheric Chemistry and Physics* 13 (1): 89–116. doi:10.5194/acp-13-89-2013.
- Yokelson, R. J., J. G. Goode, D. E. Ward, R. A. Susott, R. E. Babbitt, D. D. Wade, I. Bertschi, D. W. T. Griffith, and W. M. Hao. 1999. “Emissions of Formaldehyde, Acetic Acid, Methanol, and Other Trace Gases from Biomass Fires in North Carolina Measured by Airborne Fourier Transform Infrared Spectroscopy.” *Journal of Geophysical Research: Atmospheres* 104 (D23): 30109–30125. doi:10.1029/1999JD900817.
- Yokelson, R. J., D. W. T. Griffith, and D. E. Ward. 1996. “Open-path Fourier Transform Infrared Studies of Large-scale Laboratory Biomass Fires.” *Journal of Geophysical Research-Atmospheres* 101 (D15) (September 20): 21067–21080. doi:10.1029/96JD01800.
- Yokelson, R. J., R. Susott, D. E. Ward, J. Reardon, and D. W. T. Griffith. 1997. “Emissions from Smoldering Combustion of Biomass Measured by Open-path Fourier Transform Infrared Spectroscopy.” *Journal of Geophysical Research-Atmospheres* 102 (D15) (August 20): 18865–18877. doi:10.1029/97JD00852.

Yokelson, R. J., S. P. Urbanski, E. L. Atlas, D. W. Toohy, E. C. Alvarado, J. D. Crouse, P. O. Wennberg, et al. 2007. "Emissions from Forest Fires Near Mexico City." *Atmospheric Chemistry and Physics* 7 (21): 5569–5584.

CHAPTER 5: SUMMARY AND CONCLUSIONS

5.1. SUMMARY

The focus of this dissertation was to better characterize wildland fire emissions and plume rise dynamics. In chapter 2 emission factors were calculated for two prescribed fires in wire grass and loblolly pine leaf litter in the southeastern United States. These emissions factors were correlated with calculations of modified combustion efficiency. Comparisons were made between the two burns as well as with other literature. Chapter 3 outlined the use of WRF-Fire, a coupled fire-atmosphere model applied in large eddy simulation mode, to investigate the sensitivity of fire line rate of spread and pyrogenic plume rise heights to atmospheric stability. In Chapter 4 a plume rise analysis technique was investigated, with the use of a case study from a large southern California fire complex, to assess the accuracy of this technique for application with regional scale air quality models.

5.2. CONCLUSIONS

5.2.1. Chapter 2

A unique data set was presented for which emission measurements from two prescribed fires were collected in and near source. These data allowed for the correlation of smoke emissions factors with calculations of modified combustion efficiency. We found that comparing two low intensity prescribed burns that shared the same fuel type, canopy, surface meteorology, and ignition techniques allowed us to isolate the variability in emission factors due to moisture content of the fuels, the relative live fuel contribution,

and the influence of sampling proximity to the emission source. Our results show the strong variability present in EFs due mainly to small differences in fuel moisture content and the overall ratio of dead to live fuel. Excess trace gas concentrations increased between 2 and 500 times when the sampling platform was in-source as compared to the near source sampling location.

The time resolution and sampling techniques allowed for separation of the trace gas and particles results between flaming and smoldering combustion as well as the onset of smoldering combustion. Overall, our results agree well with similar studies which focus on prescribed fires in the southeastern United States and with those that look at smoldering combustion. However, we observed overall higher emission factors of $PM_{2.5}$ and a higher emission factor of NH_3 during smoldering from burn 2. The elevated levels of NH_3 are likely attributed to the increased live fuel activity and level of nitrogen deposition present in that location.

5.2.2. Chapter 3

This study employed the use of WRF-Fire, a coupled fire-atmosphere model, operating in large eddy simulation mode, to determine the sensitivity of wildland fire plume rise and rate of spread, to changes in atmospheric stability. We found that head-fire ROS was not significantly influenced by atmospheric stability. We also discovered that ROS was not an informative metric for understanding overall fire behavior as the rate of change of the fire area was not well represented using this. A fire area metric called rate of growth was introduced that subsequently showed significantly different behavior suggesting that neutral stability facilitated an energetically decreasing environment. The unstable atmosphere produced a constant (though variable) growth environment

suggesting an energetically stable environment. The authors know of no data sets available for which to compare these findings.

Plume rise was calculated using a center of mass approach on fire-emitted water vapor. The unstable atmosphere produced plumes which pushed through a thick thermal inversion layer. The neutral atmosphere produced plumes which stayed within and never rose above the thermal inversion layer. The difference in stability and presence of a thermal inversion produced an average 500 m difference in plume rise between the two stability cases.

Our analysis was limited in both the duration of time we could observe the plume and the distance downwind we could track the plume. These limitations were due to limitations in computing resources and the use of water vapor as a tracer for smoke respectively. The neutral plume reached its steady state position during the time frame and distance we sampled. The unstable plume did not reach a steady state height during the duration of our study.

5.2.3. Chapter 4

This study employed simulations from WRF-Sfire, a coupled fire-atmosphere model, to develop an analysis technique for evaluating plume rise of an inert tracer. The center-of-mass approach, also used in Chapter 3, was used to estimate plume height for the Witch and Quejito fires in southern California. We found that our 6-hr averages of plume rise were low but within one standard deviation of the plume heights estimated using MISR data. Instantaneous measures of plume heights agreed well with MISR data, but still trended low. The use of a background PM concentration filter was shown to lower the overall estimates of plume height. We demonstrated the ability of coupled fire-

atmosphere models to produce non-Gaussian plumes and the potential of the center-of-mass technique to assess plume rise in mesoscale models such as those used in regional air quality modeling.

5.3. FUTURE WORK

The center-of-mass technique, outlined in two of the dissertation chapters, will need to be evaluated against model runs for which the vertical grid is not stretched (evenly spaced). It will be important to ensure that the stretch vertical grid, present in most all mesoscale models, will not skew the plume rise results. Conversely, if the use of a stretched grid does influence the distribution of pollutants vertically, this influence could be characterized for future applications.

Regarding the sensitivity analysis of WRF-Fire to changes in stability conditions, two surface heat fluxes were employed to maintain the different stability scenarios. The relative influence of these surface heat fluxes on plume rise and fire behavior will be important to quantify. Likewise quantifying the ratio of fire heat flux to background surface heat flux over multiple burning scenarios will outline the relative importance of these two heat fluxes and their interaction.

The emissions factor study could be further enhanced by investigating the role of excess water vapor in relation to modified combustion efficiency. The observed variability, based on perceived changes in moisture content may be explained with the knowledge of the emission factor of water as it relates to MCE. Additionally, the interpretation of the results presented will be enhanced with knowledge of the dispersion of the plume (work currently in progress).